

AN ABSTRACT OF THE THESIS OF

Varong Pavarajarn for the degree of Doctor of Philosophy in Chemical Engineering
presented on June 12, 2002.

Title: Roles of Gas and Solid Components in the Direct Nitridation of Silicon

Redacted for privacy

Abstract approved: _____

Shoichi Kimura

The factors influencing the direct nitridation of silicon, including the effects of the native oxide layer covering the surface of silicon, the effects of hydrogen contained in the nitridation gas and the catalytic effects of metals added to the raw material silicon, were investigated, using a tubular flow reactor and a fluidized-bed reactor operated at temperatures ranging from 1150°C to 1390°C in a stream of nitrogen containing 10% hydrogen.

The nitridation of silicon is not initiated until the native oxide is removed by an assistance of hydrogen contained in argon during the pretreatment or in the nitridation gas mixture. An induction period is observed before the initiation of the nitridation and depends on the nitridation temperature as well as the pretreatment time, which is associated with the removal of the oxide layer.

The presence of hydrogen in the nitridation atmosphere is crucial for the nitridation of silicon. When pretreated silicon grains are exposed to nitrogen without

hydrogen for a time period as short as 5 minutes, the subsequent nitridation, even with hydrogen, becomes extremely slow. The concentration of hydrogen as low as 0.3% is effective for sustaining the reactivity of silicon for the nitridation. The results suggest the formation of a protective layer on the surface of silicon when silicon grains are exposed to nitrogen without hydrogen. The protective film is suspected to be silicon oxynitride, or a mixture of silicon oxynitride and silicon dioxide or silicon nitride formed from the reaction of silicon with oxygen and nitrogen, depending on the temperature of its formation. However, the protective film does not form on the native oxide layer, and the reactivity of silicon is resumed upon the removal of the native oxide.

An addition of calcium (as low as 0.125%) or yttrium (1.0-2.0%) to silicon suppresses the formation of β -silicon nitride while iron enhances the formation of β -silicon nitride. Copper promotes not only the nitridation but also the formation of α -silicon nitride at 1200°C, but enhances the β -phase formation at higher temperatures. The role of liquid phases on the formation of α -/ β -silicon nitride was also discussed based on the nitridation of silicon impregnated with copper, calcium, silver, chromium and tungsten.

©Copyright by Varong Pavarajarn
June 12, 2002
All Rights Reserved

Roles of Gas and Solid Components in the Direct Nitridation of Silicon

by

Varong Pavarajarn

A THESIS

submitted to

Oregon State University

in partial fulfillment of
the requirements for the
degree of

Doctor of Philosophy

Presented June 12, 2002

Commencement June 2003

Doctor of Philosophy thesis of Varong Pavarajarn presented on June 12, 2002.

APPROVED:

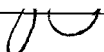

Redacted for privacy

Major Professor, representing Chemical Engineering

Redacted for privacy



Head of Department of Chemical Engineering

Redacted for privacy


Dean of Graduate School

I understand that my thesis will become part of the permanent collection of Oregon State University libraries. My signature below authorizes release of my thesis to any reader upon request.

Redacted for privacy

 
Varong Pavarajarn, Author

ACKNOWLEDGMENTS

I would like to express my deep gratitude to my advisor, Dr. Shoichi Kimura, for a number of suggestions and guidance through out the entire course of this work. His invaluable teaching has always been greatly appreciated.

I wish to express my appreciation to my committee members: Dr. Goran Jovanovic, Dr. Keith Levien, Dr. Roger Nielsen and Dr. Brian Wood for their valuable time and suggestions. I would also like to thank Dr. Douglas Keszler for not only being my committee member, but also his generosity to let me use the X-ray diffraction equipment. Special thanks to: Shin-Etsu Chemical Company for raw materials, Dr. Tsai-Chen Wang for SEM pictures and his guidance on the fluidized-bed reactor setup, Dr. Christine Pastorek for the permission to use FTIR equipment, Nick Wannenmacher and Panut Vongpayabal for their help and suggestion during the period in this study.

I am very thankful to Department of Chemical Engineering for the teaching assistantship in the first three years of my program. I am also grateful to Department of Chemistry for two years of great experience working as their teaching assistance. Special thanks to Dr. Michael Schuyler for giving me a chance for such a wonderful experience.

Finally, I would like to express my deep thanks to my parents for their support, financially and emotionally, and to my wife, Alisa, for her inspiration, patience and love. Their unconditional love has always embedded in my heart.

TABLE OF CONTENTS

	<u>Page</u>
1. INTRODUCTION.....	1
2. LITERATURE SURVEY AND OBJECTIVES.....	4
2.1 CRYSTAL STRUCTURE OF SILICON NITRIDE.....	4
2.2 COMMERCIAL TECHNIQUES FOR MASS-PRODUCING SILICON NITRIDE POWDER.....	7
2.2.1 Carbothermal Reduction and Nitridation of Silica.....	8
2.2.2 Liquid Phase Reactions/Imide Process.....	9
2.2.3 Direct Nitridation of Silicon.....	10
2.3 FACTORS INFLUENCING THE DIRECT NITRIDATION OF SILICON.....	11
2.3.1 Effects of Native Oxide Layer Covering Silicon Surface.....	12
2.3.2 Effects of Hydrogen in the Reactant Gas Mixture.....	14
2.3.3 Effects of Metals in Silicon.....	15
2.3.4 Effects of Liquid Phases Formation.....	17
2.4 OBJECTIVES.....	19
3. EXPERIMENTS.....	20
3.1 CHARACTERISTICS OF SILICON RAW MATERIAL.....	20
3.2 RAW MATERIAL PREPARATION PROCEDURE.....	21
3.3 EXPERIMENTAL APPARATUS AND EXPERIMENTAL PROCEDURE.....	23
3.3.1 Thermogravimetric Analysis.....	23
3.3.2 Tubular Flow Reactor.....	25
3.3.3 Fluidized-Bed Reactor.....	28
3.4 ANALYSIS OF PRODUCTS.....	32

TABLE OF CONTENTS (Continued)

	<u>Page</u>
4. EXPERIMENTAL RESULTS AND DISCUSSION.....	36
4.1 PRELIMINARY EXPERIMENTS.....	36
4.1.1 Preliminary Results from Thermogravimetric Analysis.....	36
4.1.2 Effects of Operating Gas Flow Rate in the Tubular Flow Reactor.....	38
4.1.3 Effects of Positions in the Tubular Flow Reactor.....	39
4.1.4 Heat Transfer Effects in the Tubular Flow Reactor.....	41
4.1.5 Consistency and Reproducibility of Results from the Tubular Flow Reactor.....	43
4.1.6 Effects of Particles Size.....	46
4.2 EFFECTS OF OXIDE LAYER.....	51
4.2.1 Results from Experiments using Tubular Flow Reactor.....	51
4.2.2 SEM Pictures of Silicon Wafer Specimen.....	58
4.2.3 Results from Experiments using Fluidized-Bed Reactor.....	65
4.3 ROLES OF HYDROGEN.....	70
4.3.1 Phase Diagram for the Si-N-O System.....	70
4.3.2 Nitridation without Hydrogen at 1300°C.....	82
4.3.3 Nitridation without Hydrogen at Different Temperatures.....	96
4.3.4 Infrared Spectrophotometry Analysis.....	99
4.3.5 Formation of Protective Film.....	104
4.4 EFFECTS OF OXIDE LAYER IN THE ABSENCE OF HYDROGEN.....	107
4.4.1 Effects of Oxide Layer in the Nitridation without Hydrogen at 1300°C.....	107
4.4.2 Effects of Oxide Layer in the Nitridation without Hydrogen at Different Temperatures.....	110

TABLE OF CONTENTS (Continued)

	<u>Page</u>
4.5 CATALYTIC EFFECTS OF METALS.....	118
4.5.1 Calcium.....	119
4.5.2 Yttrium.....	122
4.5.3 Iron.....	126
4.5.4 Copper.....	127
4.5.5 Palladium.....	131
4.5.6 Chromium, Tungsten and Silver.....	133
4.5.7 Summary for Catalytic Effects of Metals.....	136
4.5.8 Effects of Liquid Phase.....	139
4.5.9 Operation with Programmed Temperature.....	142
5. CONCLUSIONS AND RECOMMEDATIONS.....	146
5.1 CONCLUSIONS.....	146
5.1.1 Effects of the Native Oxide Layer.....	146
5.1.2 Roles of Hydrogen.....	147
5.1.3 Combined Effect of Hydrogen Interruption and Native Oxide.....	148
5.1.4 Catalytic Effects of Metals.....	148
5.2 RECOMMENDATIONS FOR FUTURE WORK.....	149
BIBLIOGRAPHY.....	152
APPENDICES.....	160
APPENDIX A Thermodynamics Data.....	161
APPENDIX B The Nitridation of Silicon Impregnated with High Contents of Metal.....	163

LIST OF FIGURES

<u>Figure</u>	<u>Page</u>
2.1 β -Si ₃ N ₄ unit cell.....	5
2.2 α -Si ₃ N ₄ unit cell.....	6
3.1 Schematic diagram of the thermogravimetric analysis system.....	24
3.2 Schematic diagram of the tubular flow reactor system.....	27
3.3 Schematic diagram of the fluidized-bed reactor system.....	29
3.4 Minimum fluidization velocity of silicon granules in 90% nitrogen – 10% hydrogen at room temperature.....	30
3.5 An example of X-ray diffraction scan of product.....	35
4.1 Change in sample mass observed in TGA.....	37
4.2 Effects of gas flow rate on the nitridation of bare silicon granules at 1200°C.....	39
4.3 Effects of position in the tubular flow reactor.....	40
4.4 Effects of sample mass used for the nitridation at 1300°C in the tubular flow reactor.....	42
4.5 Overall conversions of control samples.....	44
4.6 Conversions observed from different sample-preparation batches.....	45
4.7 Comparison of the conversions of silicon powder and silicon granules to α - and β -Si ₃ N ₄ in the 3-hour nitridation at 1300°C	47
4.8 Comparison of the overall conversions of silicon powder and silicon granules in the nitridation at 1300°C.....	48

LIST OF FIGURES (Continued)

<u>Figure</u>	<u>Page</u>
4.9 Comparison of the conversions of silicon granules with different granule sizes to α - and β -Si ₃ N ₄ in the 3-hour nitridation at 1300°C.....	50
4.10 Effects of the native oxide layer at 1150°C.....	52
4.11 Effects of the length and temperature of pretreatment.....	53
4.12 The progress of nitridation of samples prepared at different pretreatment conditions.....	55
4.13(a,b) SEM pictures of silicon-wafer specimen after heating to 1300°C.....	59
4.13(c) SEM picture of silicon-wafer specimen after heating to 1300°C.....	60
4.14(a,b) SEM pictures of silicon-wafer specimen after 1-hour pretreatment at 1300°C.....	61
4.14(c) SEM picture of silicon-wafer specimen after 1-hour pretreatment at 1300°C.....	62
4.15(a,b) SEM pictures of silicon-wafer specimen after 6-hour pretreatment at 1300°C.....	63
4.15(c) SEM picture of silicon-wafer specimen after 6-hour pretreatment at 1300°C.....	64
4.16 The progress of fluidized-bed nitridation at 1300°C samples prepared at different pretreatment conditions.....	66
4.17 The progress of fluidized-bed nitridation at 1200 and 1300°C of samples pretreated for 1 hour at 1300°C.....	67
4.18 Comparison of nitridation results obtained in the fluidized-bed reactor and tubular flow reactor.....	69

LIST OF FIGURES (Continued)

<u>Figure</u>	<u>Page</u>
4.19 Stability-field diagram for the Si-O-N system calculated based on reaction (A)-(E) at 1300°C.....	73
4.20 Schematic presentation of the Wagner's model.....	76
4.21 Stability-field diagram for the Si-O-N system at 1300°C with the active oxidation, i.e. reactions (A)-(D), incorporated.....	79
4.22 Regions of stability of different phases as a function of temperature and oxygen partial pressure in 1 atm nitrogen.....	81
4.23 Progress of nitridation at 1300°C under various reaction conditions.....	83
4.24 Effects of hydrogen concentration.....	84
4.25 Progress of nitridation when hydrogen was interrupted during the reaction.....	85
4.26(a,b) SEM pictures of silicon-wafer specimen after 6-hour pretreatment, followed by 5-minute nitridation with hydrogen at 1300°C.....	87
4.26(c) SEM picture of silicon-wafer specimen after 6-hour pretreatment, followed by 5-minute nitridation with hydrogen at 1300°C.....	88
4.27(a,b) SEM pictures of silicon-wafer specimen after 6-hour pretreatment, followed by 5-minute nitridation without hydrogen at 1300°C.....	89
4.27(c) SEM picture of silicon-wafer specimen after 6-hour pretreatment, followed by 5-minute nitridation without hydrogen at 1300°C.....	90

LIST OF FIGURES (Continued)

<u>Figure</u>	<u>Page</u>
4.28(a,b) SEM pictures of silicon-wafer specimen after 1-hour pretreatment, followed by 3-hour nitridation with hydrogen at 1300°C.....	93
4.28(c) SEM picture of silicon-wafer specimen after 1-hour pretreatment, followed by 3-hour nitridation with hydrogen at 1300°C.....	94
4.29 SEM pictures of silicon-wafer specimen exposed to nitrogen without hydrogen for 5 minutes after 1-hour pretreatment, followed by 3-hour nitridation with hydrogen at 1300°C.....	95
4.30 Effects of hydrogen interruption at different temperatures.....	96
4.31 IR spectra of products in the nitridation at 1300°C.....	102
4.32 IR spectra of products in the nitridation at 1200 and 1300°C.....	103
4.33 Effects of hydrogen interruption at 1300°C under different pretreatment conditions.....	108
4.34 Effects of hydrogen interruption in the nitridation at 1200°C with various pretreatment times.....	111
4.35 Effects of hydrogen interruption in the nitridation at 1250°C with various pretreatment times.....	111
4.36 Effects of hydrogen interruption in the nitridation at 1300°C with various pretreatment times.....	112
4.37 Effects of hydrogen interruption in the nitridation at 1350°C with various pretreatment times.....	112
4.38 Effects of hydrogen interruption at different temperatures under different pretreatment conditions.....	114

LIST OF FIGURES (Continued)

<u>Figure</u>	<u>Page</u>
4.39 Effects of hydrogen interruption time at various temperatures under different pretreatment conditions.....	117
4.40 Nitridation of calcium impregnated silicon.....	119
4.41 Nitridation at 1300°C of calcium impregnated silicon for 3 and 6 hours.....	120
4.42 Nitridation of calcium impregnated silicon as a function of temperature.....	121
4.43 Nitridation of yttrium impregnated silicon.....	123
4.44 Nitridation at 1300°C of yttrium impregnated silicon for 3 and 6 hours.....	124
4.45 Nitridation of yttrium impregnated silicon as a function of temperature.....	125
4.46 Nitridation of iron impregnated silicon.....	127
4.47 Nitridation of copper impregnated silicon.....	128
4.48 Nitridation at 1200°C of copper impregnated silicon for 3 and 6 hours.....	129
4.49 Nitridation at 1300°C of copper impregnated silicon for 3 and 6 hours.....	130
4.50 Nitridation of palladium impregnated silicon.....	132
4.51 Nitridation of chromium impregnated silicon.....	133
4.52 Nitridation of tungsten impregnated silicon.....	134
4.53 Nitridation of silver impregnated silicon.....	135

LIST OF FIGURES (Continued)

<u>Figure</u>		<u>Page</u>
4.54	Comparison of overall conversions in the nitridation of silicon impregnated with various kind of metals.....	137
4.55	Comparison of the fraction of α -phase in the product from the nitridation of silicon impregnated with various kind of metals.....	138
4.56	Comparison of the nitridation of calcium impregnated silicon with a step-wise increase in temperature to the nitridation at 1390°C.....	144
4.57	Comparison of the nitridation of yttrium impregnated silicon with a step-wise increase in temperature to the nitridation at 1390°C.....	145

LIST OF TABLES

<u>Table</u>		<u>Page</u>
3.1	Specifications of raw material silicon.....	21
4.1	Effects of temperature at which the protective film is formed.....	98
4.2	Melting points and eutectic points for metal-silicon binary systems.....	140

LIST OF APPENDIX FIGURES

<u>Figure</u>		<u>Page</u>
B1	XRD patterns of the products from the nitridation of 20% calcium-impregnated silicon.....	165
B2	IR spectra of the products from the nitridation of 20% calcium-impregnated silicon compared to that from bare silicon.....	166
B3	XRD patterns of the products from the nitridation of 20% yttrium-impregnated silicon.....	168
B4	IR spectra of the products from the nitridation of 20% yttrium-impregnated silicon compared to that from bare silicon.....	169
B5	XRD patterns of the products from the nitridation of 20% copper-impregnated silicon.....	171
B6	IR spectra of the products from the nitridation of 20% copper-impregnated silicon compared to that from bare silicon.....	172

NOTATION

D_B	diffusivity of species B , [m^2/s]
$\Delta G^\circ_{[I]}$	Gibbs free energy change for reaction I , [J/mol]
$I_\delta(hkl)$	integrated intensity of an X-ray beam diffracted from reflection (hkl) of crystalline phase δ
j	flux of oxygen, according to Wagner's model, [$\text{gram-atom/m}^2 \text{ s}$]
$K_{\delta\gamma}$	calibration constant which relates intensity ratio of diffracted X-rays from reflections of two-phases in a mixture with a mass fraction ratio of these phases
$K_{[I]}$	equilibrium constant for reaction I
M_B	molar mass of species B , [g/mol]
$P_{\text{O}_2, [I]}$	partial pressure of O_2 associated with reaction I , [atm]
$P_{\text{N}_2, [I]}$	partial pressure of N_2 associated with reaction I , [atm]
$P_{\text{SiO}, [I]}$	partial pressure of SiO associated with reaction I , [atm]
R	universal gas constant, [8.314 J/mol K]
T	temperature, [$^\circ\text{C}$ or K]
W_δ	mass fraction of phase δ in a mixture
X	overall conversion of silicon, [% or dimensionless]
X_α	conversion from silicon into α -silicon nitride, [% or dimensionless]
X_β	conversion from silicon into β -silicon nitride, [% or dimensionless]

Greek Letters

δ	thickness of the effective boundary layer for diffusion, [m]
----------	---

ROLES OF GAS AND SOLID COMPONENTS IN THE DIRECT NITRIDATION OF SILICON

1. INTRODUCTION

In the last decade, silicon nitride (Si_3N_4) became a very promising material for high-temperature and high mechanical-stress applications because it offers high thermal shock resistance and high strength retention at elevated temperature as well as high-temperature deformation resistance and low creep. It has much higher creep resistance than metals and its thermal shock resistance is much better than that of most ceramics. Moreover, silicon nitride is inert to many chemicals. Thus, another benefit of silicon nitride is its corrosion resistance. It can withstand erosion from many molten metals, including molten aluminum.

The applications of silicon nitride depend primarily on its high temperature strength, good thermal shock resistance and chemical inertness. Early applications of silicon nitride include use as a mold for molten nonferrous metals, as a material for components in molten aluminum handling and casting, and as a thermocouple sheath used for hot-metal processing. Silicon nitride is also used for high-temperature rollers and ball bearings in applications, including abrasive environment in oil drilling and vacuum pumps. A silicon nitride bearing has a longer life than a conventional high-density steel and hard-metal bearing because of its wear resistance, low friction, high stiffness and low density.

The prospect of high-efficiency ceramic gas-turbine engine and reciprocating engines running at much higher temperatures than the conventional metallic engines has driven the development of silicon nitride for components in automobile engines, such as stator blades, exhaust valves, valve spring retainers, bucket tappets, rocker arm pads, and valve springs. Moreover, since the introduction of turbocharger rotors made by ceramics, silicon nitride seems particularly suited to such applications. The low specific density of silicon nitride improves the response of the engine during acceleration compared to the heavier metal turbocharger. The nozzles of certain rockets have already been prepared by using silicon nitride. Although these applications are not very-high-temperature applications originally envisaged, they rely on the high strength and toughness required to withstand the impact damage and wear, together with low density of silicon nitride.

Silicon nitride exists as amorphous and crystalline forms. There are two well known phases of crystalline silicon nitride, designated as α and β forms, respectively. β -silicon nitride is more desirable polymorph for high temperature engineering applications because it has high temperature strength as well as excellent thermal shock and oxidation resistance [Lange, 1979]. However, the β -form can not be directly used as the starting material for making good quality components. Instead, fabricating β -silicon nitride parts usually starts from α -silicon nitride powder mixed with sintering additives, normally Al_2O_3 and Y_2O_3 mixture. The mixture is then shaped into a desired component. Finally, the component is sintered at high temperatures (1700-1800°C) where phase transformation from α to β occurs,

providing a micro structure having high mechanical and thermal strength [Ault and Yeckley, 1994; Lange, 1979]. Thus, a desired starting material for making silicon nitride component is a powder of a few tenths of micron size, containing at least 90% of α -form. A higher content of α -form (higher than 95%) is often desired.

The cost of silicon nitride products is presently high compared to other commercial ceramics, such as alumina and silicon carbide. This is largely due to the production cost of silicon nitride. There are four typical processes for producing silicon nitride powder [Yamada, 1993]. Each process is discussed in the next section. One of the most commonly used processes is the direct nitridation of silicon, which has been recognized as one of commercial methods for mass-production of silicon nitride containing predominantly α -form. This process is an inexpensive option for the applications in which metal impurities, originating from silicon, contained in the product silicon nitride can be tolerated. However, the product from this process is often considered as lower quality product than product from the more expensive diimide process, since the content of α -form from the direct nitridation process is normally lower than product obtained from the diimide process.

The main purpose of this work is to further understand factors that affect the formation of silicon nitride in the direct nitridation of silicon, in order to improve the quality of product from the direct nitridation process while maintaining low production cost.

2. LITERATURE SURVEY AND OBJECTIVES

2.1 CRYSTAL STRUCTURE OF SILICON NITRIDE

It has been generally accepted that there are two forms of crystalline silicon nitride, designated as α and β forms. Although the third polymorph of silicon nitride, designated as c -Si₃N₄, was recently discovered [Zerr, *et al.*, 1999], it had to be synthesized under extremely high pressure (15 GPa) and extremely high temperature (2200 K), yet the amount obtained was very small. Thus, this work will focus mainly on the more common polymorphs, α and β forms.

Detailed X-ray diffractometry (XRD) examinations have proved that the crystal structures of both α and β polymorphs are hexagonal. However, their respective structural dimensions are different. There is a wide spread in the reported lattice parameters for the two phases. Values for the α -phase have ranged from 0.7748-0.7818 nm for a and from 0.5591-0.5628 nm for c , while the axial ratios c/a are reasonably constant [Wang, *et al.*, 1996]. The lattice parameters for the β -phase have been reported in the range from 0.7595-0.7608 nm for a and from 0.2900-0.2911 nm for c [Wang, *et al.*, 1996]. It can be seen that the c -axis dimension of the unit cell of the α -phase is approximately twice that of the β -phase.

In both the forms, the basic building unit is the silicon-nitrogen tetrahedron in which a silicon atom lies at the center of a tetrahedron, and four nitrogen atoms at

each corner. Each nitrogen atom is shared among three tetrahedra so that each silicon atom has four nitrogen atoms as nearest neighbors, and each nitrogen atom has three silicon atoms as nearest neighbors [Ruddlesden and Popper, 1958]. The structures also can be regarded as puckered eight-membered rings of alternating silicon and nitrogen atoms. Basal planes are formed by the joining of six of these rings forming a larger central void encapsulated by six silicon atoms. Stacking of the basal planes forms the structure of β -phase, as shown in Figure 2.1. The large void between the hexagonal arrangement of atoms is continuous through the β -phase lattice forming a c -axis channel that has an equivalent cylindrical radius of 1.5\AA . Theoretically, it may enable large atoms to diffuse readily through the lattice [Thompson and Pratt, 1967].

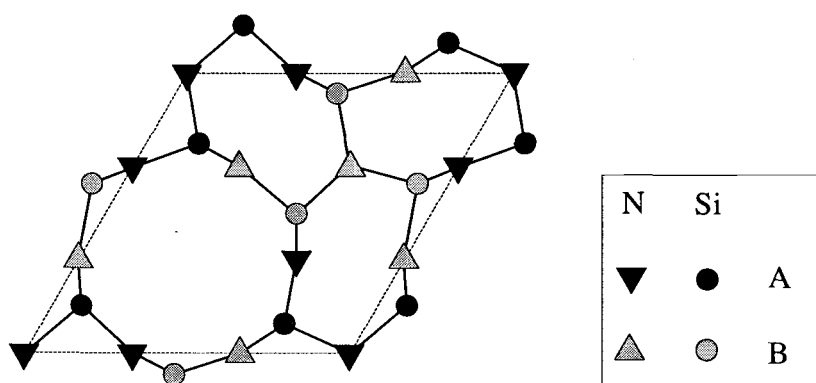


Figure 2.1 β - Si_3N_4 unit cell: the structure of β - Si_3N_4 can be described as a stacking of Si-N layers in ... ABAB ... sequence.

The structure of α - Si_3N_4 was determined to be closely related to that of β - Si_3N_4 , consisting of alternate basal layers of β - Si_3N_4 and its mirror image, as shown in Figure 2.2. Because of the operation of a c glide plane, the continuous voids are interrupted to form a series of large interstices, which are roughly spherical in shape with a radius of approximately 1.5\AA , linked by tunnels having a radius of 0.7\AA . Consequently, large foreign atoms or molecules could be trapped within the lattice while small ones, such as oxygen, will be able to diffuse within the lattice [Thompson and Pratt, 1967].

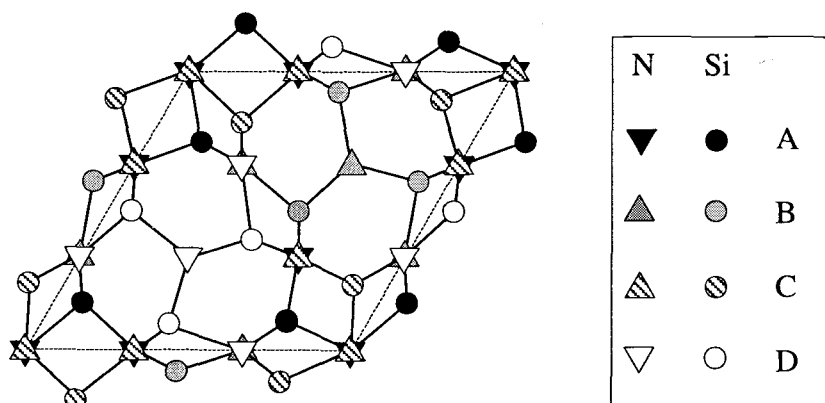


Figure 2.2 α - Si_3N_4 unit cell: the structure of α - Si_3N_4 can be described as a stacking of Si-N layers in ... ABCDABCD ... sequence.

The α to β transformation of silicon nitride is commonly observed during the sintering process, at temperature exceeding 1500°C . It has been suggested that the transformation is a reconstructive transformation involving breaking and reforming

of six Si-N bonds in each unit cell, with a change in the position of one nitrogen and a small displacement of neighboring atoms [Messier, *et al.*, 1978; Thompson and Pratt, 1967]. The α to β transformation process apparently can occur only in the presence of a liquid phase, which is believed to lower the transformation activation energy [Messier, *et al.*, 1978; Suematsu, *et al.*, 1997]. The reverse β to α transformation has never been observed experimentally, but it has been expected to be too slow to be detected [Jennings, 1983; Riley, 2000].

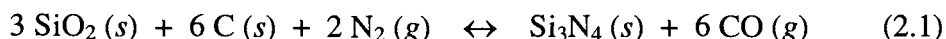
2.2 COMMERCIAL TECHNIQUES FOR MASS-PRODUCING SILICON NITRIDE POWDER

Silicon nitride is not found in nature, but can be synthesized by a number of different techniques. For industrial production of silicon nitride powder, silicon, silica and silicon tetrachloride are the three commonly used starting materials because they are available in high purity on an economic basis or can be easily purified.

There are three typical methods which have already been used for producing silicon nitride on a commercial scale [Yamada, 1993]. Their final products are different in quality as well as the production cost.

2.2.1 Carbothermal Reduction and Nitridation of Silica

In the presence of carbon and nitrogen, fine silica powder reacts according to the overall equation [Segal, 1985]:



Fine α -silicon nitride powder can be produced directly by using very fine silica. The reaction is usually performed at temperature in the range of 1200-1450°C, depending on the reactivity of raw materials. Since an excess amount of carbon is required for full transformation of silica to silicon nitride, some free carbon can remain in the nitrated powder. By annealing this powder in air, the remaining carbon can be partially oxidized, but so is the silicon nitride. Consequently, the product powder produced by this method often suffers from purity problem associated with residual carbon and oxygen content. The content of α -silicon nitride obtained from this process is at most 88%.

2.2.2 Liquid Phase Reactions/Imide Process

This process could be described as a two-step process. The first step is the liquid phase reaction between silicon tetrachloride and ammonia at room temperature, as follows:



In principle, the liquid phase reaction of silicon tetrachloride with ammonia can be performed in three different ways: (a) liquid SiCl_4 with liquid NH_3 , (b) gaseous SiCl_4 with liquid NH_3 and (c) liquid SiCl_4 and gaseous NH_3 . In all three cases, fine silicon diimide and ammonium chloride particles are formed. The ammonium chloride can be removed by series of washing with liquid ammonia.

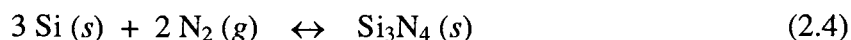
After removing the ammonium chloride, the silicon diimide is given a polymerization via heat treatment in nitrogen or ammonia [Yamada, 1993]. The polymer is then pyrolyzed at 1100°C in nitrogen to produce amorphous silicon nitride. Subsequent heat treatment at temperature higher than 1430°C initiates conversion of amorphous product into α -crystalline form, which may be represented by an overall stoichiometric equation as



Since reactants are liquids or gases, very pure silicon nitride with a high content of α -form (> 95%) can be prepared [Ault and Yeckley, 1994]. However, the production cost is high due to complexities of the process and extensive efforts to purify the intermediate silicon diimide.

2.2.3 Direct Nitridation of Silicon

The direct nitridation of silicon is one of the most commonly used process in the production of α -silicon nitride [Cambier and Leriche, 1990]. The process is based on contacting elemental silicon with nitrogen at temperature in the range of 1200-1400°C. Although the true mechanism is unknown, the overall reaction of this process can be represented by the following equation:



The reaction is highly exothermic. Extreme care must be taken to prevent temperature run-away, which results in melting of silicon particles. β - Si_3N_4 is found in greater abundance when the reaction is carried out at temperature near the melting point of silicon, 1410°C [Jennings, 1983].

The direct nitridation process is more complicated than Equation (2.4) implies. Several models have been proposed to describe the nitridation of silicon

[Atkinson, *et al.*, 1973; Jennings, 1983; Pigeon and Varma, 1993; Varma, *et al.*, 1991], but there is no general agreement regarding the mechanism of the nitridation.

The production cost for this process is low, compared to other processes mentioned earlier, since the process is one simple step using inexpensive reactants. This process is an inexpensive option for the applications in which metal impurities, originating from silicon, contained in the product silicon nitride can be tolerated. It has been reported that the commercial product obtained by this method normally contains 92% α -form [Segal, 1985].

2.3 FACTORS INFLUENCING THE DIRECT NITRIDATION OF SILICON

There are many reaction variables involved in the direct nitridation process, such as reaction time, temperature, heating rate, particle characteristics, and reactant gas composition. Their influences on the microstructure, phase development, and reaction rates have been extensively examined by a number of different researchers [Atkinson and Moulson, 1976; Jennings, 1983]. Determining the dependence of each process variable is complicated by the mutual interactions among them. In this work, the effects of oxide layer naturally covering the surface of silicon raw materials, the effects of hydrogen experimentally added to nitrogen and the effects of metals added to silicon on the direct nitridation of silicon are individually discussed.

The effects of reaction temperature are also studied together with the effects of the factors mentioned above.

2.3.1 Effects of Native Oxide Layer Covering Silicon Surface

Oxygen is a major contaminant in silicon powder. Majority of oxygen is naturally localized on the surface of silicon particles as a thin layer of silica (SiO_2), which is usually referred to as “native oxide layer” or “native silica”. Although it varies for various samples, the thickness of the native oxide layer is typically 1-3 nm [Atkinson and Moulson, 1976].

Roles of the oxide layer have been discussed widely in the literature. It is generally accepted that the native silica layer has a retarding effect on the nitridation of silicon [Dervišbegovic and Riley, 1981; Rahaman and Moulson, 1984; Shaw, 1982]. High oxygen silicon powders usually achieve a lower conversion than low oxygen silicon powders [Pompe, *et al.*, 1985].

It has been found that SiO_2 can also form at high temperature during the nitridation from oxygen in the nitriding atmosphere, which inhibits the subsequent nitridation [Lin, 1975; Messier and Wong, 1973]. Silicon powder that is deliberately partially oxidized in air at 1000°C for 2 hours can not be nitrided [Atkinson and Moulson, 1976; Moulson, 1979]. However, it should be noted that SiO_2 formed during the reaction seems to have different morphology than the SiO_2 originally

residing on silicon particles. The native oxide film on the surface of silicon is amorphous SiO_2 [Riley, 2000]. On the contrary, strong α -cristobalite (crystalline form of SiO_2) peaks are observed from the X-ray diffraction patterns obtained from the surface of silicon specimen nitrided in the atmosphere containing oxygen at high temperature [Messier and Wong, 1973].

Hence, it was suggested that the removal or disruption of the native oxide layer from the surface of silicon particles would enhance the formation of silicon nitride [Dervišbegovic and Riley, 1981; Lin, 1975; Rahaman and Moulson, 1984; Shaw, 1982]. The native oxide film on the surface of silicon particles may be removed at high temperature, in a stream of dry hydrogen or in a stream of inert gas at low oxygen potential [Atkinson and Moulson, 1976; Shaw, 1982]. An addition of hydrogen to the nitriding gas mixture was also proved to be more effective for the removal of the surface oxide layer compared to pure nitrogen [Lin, 1975]. However, it was proposed that a short pretreatment of silicon powder under reducing conditions was more effective than the addition of a small proportion of hydrogen to the nitriding gas [Dervišbegovic and Riley, 1981; Rahaman and Moulson, 1984].

The native oxide is often mentioned as part of the nitridation mechanism. Many researchers have believed that SiO vapor, generated from the reaction between silicon and the native silica or from the reaction between the native silica and hydrogen, has a major role in the nitridation mechanism [Barsoum, *et al.*, 1991; Campos-Loriz and Riley, 1978; Lindley, *et al.*, 1979; Moulson, 1979; Pigeon, *et al.*,

1993]. However, no consensus has been reached regarding the role (if any) of the silicon monoxide in the nitridation reaction.

2.3.2 Effects of Hydrogen in the Reactant Gas Mixture

One of the key factors that significantly affect the extent of nitridation reaction is the presence of hydrogen in the reactant gas mixture. Although exact roles of hydrogen are unclear, an addition of hydrogen to the nitriding atmosphere has long been known to increase the overall rate of the nitridation of silicon, especially at lower temperatures [Barsoum, *et al.*, 1991; Parr, *et al.*, 1961; Popper and Ruddlesden, 1961; Rahaman and Moulson, 1984]. The nitridation with pure nitrogen usually requires a very long reaction time (more than 10 hours), and the conversion is low. By adding hydrogen to nitrogen, a high level of conversion is usually achieved within a short period of reaction time [Dervišbegovic and Riley, 1981; Rahaman and Moulson, 1984].

It was reported that the induction period in the nitridation was eliminated and the continuing reaction rate was faster when hydrogen was added to nitrogen [Dervišbegovic and Riley, 1981]. It was also reported that the nitridation rate increased with hydrogen concentration (in the range of 5-10%), but high a hydrogen content (50%) resulted in a slow reaction rate due to the nitrogen diluent effect [Dervišbegovic and Riley, 1981; Maalmi and Varma, 1996]. However, since a

change in the concentration of one component in a binary mixture inevitably causes a change in the concentration of another component, Jovanovic *et al.* [1994] fixed the nitrogen concentration and used argon as an inert balance while varying the concentration of hydrogen. It was found that an increase in the hydrogen concentration (up to 40%) slowed down the nitridation during the initial stage of reaction, but the final conversions were approximately the same. Furthermore, the induction period did not change with an increase in the hydrogen concentration [Jovanovic, 1994].

Hydrogen affects the morphology of silicon nitride product as well. It was observed that an addition of hydrogen to nitrogen aided the formation of finer and more uniform microstructures, as compared to pure nitrogen [Rahaman and Moulson, 1984]. It was also reported that an addition of hydrogen resulted in higher α/β ratios [Shaw, 1982]. Jennings [1983] proposed that hydrogen discouraged the formation of atomic nitrogen, and hence slowed down nitrogen diffusion through the silicon nitride matrix to react with silicon underneath, which was believed to have resulted in β -silicon nitride.

2.3.3 Effects of Metals in Silicon

It has been known that transition metals contained in silicon as impurities regulate the kinetics of its nitridation as well as the α/β -phase formation [Boyer and

Moulson, 1978; Cofer and Lewis, 1994; Hüttinger and Pieschnick, 1994; Jennings, 1983; Lin, 1977; Lin, 1975; Mitomo, 1977; Moulson, 1979; Mukerji and Biswas, 1981; Pigeon, *et al.*, 1993; Sanyal, *et al.*, 1991]. Many researchers have studied the effects of several transition metals on the nitridation of silicon by intentionally adding metals into silicon before the nitridation. Aluminum, titanium, hafnium, zirconium and chromium are known as metals that accelerate the growth of β -silicon nitride [Cofer and Lewis, 1994; Lin, 1977; Mitomo, 1977; Mukerji and Biswas, 1981; Pigeon, *et al.*, 1993]. Calcium is known to promote the development of α -silicon nitride [Pigeon, *et al.*, 1993]. Copper is recently studied for the aid of silicon nitride production [Deckwerth and Rüssel, 1994], though the process presented in the literature is not the direct nitridation and its catalytic effect on the α -/ β -phase formation has not been dealt with. Iron is the metal that has been studied most frequently, since it is the most common metal impurity in commercially available silicon powders. However, the effects of iron on the α -/ β -silicon nitride formation, reported in the literature, are inconsistent. It has been suggested that iron appears to inhibit the α -silicon nitride formation while favors the growth of β -silicon nitride as the iron-rich region forms a liquid below 1350°C [Campos-Loriz and Riley, 1978; Mukerji and Biswas, 1981]. It has also been claimed that iron promotes the formation of α -silicon nitride [Mitomo, 1977]. On the other hand, based on the reports by Boyer and Moulson [1978], iron devitrifies the surface silica by reducing its adhesion to the underlying silicon and consequently enhances the formation of both α - and β -silicon nitride.

The inconclusive results of previous research seem to have resulted from the fact that many factors are involved in the nitridation process and that the work has been conducted under different reaction conditions depending on researchers. It is thus suggested that the results be compared systematically based on the nitridation under the same reaction conditions. By studying the effects of various transition metals on the nitridation of silicon, a higher content of α -silicon nitride could be achieved by adding a small amount of metals in the raw material silicon before its nitridation, and this could enhance the formation of α -phase or suppress the formation of β -phase. In this work, the effect of yttrium is also studied, since yttrium is often added as yttria (Y_2O_3) during the process of sintering silicon nitride, while no result regarding the catalytic effect of yttrium or yttria on the nitridation of silicon have been reported.

2.3.4 Effects of Liquid Phases Formation

The liquid phase is often mentioned to describe the nitridation mechanisms. It is considered to result from molten alloys of silicon and metal impurities and believed to affect the nitridation of silicon. Many researchers intentionally added transition metals into silicon and nitrided it at temperature higher than the eutectic point of the metal-silicon binary compound to study the effects of metals on the nitridation of silicon. Then, any enhancement observed is reported as having resulted from the presence of liquid phases formed during the reaction.

Jennings [1983] and Boyer and Moulson [1978] have suggested, by intentionally adding iron into silicon, that the presence of liquid phases provides an easy diffusion path for nitrogen to react with silicon and results in the enhancement of the formation of β -silicon nitride. They have also suggested that the liquid phase prevents the formation of coherent nitride layer, and that this keeps the silicon underneath from vaporizing and reacting with nitrogen gas to form α -silicon nitride.

Mukerji and Biswas [1981] have studied the nitridation of silicon containing titanium and hafnium and supported the mechanism proposed by Boyer and Moulson [1978]. Pigeon *et al.* [1993] have also proposed the enhancement of α -silicon nitride formation by the presence of liquid phase, while suggesting that the enhancement of β -silicon nitride formation is not strictly limited to the presence of liquid phases.

Most of the previous studies have focused on limited choices of metals and narrow ranges of metal contents. In this study, the effects of metals on the silicon nitridation are investigated systematically using a larger number of metal species over wider ranges of contents. Moreover, the involvement of liquid phases in the α -/ β -silicon nitride formation is discussed based on the results from the nitridation of silicon impregnated with calcium, copper, chromium, silver, and tungsten, among which the last two metals have never been tested in the silicon nitridation.

2.4 OBJECTIVES

The objective of this study is to investigate factors that affect the nitridation of silicon in order to further understand and improve the direct nitridation of silicon process. The specific objectives of this research are:

- to investigate the factors that affect the nitridation of silicon, including, in particular, hydrogen and oxygen
- to find a metal that offers the catalytic effect to enhance the α -content in the product from the direct nitridation of silicon, and
- to determine an appropriate range of operating conditions for the direct nitridation process that result in a high overall conversion and high α -content in the product.

3. EXPERIMENTS

3.1 CHARACTERISTICS OF SILICON RAW MATERIAL

It has been reported that the extent of the nitridation of silicon powder depends critically on the particle size [Evans and Chatterji, 1958; Jennings and Richman, 1976]. Higher conversion is usually achieved from smaller particles. Moreover, it has also been found that small particle size yields a high α/β ratio. Although it has been proved that silicon nitride containing almost 100% α -form can be produced from the direct nitridation of very fine silicon powder in a fluidized-bed reactor [Liu and Kimura, 1999], the fluidization of fine silicon powder of a few micro-meters in size is extremely difficult due to its strong cohesivity that firms the bed structure and causes slugging of or channeling in the bed [Geldart and Abrahamsen, 1978]. Such fine silicon powder needs to be mixed with a large amount of fluidization conditioners, such as silicon nitride particles of fluidizable sizes, to overcome the fluidization problem [Liu, 1996; Liu and Kimura, 1999]. The process for the nitridation of fine silicon powder in a fluidize-bed reactor is still under development and further study is needed.

To overcome the above size problem, particles composed of fine silicon grains which are partially sintered into larger porous granules were used in this work. These particles were prepared by Shin-Etsu Chemical Company, Ltd. from silicon

grains of 2 μm in average size, granulated and briefly sintered to become slightly cemented together. For majority of the runs made in this study, granules were sieved and those with size ranging from 295 to 500 μm were used. The specifications of the silicon raw material used are given in Table 3.1.

Table 3.1 Specifications of raw material silicon.

Trace impurities (% by mass)*					BET area** (m^2/g)
Fe	Al	Ca	C	O	
0.08	0.10	0.02	0.02	0.51	1.7-2
source: * Shin-Etsu Chemical Company Ltd.; **Micromeritics ASAP 2000					

3.2 RAW MATERIAL PREPARATION PROCEDURE

For the study of catalytic effects of metals on the silicon nitridation, small amounts of metals were intentionally added to the silicon raw material. Metals used in this work are calcium, copper, chromium, iron, silver, tungsten and yttrium. For preparing samples, silicon granules of about 12 g were first immersed in 40 ml of methanol solutions of metal-nitrate compounds, except tungsten, followed by the natural evaporation of all the methanol at room temperature. HPLC grade (99.9%)

methanol was used for preparing the solutions. The samples were then put in an oven at 110°C for 12 hours to ensure the elimination of all possibly remaining methanol and moisture. The amount of each metal-nitrate compound dissolved in methanol was adjusted so that a desired level of metal impregnation was achieved after the decomposition and reduction of the nitrate compound at high temperature before the silicon-nitridation reaction. In this work, the final contents of each metal were adjusted to be 0.125, 0.45, 1.00 and 2.00 percent by mass, respectively. It was suggested by preliminary runs that nitrate derivatives were removed from samples and each metal compound was converted to corresponding reduced metal under the reducing atmosphere of 90% argon and 10% hydrogen, which was used for the pretreatment of samples prior to the silicon-nitridation. The decrease in sample mass agreed well with the mass of nitrate derivatives associated with the decomposition of each metal-nitrate compound. Tungsten and palladium were added as tungsten chloride and palladium chloride, respectively, following the same procedure as described above.

3.3 EXPERIMENTAL APPARATUS AND EXPERIMENTAL PROCEDURE

3.3.1 Thermogravimetric Analysis

As mentioned earlier, the oxide layer residing on the surface of silicon greatly affects the nitridation. Although it has been reported that the native oxide film can be removed by pretreatment at high temperature, in a stream of dry hydrogen or inert gas at low oxygen potential [Atkinson and Moulson, 1976; Shaw, 1982], the duration of the pretreatment required to remove majority of the oxide layer depends upon nature of raw materials. Thus, thermogravimetric analysis (TGA) was used to preliminarily study the removal of the native oxide layer on the surface of silicon granules used in this work.

A thermal gravimetric analyzer (Omnitherm TGA/1500), capable of detecting a mass change as small as 0.001 mg, is schematically illustrated in Figure 3.1. A sample of solids, about 15 mg, was placed in the platinum basket and heated up to desired temperatures under constant flow of argon ($32.5 \text{ cm}^3/\text{min}$). The sample mass and temperature were recorded at specified intervals after the system was initiated.

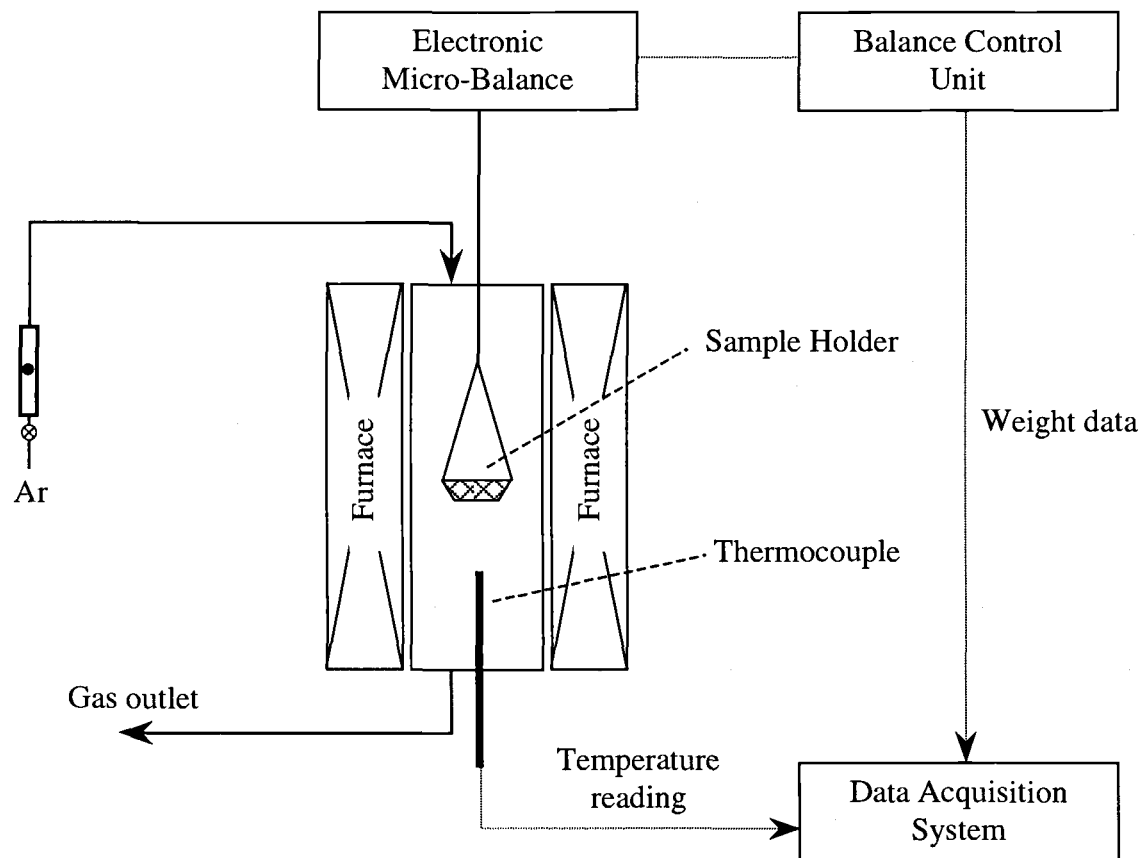


Figure 3.1 Schematic diagram of the thermogravimetric analysis system.

3.3.2 Tubular Flow Reactor

Figure 3.2 illustrates a horizontal tubular flow reactor used for this study.

The reactor is an alumina tube (38.1 mm inside diameter \times 1524 mm long) placed inside a two-heating-zone furnace (Lindberg-54454). The uniform temperature zone is 130 mm long, where the temperature variation is within $\pm 2^\circ\text{C}$.

For each run in the tubular flow reactor, a desired amount of sample granules was put in an alumina tray (25 mm \times 15 mm \times 5 mm deep). Five alumina trays of different samples can be placed next to each other in series in the uniform temperature zone of the reactor. The amount of sample granules was adjusted, based on preliminary runs, so that the thickness of the particle layer in each tray was 2 mm or smaller to avoid any mass and heat transfer effects from intruding in the nitridation, as described in more details in later sections. Samples were then heated to a prescribed temperature, in the range of 1150-1300°C, at a rate of 10°C/min, under the continuous flow of argon. After the system had reached the prescribed temperature, if the pretreatment was desired, a gas mixture containing 90% argon and 10% hydrogen was supplied to the reactor as a pretreatment agent to remove surface oxide on silicon as well as to convert metal nitrates/chloride impregnated into reduced metals. The pretreatment temperature and duration are subject to study in this work.

After pretreatment, the nitridation was initiated by supplying a gas mixture of 90% nitrogen and 10% hydrogen. The flow rate of the reactant gas mixture was

fixed at $92.96 \text{ cm}^3/\text{s}$ (at room temperature), which was known, based on preliminary runs, to be high enough for eliminating the gas-film mass-transfer resistance. A reaction time of 3 hours was selected for majority of the runs in this work, since it was shown that the nitridation of the silicon granules reached a stage of very slow progress in about 3 hours [Jovanovic, *et al.*, 1994; Pavarajarn and Kimura, 2001]. For experiments in which pretreatment temperature was different from the reaction temperature, only argon was fed to the system while the reactor temperature was altered. The heating/cooling rate of the furnace was fixed at $10^\circ\text{C}/\text{min}$. In the programmed temperature operation, the nitridation reaction was carried out at 1300°C for one hour and then at 1390°C for two hours, as suggested elsewhere [Jovanovic, *et al.*, 1994]. It took 9 minutes to raise the reaction temperature, and during this transitional time period the feed of reactant gas was maintained unchanged.

For the study of the effects of hydrogen, the hydrogen feed was shut off after the pretreatment. Only argon was fed to the reactor while the reactor temperature was adjusted to the nitridation temperature. The argon feed was maintained for additional 5 minutes, after the temperature had reached the nitridation temperature, to purge possibly remaining hydrogen out of the system. Then, the nitridation was initiated without hydrogen for certain periods, i.e., 5, 10, 30 and 60 minutes. During these periods, only nitrogen was supplied to the reactor. After the nitridation without

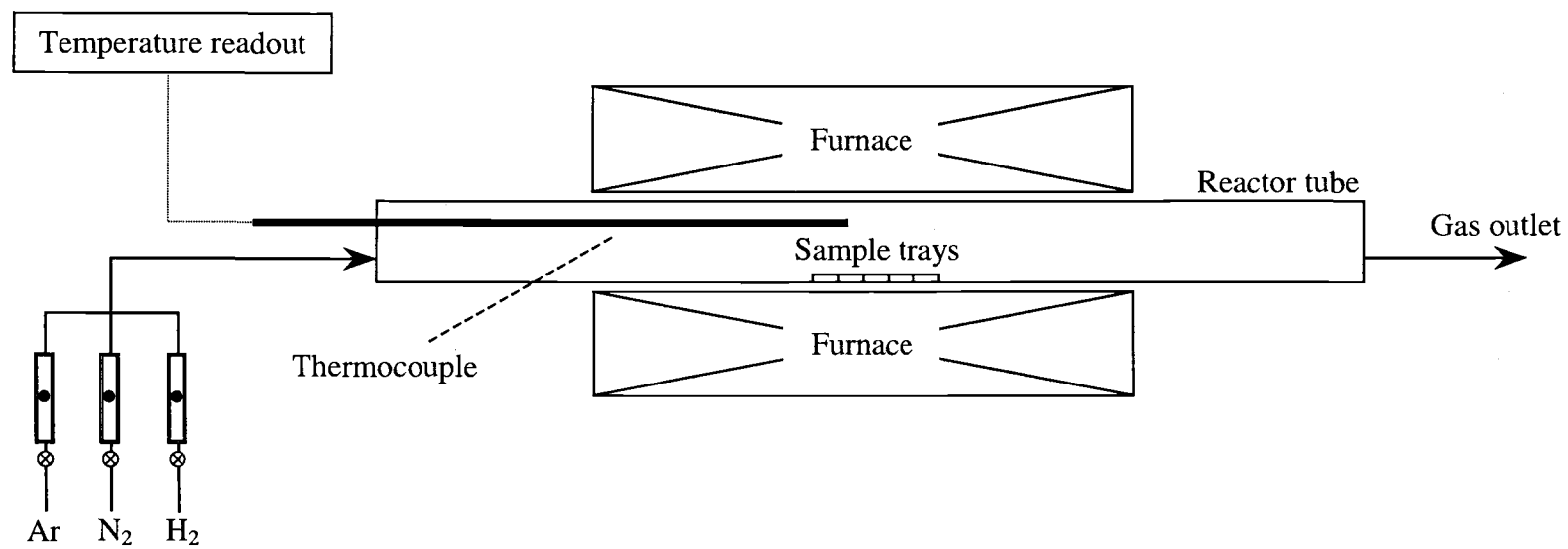


Figure 3.2 Schematic diagram of the tubular flow reactor system.

hydrogen, hydrogen was reintroduced to the system. The flow rate and the content of the reactant gas mixture were the same as for experiments with uninterrupted flow of hydrogen.

3.3.3 Fluidized-Bed Reactor

Figure 3.3 illustrates a schematic diagram of the fluidized-bed system used for this study. An alumina tube (55 mm inside diameter \times 1200 mm long) was used as a fluidized-bed reactor with a perforated alumina disk used as the gas distributor. The reactor was placed inside an alumina furnace-tube (100 mm inside diameter \times 1500 mm long) which was heated in a three-heating-zone furnace (Lindberg-58475). Bed temperature was measured with an R-type thermocouple, shielded in an alumina tube, inserted into the bed to about 3 cm above the distributor.

Silicon granules were pneumatically charged directly into the bed through a mullite tube (12 mm inside diameter). The products were also pneumatically discharged from the fluidizing surface through another mullite tube (9 mm inside diameter) into a sampling flask. The composition of the reactant gas mixture was adjusted with calibrated rotameters. The operating pressure of the system was slightly higher than atmospheric pressure. The pressure drop of the bed and its fluctuations were measured with a pressure transducer. The standard deviation of the

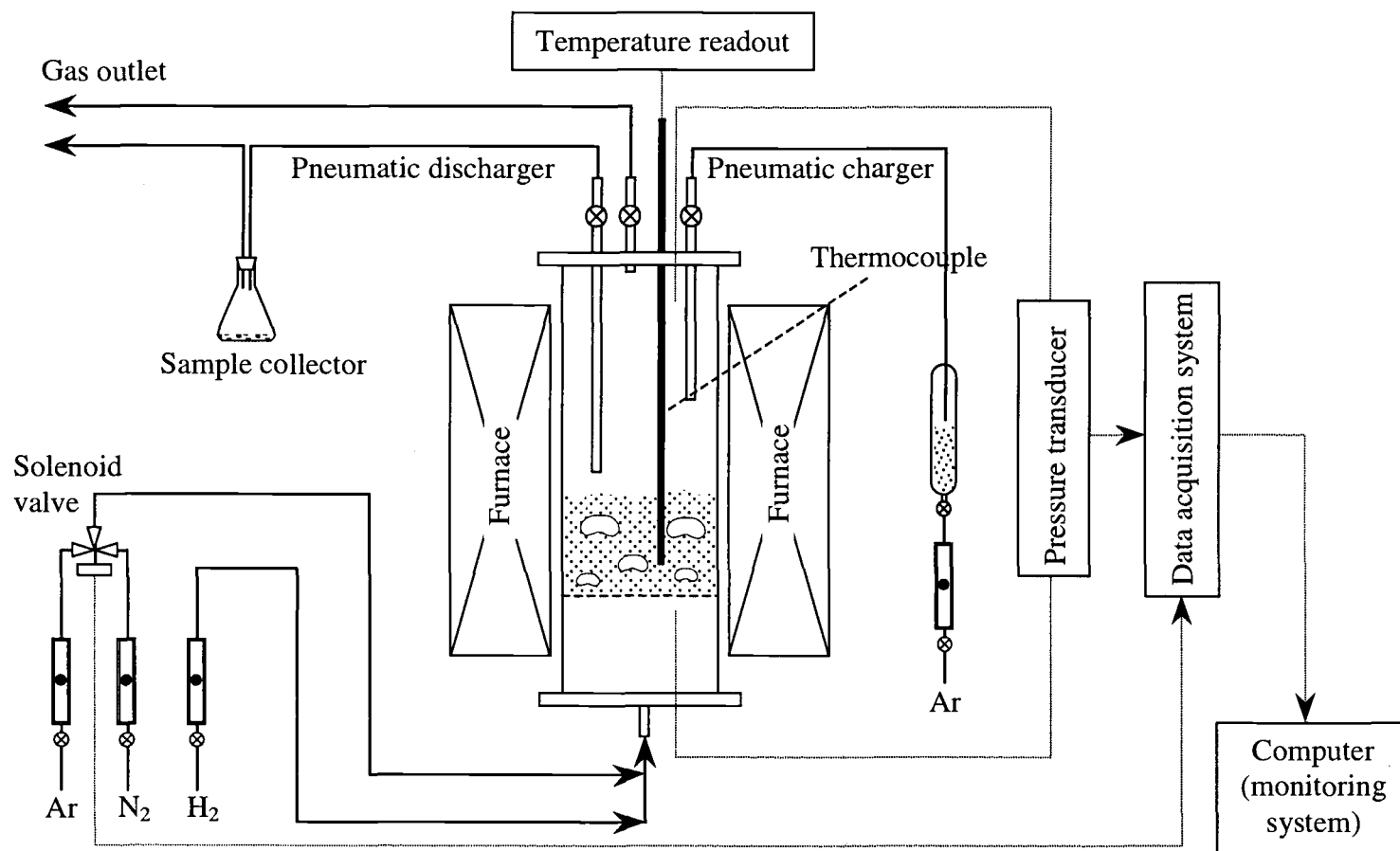


Figure 3.3 Schematic diagram of the fluidized-bed reactor system.

pressure fluctuations was computed at an interval of 10 seconds by a data acquisition system and was used to monitor the fluidization condition of the bed.

The minimum fluidization velocity of the silicon granules was found to be about 8 cm/s at room temperature, as shown in Figure 3.4. The operating gas velocity was chosen to be 25 cm/s, which is well above the minimum fluidization velocity of the silicon granules.

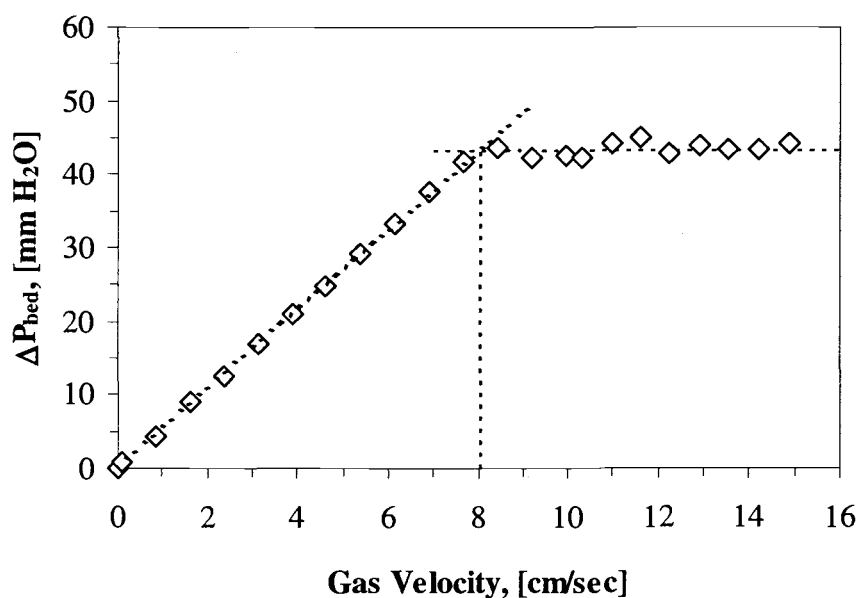


Figure 3.4 Minimum fluidization velocity of silicon granules in 90% nitrogen – 10% hydrogen at room temperature.

The empty bed was first heated to a prescribed operating temperature, in the range of 1200-1300°C, at a rate of 10°C/min, under the continuous flow of argon.

After the reactor temperature reached the set point, the flow of argon was adjusted to the operating velocity. Then, silicon granules about 100 g, which were first fluidized for 5 minutes by argon in a feeding container to decrease the oxygen content in the voids, were pneumatically charged into the bed using argon as a carrier gas. Since the cold silicon granules were suddenly supplied to the bed, the bed temperature dropped about 300-400°C below the set-point temperature. After the bed temperature had returned to the set-point (in about 10 minutes), the argon stream was switched to a mixture of 90% argon and 10% hydrogen, for the pretreatment, while the gas velocity was kept unchanged.

The nitridation was initiated by actuating a solenoid valve that switched argon to nitrogen without changing the flow rate. It should be noted that hydrogen was fed separately to the reactor and unaffected by an action of the solenoid. Thus, hydrogen was maintained at constant concentration at all time. As the bed temperature started to rise due to the heat released by the nitridation, the solenoid valve was deactivated, switching nitrogen back to argon to quench the reactor. The DC signal used to actuate the valve also triggered a timer in the data acquisition system providing the cumulative reaction and quenching times with a resolution of 1 second. At the same time, the set point on the furnace controller was lowered to adjust the energy input to the furnace, which provided a stable bed operating temperature without frequent quenching. This on/off procedure was used during the initial stage of nitridation, in particular, to keep the bed temperature within $\pm 3^{\circ}\text{C}$ of the set point during most of the reaction time.

At various reaction times, samples of reacted solids were withdrawn from the reactor through the pneumatic discharge line without disturbing the reaction conditions in the bed. Each sampling mass was about 1 g and the total mass of sample solids withdrawn throughout the run was kept small so that the fluidization condition was not altered significantly.

3.4 ANALYSIS OF PRODUCTS

The silicon/ α -, β -silicon nitride phase composition of products from the reaction were determined by powder X-ray diffraction (XRD) using Norelco-12045 diffractometer with CuK_α radiation. Each sample was scanned in the range of $2\theta = 26\text{--}38^\circ$ with a step size of $2\theta = 0.01^\circ$. Peak areas, background noise, and separation of overlapped peaks were determined by fitting the diffraction patterns using the Pseudo-Voight function [McCusker, *et al.*, 1999] in the Xfit-Koalariet software package from the Collaborative Computational Project number 14 (CCP14). Then, the mass fraction of each phase as well as the conversion from silicon to each α - and β -silicon nitride were calculated from the method proposed by Jovanovic and Kimura [1994], using the integrated intensity of (111) peak of Si, the integrated intensities of (102), (210) and (201) peaks of α -silicon nitride and those of (101) and (210) peaks of β -silicon nitride, as follows:

$$\frac{I_{\alpha}(102) + I_{\alpha}(210)}{I_{\beta}(101) + I_{\beta}(210)} = K_{\alpha/\beta} \frac{W_{\alpha}}{W_{\beta}} \quad (3.1)$$

$$\frac{I_{Si}(111)}{I_{\alpha}(201)} = K_{Si/\alpha} \frac{W_{Si}}{W_{\alpha}} \quad (3.2)$$

and

$$W_{\alpha} + W_{\beta} + W_{Si} = 1 \quad (3.3)$$

where $I_{\delta}(hkl)$ signifies the integrated intensity of the hkl reflection of phase δ , and W_{δ} is the mass fraction of corresponding phase δ in a mixture. The linear regression calibration constants, $K_{\alpha/\beta}$ and $K_{Si/\alpha}$ were evaluated to be 0.647 and 5.53 respectively [Jovanovic, *et al.*, 1994].

From measured mass composition, the overall conversion of silicon, X , was calculated as:

$$X = \frac{1 - W_{Si}}{1 + \left(\frac{M_{SN}}{3M_{Si}} - 1 \right) W_{Si}} \quad (3.4)$$

where M_{SN} and M_{Si} are the molar masses of silicon nitride and silicon, and

$(M_{SN} / 3M_{Si}) - 1 = 0.665$ is a converting factor.

Thus, the mass fractional yields of α -silicon nitride, X_{α} , and β -silicon nitride, X_{β} , were calculated as:

$$X_{\alpha} = \frac{1 - W_{Si}}{1 + 0.665W_{Si}} \left(\frac{W_{\alpha}}{W_{\alpha} + W_{\beta}} \right) \quad (3.5)$$

and

$$X_{\beta} = \frac{1 - W_{Si}}{1 + 0.665W_{Si}} \left(\frac{W_{\beta}}{W_{\alpha} + W_{\beta}} \right) \quad (3.6)$$

The overall conversion of silicon, X , is therefore the sum of the mass fractional yields of α - and β -silicon nitride:

$$X = X_{\alpha} + X_{\beta} \quad (3.7)$$

An example of X-ray diffraction patterns is shown in Figure 3.5. This XRD scan is the result from nitridation of silicon impregnated with 2.0% iron in the tubular flow reactor at 1300°C for 1 hour using 90% nitrogen and 10% hydrogen.

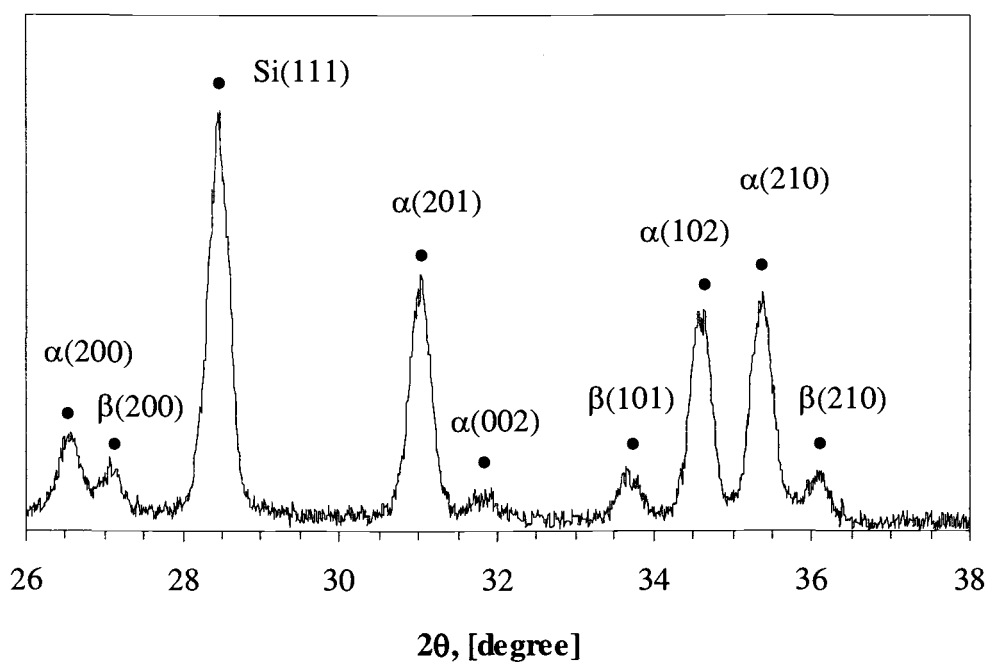


Figure 3.5 An example of X-ray diffraction scan of product.

4. EXPERIMENTAL RESULTS AND DISCUSSION

4.1 PRELIMINARY EXPERIMENTS

4.1.1 Preliminary Results from Thermogravimetric Analysis

A thermogravimetric analyzer was used for continuous observation of sample mass change under a stream of argon at high temperature. It should be noted that hydrogen was not used in these preliminary experiments because hydrogen would severely damage the heating elements of the furnace.

The thermogram of an empty sample holder shows a mass increase during the heating-up process, under flow of argon. However, no mass change was observed after the furnace temperature had stabilized (Figure 4.1). Since the flow rate of argon at the inlet (measured at room temperature) was fixed, the velocity of gas that passed through the sample holder inside the furnace increased with temperature, resulting in an increase in mass detected by the micro-balance. It should be noted that, the mass of the sample holder after the system had been cooled down to room temperature was the same as its mass before heating up.

For the experiment using silicon granules, the system and the sample were purged with argon overnight to eliminate air remaining in the system and in the pores of silicon granules. During the process of heating up, an increase in mass, at roughly

the same rate as the empty sample holder, was observed. However, the mass of the solid samples started decreasing when the temperature was roughly 1250°C. A significant mass decrease was observed for about 50 minutes after the system had reached 1300°C. After that, the sample mass remained roughly constant. Total mass loss was approximately 4% of the original sample mass.

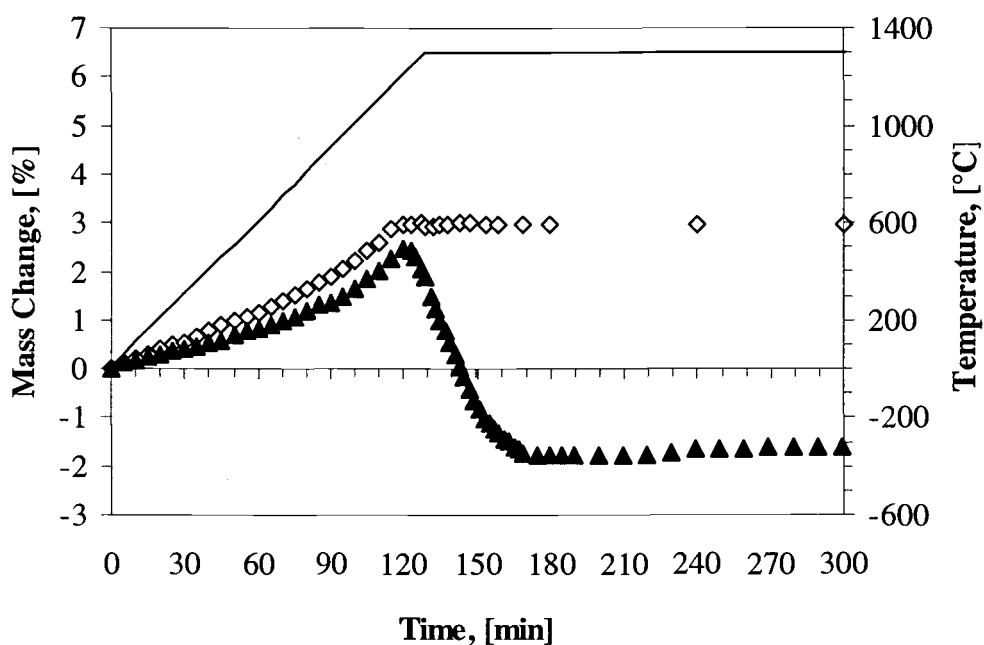


Figure 4.1 Change in sample mass observed in TGA: (◇) – empty sample holder; (▲) – silicon particles; (—) – temperature.

The result from TGA suggests that majority of the oxide layer can be removed in about 1 hour in the flow of argon at 1300°C. However, the removal of the oxide layer starts gradually when the temperature is higher than 1200°C.

4.1.2 Effects of Operating Gas Flow Rate in the Tubular Flow Reactor

Before the experiments were conducted, proper operating conditions were determined, including the flow rate of the reactant gas mixture. In the tubular flow reactor, the operating gas flow rate has to be high enough to minimize the film mass transfer resistance. Figure 4.2 shows the effect of the film mass transfer resistance in the tubular flow reactor on the nitridation of bare silicon granules (silicon granules with no metal impregnated) at 1200°C. All samples were pretreated for 1 hour at the same temperature as the reaction temperature and the nitridation was conducted for 3 hours.

It is clear that the flow rate lower than 35 cm³/sec is too low to eliminate the film mass transfer resistance. The reaction barely occurred at the flow rate of 33.35 cm³/sec. On the other hand, the effect of the mass transfer resistance is minimized at a flow rate higher than 66.5 cm³/sec. Almost the same conversion was obtained at 66.5 and 92.7 cm³/sec. Therefore, on the basis of these measurements, the operating gas flow rate was chosen to be 92.7 cm³/sec, which had well demonstrated to minimize the effect of the film mass transfer resistance.

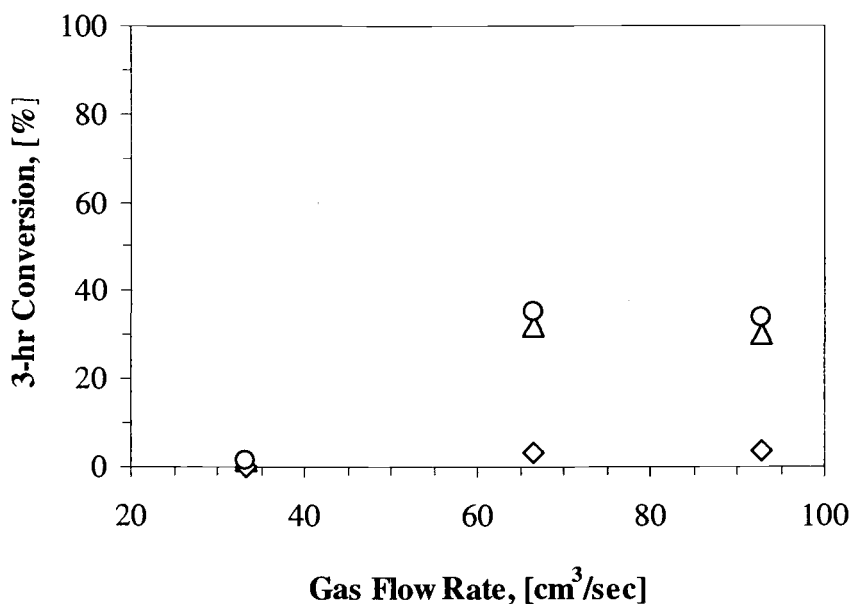


Figure 4.2 Effects of gas flow rate on the nitridation of bare silicon granules at 1200°C: (Δ) – conversion of silicon into α -Si₃N₄; (◇) – conversion of silicon into β -Si₃N₄; (○) – overall conversion of silicon.

4.1.3 Effects of Positions in the Tubular Flow Reactor

The uniform temperature zone in the tubular flow reactor is 130 mm long, which can hold five alumina trays of samples (25 mm × 15 mm × 5 mm deep) placed next to each other in series. Before using five trays at the same time, it has to be verified that the reaction conditions for all the trays are the same.

Two experiments, at two different temperatures, were conducted to verify the effect of position in the reactor. The 3-hour nitridation was done at 1300°C by using bare silicon granules and at 1200°C by using silicon granules impregnated with 0.1%

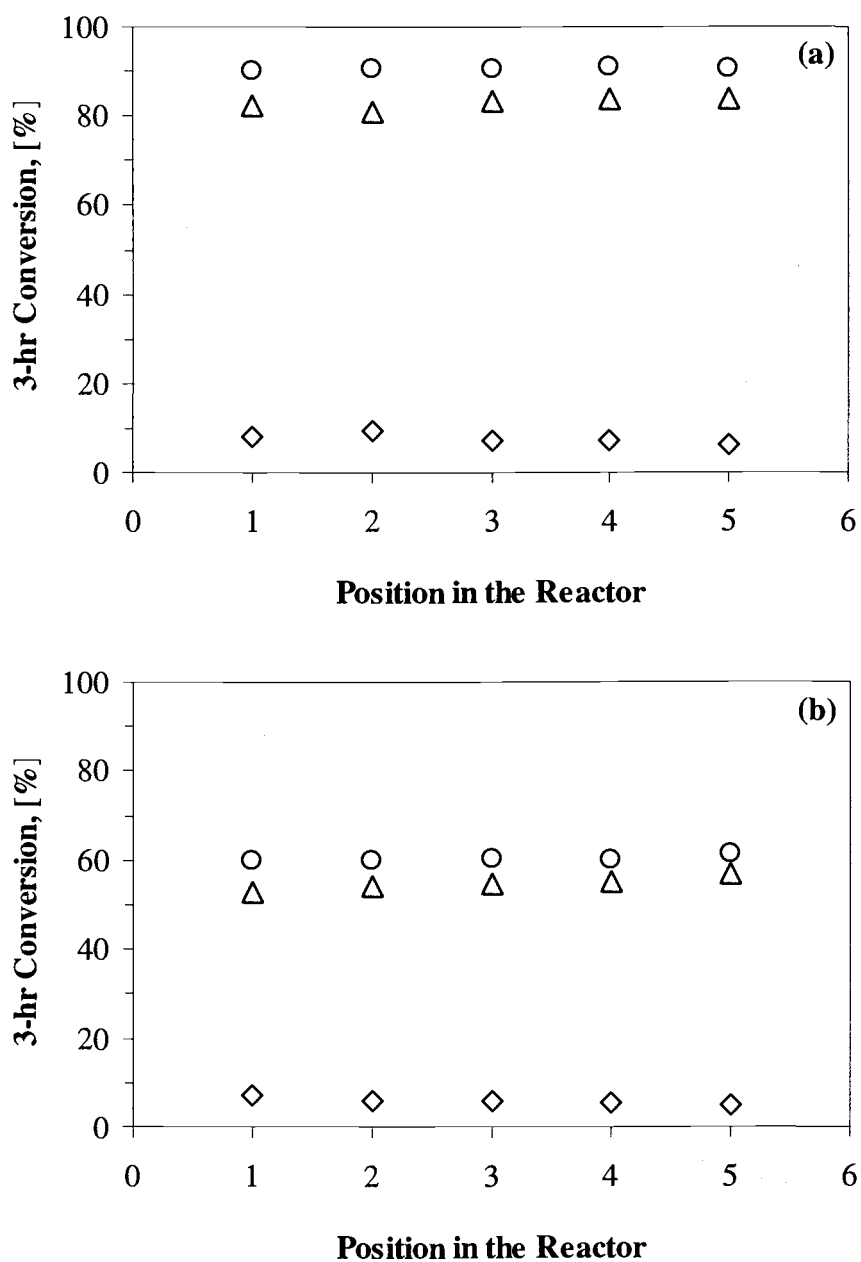


Figure 4.3 Effects of position in the tubular flow reactor: (O) – overall conversion; (Δ) – conversion of silicon into α - Si_3N_4 ; (\Diamond) – conversion of silicon into β - Si_3N_4 .
 (a) Nitridation of bare silicon at 1300°C.
 (b) Nitridation of silicon impregnated with 0.1% copper, at 1200°C.

copper. In both the runs, samples were pretreated with 90% argon and 10% hydrogen for 1 hour at the same temperature as the nitridation temperature, in order to remove the native oxide layer on the surface of silicon. It was found that there was no difference depending on the position. The 3-hour conversions obtained from 5 trays containing the same samples were not different, for both the experiments (Figure 4.3).

4.1.4 Heat Transfer Effects in the Tubular Flow Reactor

The nitridation of silicon is a highly exothermic reaction. Unlike the nitridation in the fluidized-bed reactor, in which the temperature can be controlled by switching from nitrogen to argon to quench the reaction mixture, the nitridation in the tubular flow reactor has higher chance to have a problem associated with heat generated from the reaction. In a large batch of silicon nitridation, in which heat transfer is limited, high heat released from the reaction can induce the temperature to run away, causing melting of the silicon granules. However, with a small sample size, the heat transfer effect can be minimized.

To test the heat transfer effect in the tubular flow reactor, various amounts of silicon granules were used in the nitridation. If heat transfer from the sample bed to the bulk gas stream was limited, heat would accumulate in the sample bed, resulting in the dramatic increase in bed-temperature and consequently the conversion of the

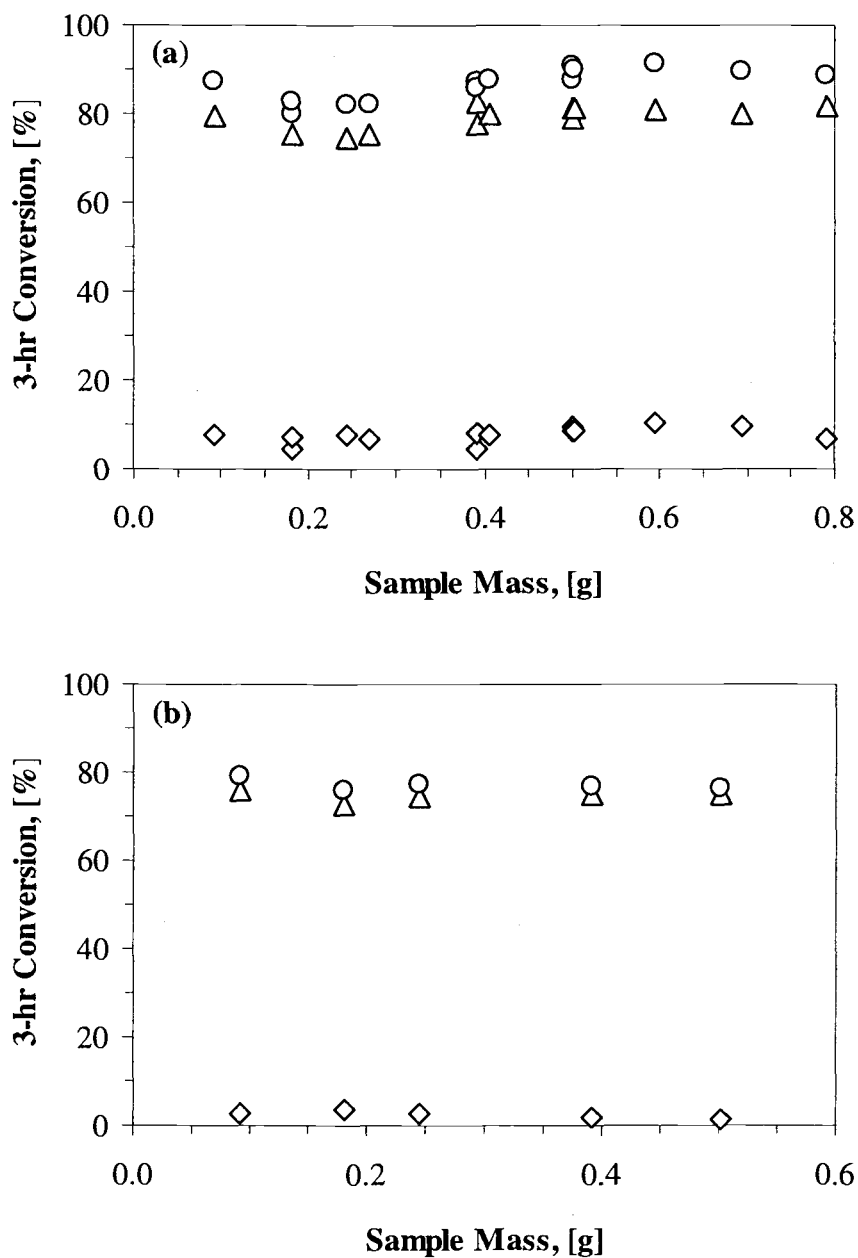


Figure 4.4 Effects of sample mass used for the nitridation at 1300°C in the tubular flow reactor: (O) – overall conversion; (Δ) – conversion of silicon into α - Si_3N_4 ; (\diamond) – conversion of silicon into β - Si_3N_4 .
 (a) Nitridation of bare silicon.
 (b) Nitridation of silicon impregnated with 1.0% yttrium.

reaction. However, it was found that the conversions obtained from the 3-hour nitridations of different amounts of samples, ranging from 0.09 to 0.79 g, were not significantly different at 1300°C (Figure 4.4). The conversion achieved from the greatest sample mass (0.79 g), where the thickness of the sample layer in the sample tray was 5 mm, was roughly the same as the conversion achieved from the smallest sample mass (0.09 g), where only one layer of silicon granules were loosely placed into the sample tray. These results indicate that the heat transfer effect in the range of sample mass used was not significant. Heat generated from the reaction in the bed of particles was transferred to the gas stream effectively.

4.1.5 Consistency and Reproducibility of Results from the Tubular Flow Reactor

Bare silicon granules were put in the most upstream sample tray for every experiment as a control sample. The conversion of the control sample in each run was recorded to observe the consistency of the results. As shown in Figure 4.5, the results among experiments under the same operating conditions were generally consistent. The samples in all runs were pretreated for 1 hour at the same temperature as the nitridation temperature. The nitridation was observed for 3 hours.

The reproducibility for sample preparations was also confirmed. The samples impregnated from different batches yielded roughly the same conversion, as

illustrated in Figure 4.6. The nitridation was done at 1300°C for 3 hours, after 1-hour pretreatment at the same temperature.

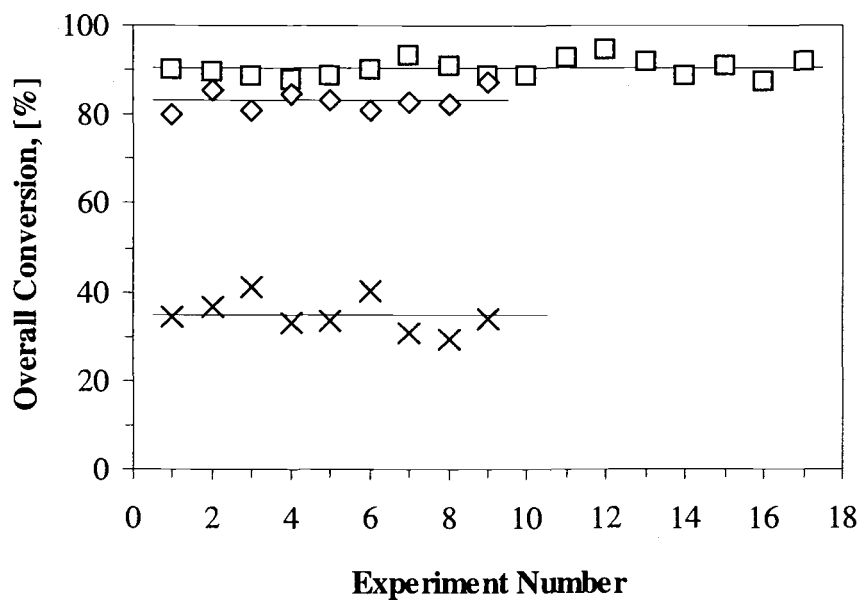


Figure 4.5 Overall conversions of control samples: (X) – nitridation at 1200°C; (◇) – nitridation at 1250°C; (□) – nitridation at 1300°C; (—) – average values.

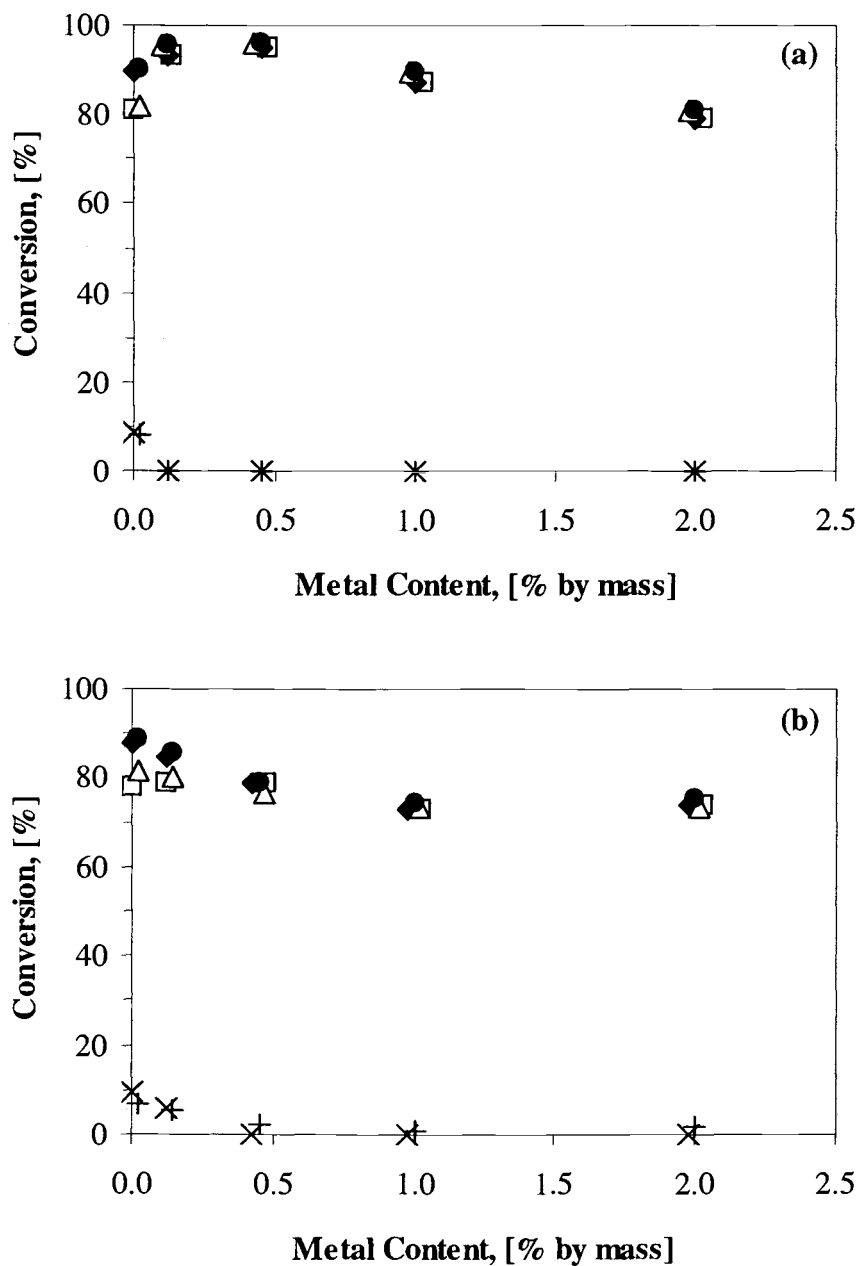


Figure 4.6 Conversions observed from different sample-preparation batches: (□) and (Δ) – conversion of silicon into α - Si_3N_4 , from different batches; (X) and (+) – conversion of silicon into β - Si_3N_4 , from different batches; (◆) and (●) – overall conversion, from different batches. Noted that some data points are intentionally shifted in X-direction for clarity.

(a) Nitridation of silicon impregnated with calcium.

(b) Nitridation of silicon impregnated with yttrium.

4.1.6 Effects of Particles Size

As mentioned earlier, the impregnation of metal into silicon granules was done by immersing silicon granules in the solution of metal-nitrate or metal-chloride in methanol. Although an ultrasonic bath was used to assist the transport of the impregnating solution into pores of particles, it was unsure whether the solution could reach the silicon grains at the center of granules. Direct measurement of the metal content on the grains inside granules is quite difficult because the grain size is very small. Instead, the nitridation of silicon granules (particle size of 295-500 μm) impregnated with various kinds of metals was compared to the nitridation of silicon powder (average size 7.8 μm) prepared by the same sample preparation procedures. Yttrium, calcium, copper, and iron were used. The content of each metal was 0.125% by mass. The reaction was carried out at 1300°C for 3 hour after 1-hour pretreatment at the same temperature. The results are shown in Figure 4.7 and 4.8.

It has been reported that the overall conversion as well as α/β ratio from silicon with smaller grain-size is greater than those from bigger grain-size samples [Campos-Loriz and Riley, 1978]. Thus, the direct comparison of the conversions obtained from silicon granules and powder may not give the useful information, since the granules which have more grain boundaries than powder would have less surface to react with nitrogen. Instead, the overall conversion of granules having different sizes were compared. As shown in Figure 4.7 and 4.8, when metal is added to silicon, a deviation in the conversion from bare silicon is observed. This deviation

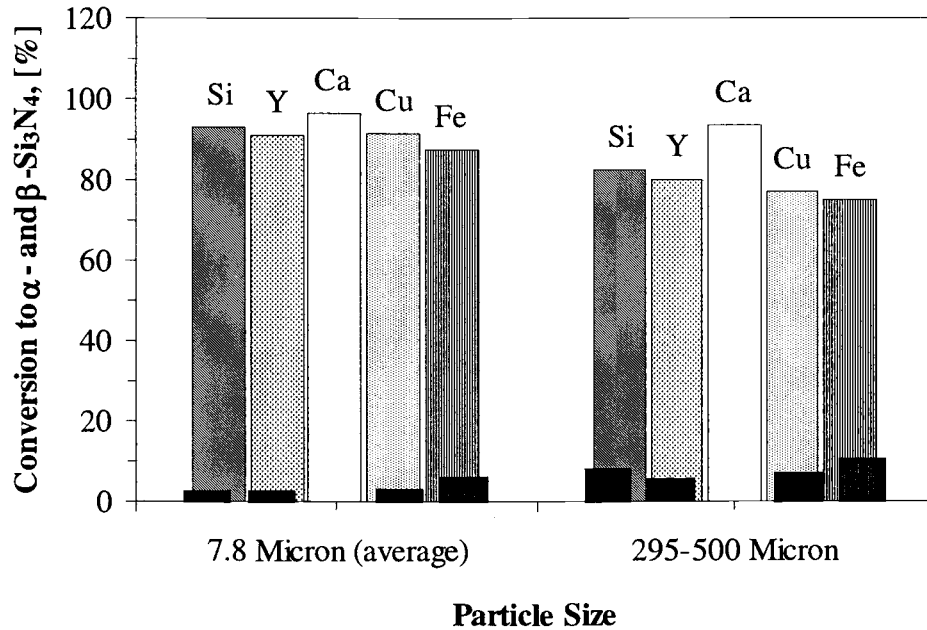


Figure 4.7 Comparison of the conversions of silicon powder and silicon granules to α - and β - Si_3N_4 in the 3-hour nitridation at 1300°C:

- (▨) – conversion to α - Si_3N_4 , from bare silicon;
- (⋯) – conversion to α - Si_3N_4 , from yttrium impregnated silicon;
- (□) – conversion to α - Si_3N_4 , from calcium impregnated silicon;
- (▤) – conversion to α - Si_3N_4 , from copper impregnated silicon;
- (▥) – conversion to α - Si_3N_4 , from iron impregnated silicon;
- (▩) – conversion to β - Si_3N_4 , from bare silicon;
- (▧) – conversion to β - Si_3N_4 , from yttrium impregnated silicon;
- (■) – conversion to β - Si_3N_4 , from calcium impregnated silicon;
- (▦) – conversion to β - Si_3N_4 , from copper impregnated silicon;
- (▨) – conversion to β - Si_3N_4 , from iron impregnated silicon.

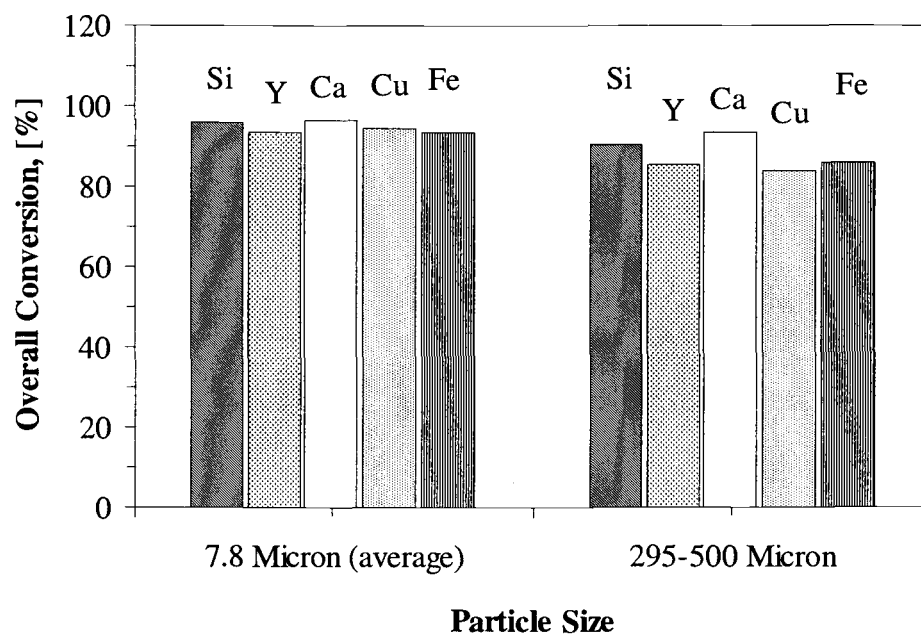


Figure 4.8 Comparison of the overall conversions of silicon powder and silicon granules in the nitridation at 1300°C:

- (▨) – overall conversion from bare silicon;
- (▤) – overall conversion from yttrium impregnated silicon;
- (□) – overall conversion from calcium impregnated silicon;
- (▥) – overall conversion from copper impregnated silicon;
- (▧) – overall conversion from iron impregnated silicon.

in the conversion is characteristic of metal impregnated and is observed from both the batches of samples, regardless of the granule-size. For instance, both large and small silicon granules impregnated with calcium showed enhancement in the formation of α - Si_3N_4 and great suppression of the formation of β - Si_3N_4 , while both the samples impregnated with iron showed enhancement in the formation of β -silicon nitride. Hence, it implies that, by using the impregnation procedures described earlier, the impregnation solution can reach into the center of granules.

Furthermore, the nitridation of granules with different sizes was carried out as well. The conversion of silicon granules that were larger than 500 μm was compared to the conversion of granules of a size in the range of 295-500 μm . The granules were impregnated with 0.125-2.0% by mass of yttrium and calcium, and nitrided at 1300°C for 3 hours.

Figure 4.9 shows that the granule size in the range investigated does not affect the conversion of silicon. The conversion obtained from samples that are larger than 500 μm was roughly the same as the conversion obtained from smaller samples (295-500 μm), for both samples impregnated with yttrium and calcium.

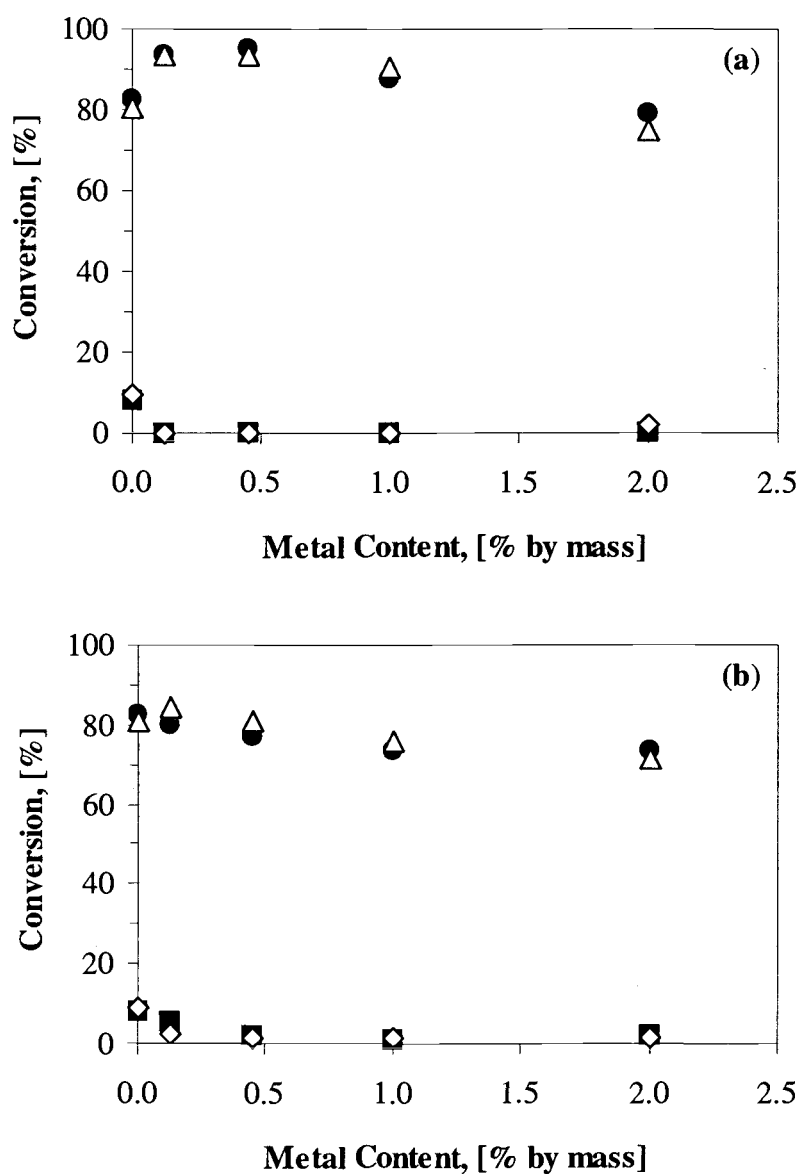


Figure 4.9 Comparison of the conversions of silicon granules with different granule sizes to α - and β - Si_3N_4 in the 3-hour nitridation at 1300°C:
 (Δ) – conversion to α - Si_3N_4 from silicon granules larger than 500 μm ;
 (\bullet) – conversion to α - Si_3N_4 from silicon granules between 295 to 500 μm ;
 (\diamond) – conversion to β - Si_3N_4 from silicon granules larger than 500 μm ;
 (\blacksquare) – conversion to β - Si_3N_4 from silicon granules between 295 to 500 μm .
 (a) Samples impregnated with calcium.
 (b) Samples impregnated with yttrium.

4.2 EFFECTS OF OXIDE LAYER

4.2.1 Results from Experiments using Tubular Flow Reactor

As mentioned earlier, it is generally accepted that the native oxide has a retarding effect on the nitridation of silicon and the removal of oxide is an essential step. However, most of the early works did not control the amount of oxide on the silicon surface. In this study, the amount of oxide on silicon particles is adjusted, prior to the nitridation, by controlling the temperature and duration of the pretreatment. According to the preliminary study in TGA, the pretreatment temperature must be higher than 1200°C in order to remove the native oxide layer effectively and the longer the pretreatment period, the less oxide remained.

It is found that the inhibiting effect by the oxide layer is critical for the nitridation at low temperature. For the reaction at 1150°C, silicon can not be nitrided if the pretreatment temperature is 1150°C, even though the pretreatment is carried out for 6 hours, because 1150°C is too low for the removal of the oxide layer. On the other hand, silicon can be nitrided at 1150°C after only 1 hour of pretreatment at 1300°C (Figure 4.10).

The removal of the oxide layer by the pretreatment at 1150°C is far less effective than the pretreatment at 1300°C. The oxide layer still remains on the surface of silicon that has experienced the pretreatment at 1150°C, while majority of oxide on the sample pretreated at 1300°C is removed. Since it is found that the

subsequent nitridation occurred only on the samples pretreated at 1300°C, it is evident that the nitridation of silicon with a higher amount of oxide covering its surface is more difficult, especially at low reaction temperature.

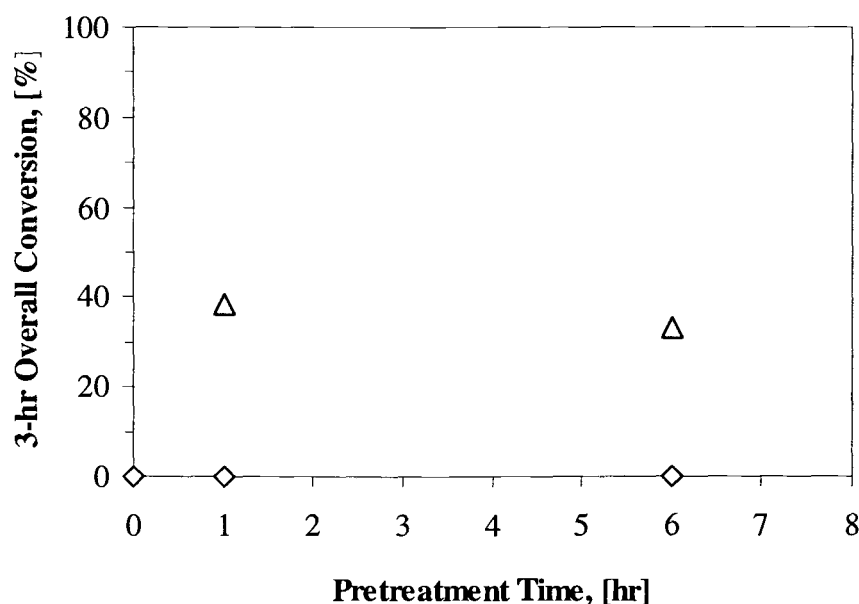


Figure 4.10 Effects of the native oxide layer at 1150°C: (◇) – samples pretreated at 1150°C; (△) – samples pretreated at 1300°C.

More supporting results are presented in Figure 4.11 which compares the nitridation of silicon grains pretreated for different lengths of time at two different temperatures based on the overall conversion of 3-hour nitridation. Considering the pretreatment and nitridation at 1200°C, it is shown that the conversions from samples pretreated for 1 or 3 hours are relatively low, roughly the same as the conversion

obtained from untreated sample. However, the conversion is significantly increased when 6-hour pretreatment is used. As mentioned earlier, the pretreatment at low temperature such as 1200°C is less effective. It takes a longer time, more than 3 hours, to remove majority of the oxide at this low temperature. Once the oxide is removed, the following nitridation proceeds appreciably.

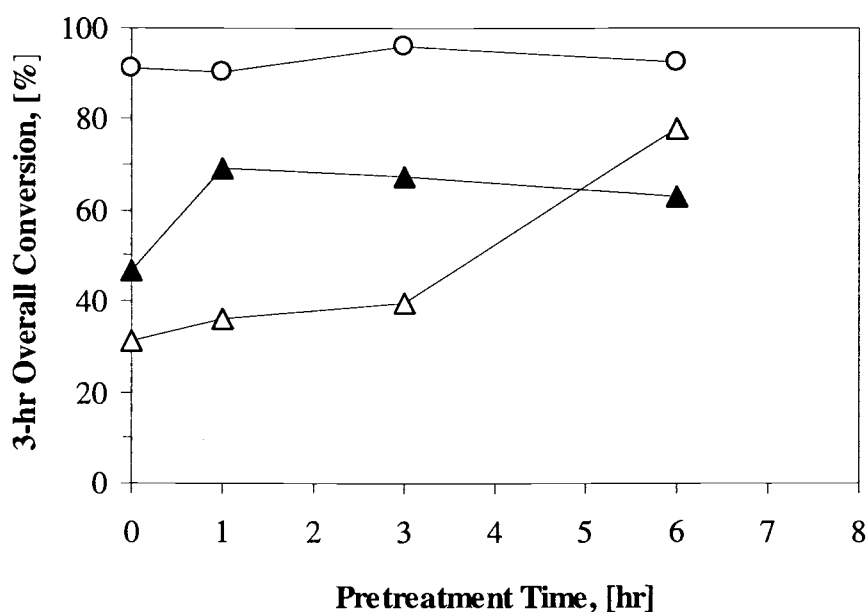


Figure 4.11 Effects of the length and temperature of pretreatment:
(Δ) – pretreatment and nitridation at 1200°C ; (▲) – pretreatment at 1300°C , nitridation at 1200°C ; (O) – pretreatment and nitridation at 1300°C .

When silicon grains are pretreated at 1300°C and subsequently nitrided at 1200°C, the 3-hour conversion depends on the pretreatment time differently from those pretreated and nitrided at 1200°C. Considering the nitridation at 1200°C of granules pretreated at 1300°C, a significant amount of oxide is removed within a short period of time, allowing nitrogen to react with exposed silicon. As the results, the conversions from samples pretreated for 1 and 3 hours are higher than the conversion from untreated samples and also higher than those from samples pretreated at 1200°C. However, when the pretreatment is carried out for 6 hours at 1300°C, the 3-hour conversion in the following nitridation at 1200°C is lower than that achieved by silicon grains pretreated for 6 hours at 1200°C. This observation is not explainable based on the removal of surface oxide. The exposure of silicon grains at high temperature for a long time may have caused a change in the surface structure, which will be discussed in a later section. It should be also noted that the untreated sample was heated to 1300°C in argon before immediately cooled down to the reaction temperature of 1200°C. This may have provoked partial removal of surface oxide during heating up beyond 1200°C, resulting in a higher conversion than untreated sample which is heated up to only 1200°C.

At higher reaction temperature, i.e. 1300°C, the inhibiting effect of the oxide layer is less potent. As shown in Figure 4.11, the conversions from 3-hour nitridation at 1300°C with and without pretreatment are roughly the same. However,

it is found that the progress of the nitridation of silicon grains covered with oxide is slightly different than that from uncovered grains.

Figure 4.12 shows the results of the nitridation at 1200 and 1300°C of silicon granules pretreated for different periods of time. It should be noted that the pretreatment was done at 1300°C for all the runs. The samples which were not pretreated were also heated to 1300°C before cooled down to the reaction temperature.

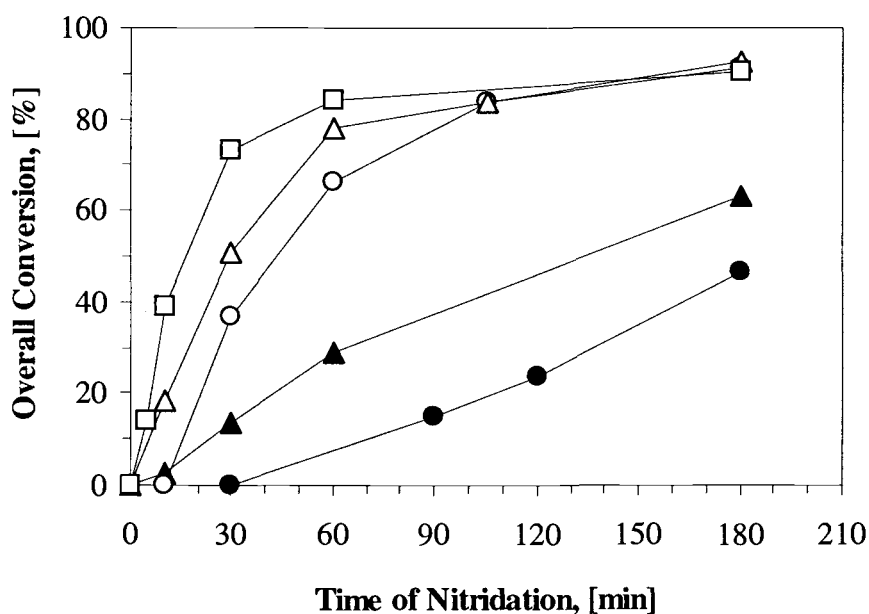


Figure 4.12 The progress of nitridation of samples prepared at different pretreatment conditions: (●) – no pretreatment, nitridation at 1200°C; (▲) – 6-hr pretreatment at 1300°C, nitridation at 1200°C; (○) – no pretreatment, nitridation at 1300°C; (□) – 1-hr pretreatment at 1300°C, nitridation at 1300°C; (△) – 6-hr pretreatment at 1300°C, nitridation at 1300°C.

The nitridation at 1300°C of silicon grains without the pretreatment shows a lag time, about 10 minutes, before the initiation of the reaction, while none is observed in the nitridation of pretreated samples. The same observation is found for the nitridation at 1200°C. The nitridation at 1200°C of untreated silicon grains shows even a longer lag time than that nitrified at 1300°C. It was reported that the delay of nitridation, or “induction period”, during the initial stage is attributed to the presence of remaining oxide layer on the grains [Dervišbegovic and Riley, 1981].

Since there is no evidence for the reaction between nitrogen and silicon dioxide [Du, *et al.*, 1989; Nemetz and Tressler, 1983; Raider, *et al.*, 1975], it is considered that the native oxide must be removed for the silicon underneath to react with nitrogen. In other words, the reaction to form silicon nitride does not occur until the silicon is exposed to the nitridation gas mixture. Thus, for silicon grains covered with native oxide, such as untreated samples, no silicon nitride is formed during the initial stage of nitridation, seen as the induction period. During this period, only the oxide removal process occurs, since the nitridation gas mixture contains hydrogen (10%) which reduces the oxygen partial pressure in the system and consequently provokes the removal of the native oxide [Atkinson and Moulson, 1976].

Furthermore, the effectiveness of the oxide removal process also depends upon the reaction temperature. The lower the reaction temperature, the less effective the removal process, resulting in a longer induction period. Considering untreated samples which contain a considerable amount of native oxide, it is obvious that the

reaction temperature of 1200°C is not high enough for the effective removal of oxide. Hence, it takes a longer time and a long induction time is observed. On the other hand, for the nitridation at 1300°C, the reaction temperature is high enough and the oxide is removed within a short period of time.

Nevertheless, the induction period may not be the time required to remove all the remaining native oxide. It is believed that the removal of native oxide is done by the reaction between silicon and silicon dioxide to form silicon monoxide (SiO) vapor. This reaction becomes possible only when the product silicon monoxide is continuously removed from the Si/SiO₂ interface to maintain SiO partial pressure there at a very low level (P_{SiO} less than 10^{-4} atm). The removal of native oxide is likely to be patch-wise, starting at defects on the surface, leaving islands of the oxide. As the removal process progresses, the size of oxide islands decreases and more silicon is uncovered. Once part of the covered silicon is exposed, the nitridation can take place.

Note that there is a difference in the progress of nitridation between silicon granules pretreated for 1 hour and those pretreated for 6 hours. 1-hr pretreatment yields faster initial rate of nitridation, although the levels of overall conversion in 3 hours are roughly the same. This phenomena is the same as observed in Figure 4.11, suggesting a change in the surface structure due to a long-time exposure of silicon to high temperature.

4.2.2 SEM Pictures of Silicon Wafer Specimen

Scanning electron microscope (SEM) was used to observe the surface of silicon and nitrided products. However, since the grain size of silicon granules is very small and it is very difficult to get a cross sectional view of such small grains, most of the SEM pictures were taken from silicon-wafer specimens (10 mm × 20 mm) nitrided by the same procedure as the silicon grains.

Silicon-wafer specimens pretreated for different periods of time have visually different surface features. The surface of silicon-wafer specimen pretreated for 1 hour is matted, while the specimen pretreated for 6 hours as well as that heated to 1300°C and then cooled down to room temperature without pretreatment is still shiny and glossy. The SEM pictures also confirm the visual observations. The SEM pictures of the wafer specimen which was heated to 1300°C and cooled down, without pretreatment, show that the surface is smooth, although some defects are found (Figure 4.13). After 1 hour of pretreatment with 90% argon and 10% hydrogen at 1300°C, a number of defects are found on the surface (Figure 4.14). These defects are holes, about 2 μm in diameter and about 10 μm deep, and they are scattering all over the surface of the wafer. However, no such defect is observed after 6 hours of pretreatment at the same temperature (Figure 4.15). The surface reconstruction is possible during the long-time exposure to high temperature, close to the melting point of silicon, because atoms have higher mobility.

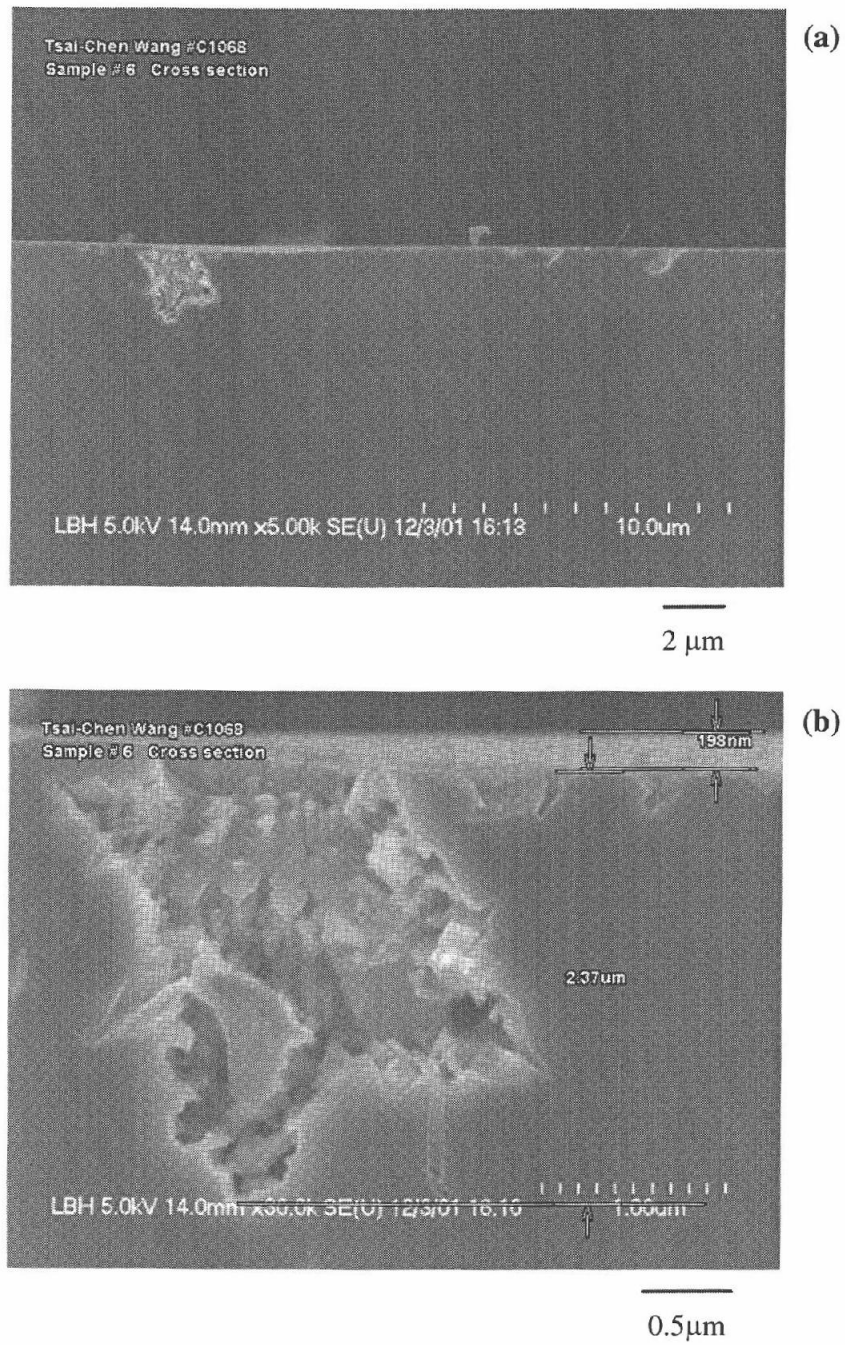


Figure 4.13 SEM pictures of silicon-wafer specimen after heating to 1300°C.
 (a) Cross sectional view, low magnification.
 (b) Cross sectional view, high magnification.

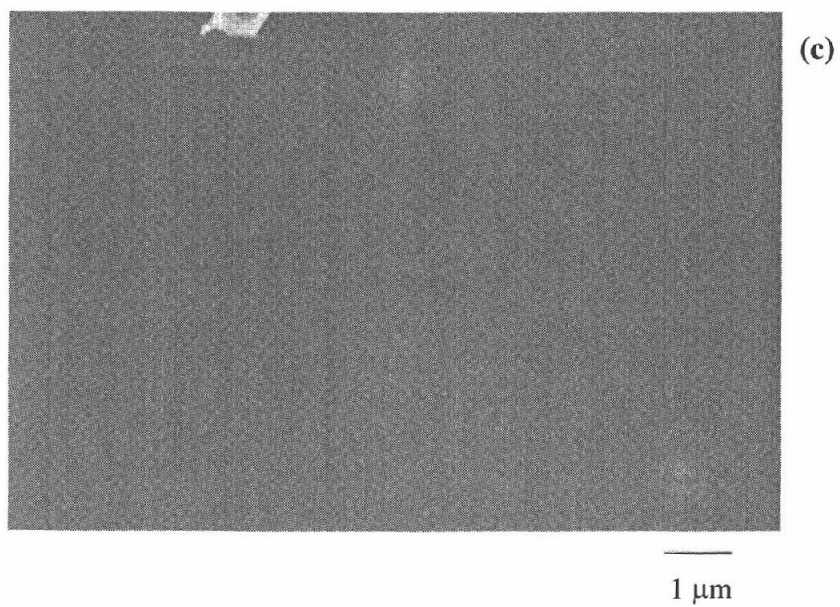


Figure 4.13(c) SEM picture of silicon-wafer specimen after heating to 1300°C: Surface.

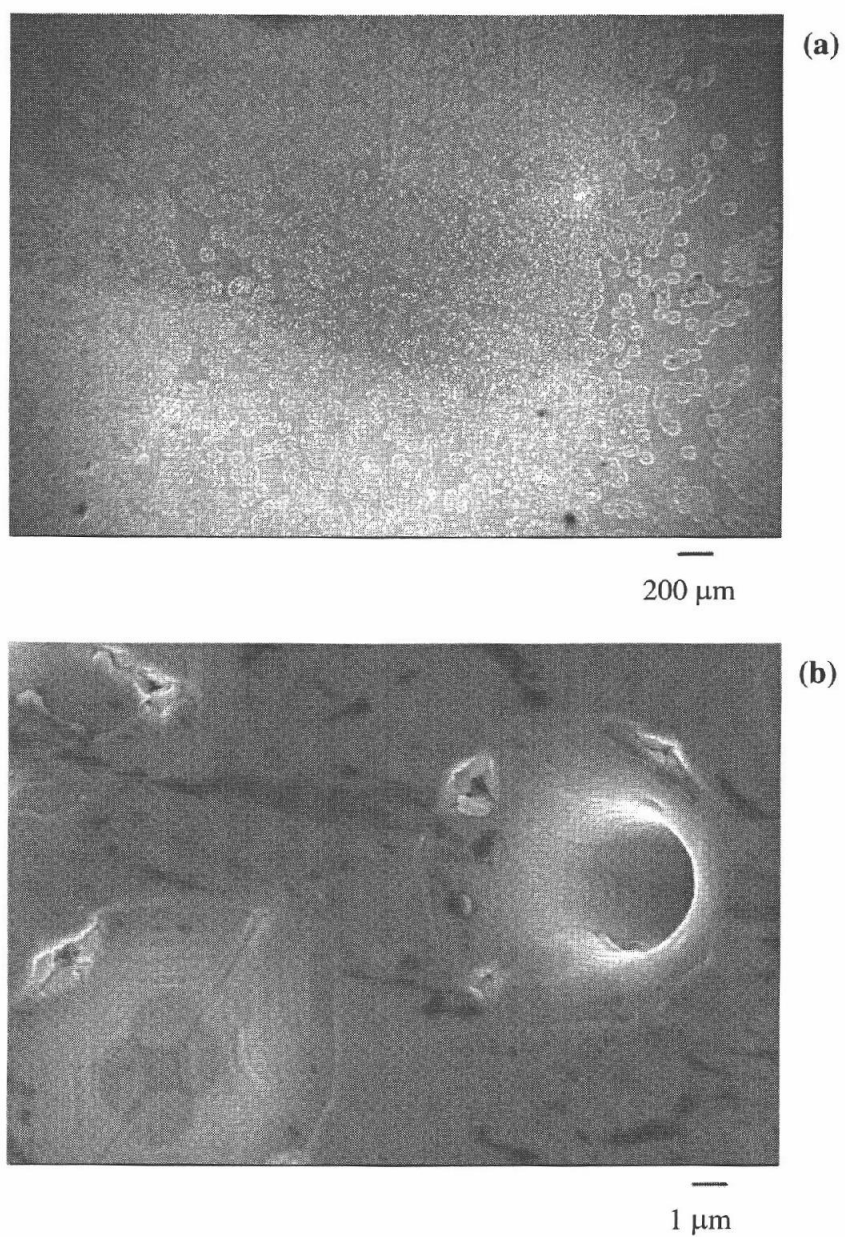


Figure 4.14 SEM pictures of silicon-wafer specimen after 1-hour pretreatment at 1300°C.
(a) Surface at low magnification.
(b) Surface at high magnification.

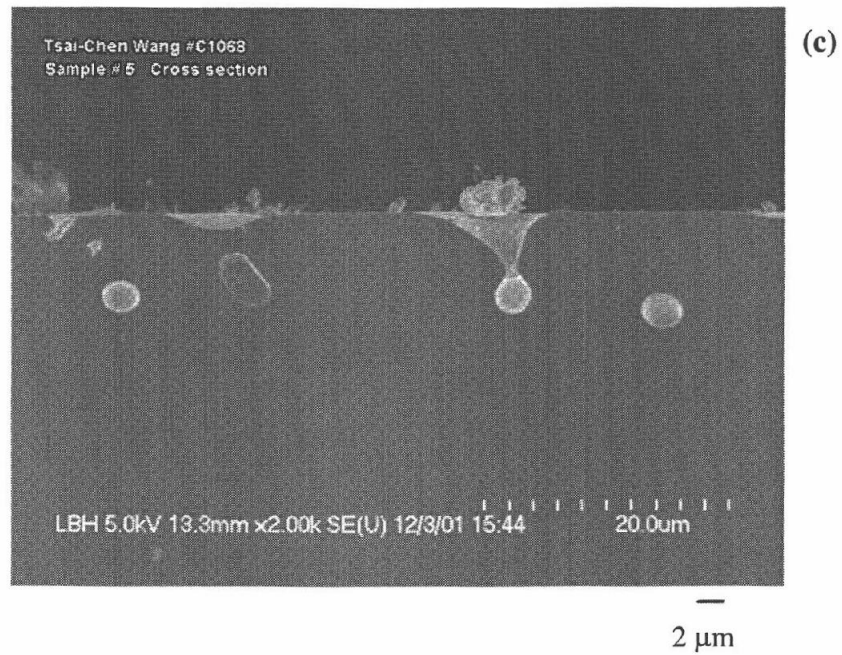
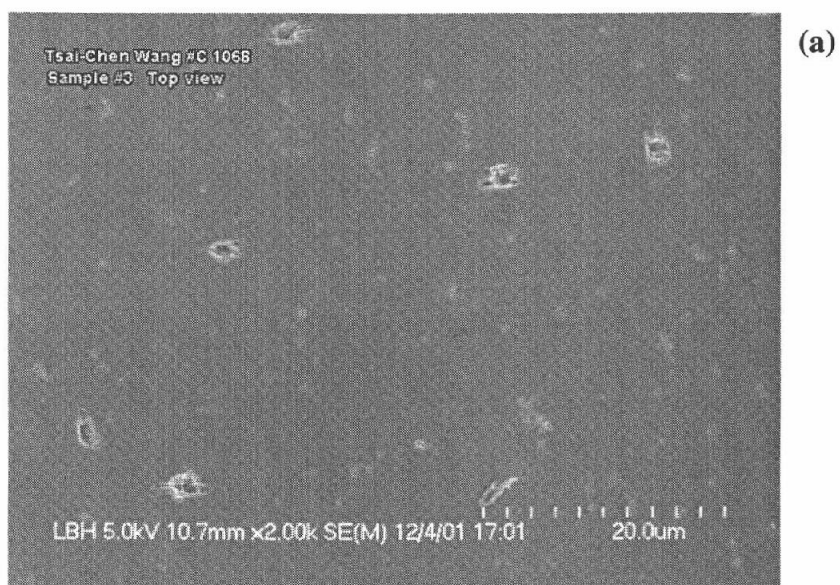
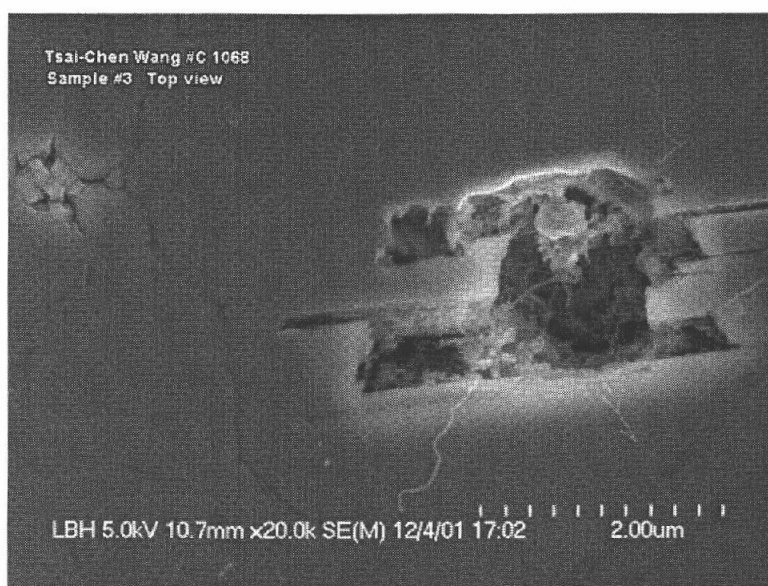


Figure 4.14(c) SEM picture of silicon-wafer specimen after 1-hour pretreatment at 1300°C: Cross sectional view.



(a)

2 μm 

(b)

1 μm

Figure 4.15 SEM pictures of silicon-wafer specimen after 6-hour pretreatment at 1300°C.

- (a) Surface at low magnification.
- (b) Surface at high magnification.

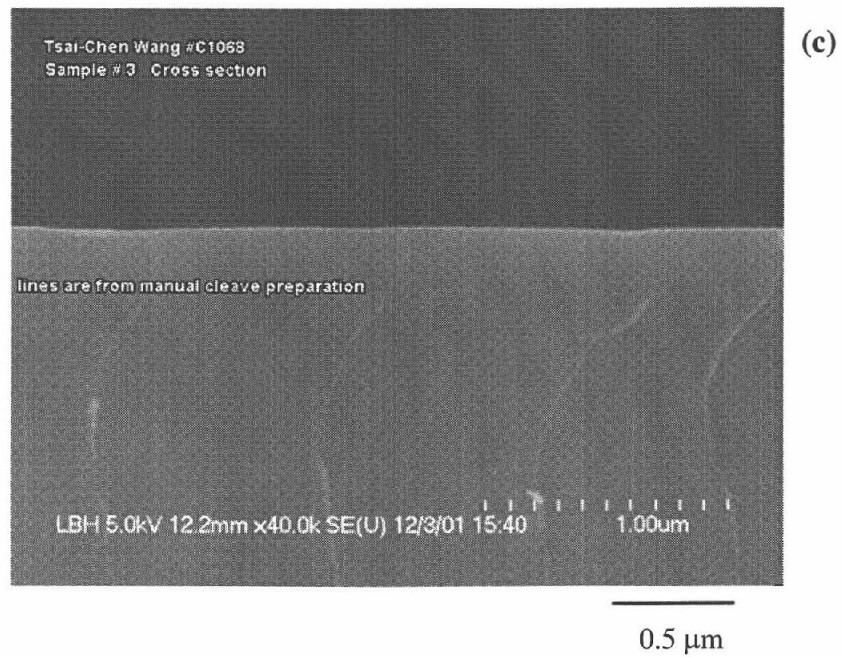


Figure 4.15(c) SEM picture of silicon-wafer specimen after 6-hour pretreatment at 1300°C: Cross sectional view.

As discussed earlier, the nitridation rate of silicon granules pretreated for 1 hour is higher than that of any silicon granules pretreated under different conditions, while the nitridation rate of untreated silicon grains is roughly the same as that of 6-hour pretreated silicon granules. Since it is found from SEM pictures that the surface of untreated silicon wafer is roughly the same as that of silicon wafer pretreated for 6 hours and a number of surface defects are found on the 1-hour pretreated silicon wafer, it is suggested that those defects may have provoked higher nitridation.

4.2.3 Results from Experiments using Fluidized-Bed Reactor

A fluidized-bed reactor was also used to study the effects of native oxide layer on the nitridation of silicon. The progress of nitridation can be conveniently obtained because a small amount of sample granules can be drawn out of the reactor at any time without disturbing the reaction. Graphs in Figure 4.16 illustrate the progress of nitridation at 1300°C of silicon granules pretreated for different lengths of time (1 hour and 3 hours).

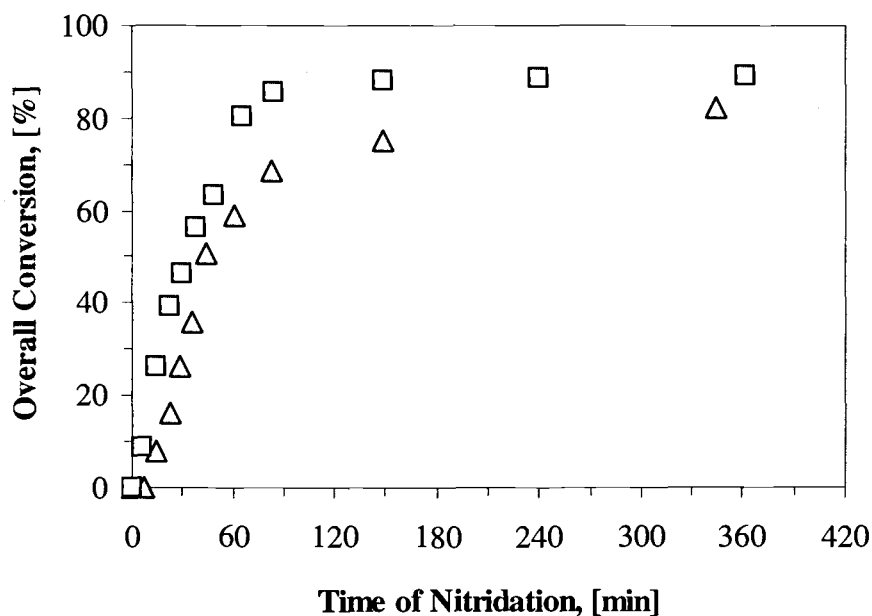


Figure 4.16 The progress of fluidized-bed nitridation at 1300°C samples prepared at different pretreatment conditions: (Δ) – 1-hr pretreatment at 1300°C; (\square) – 3-hr pretreatment at 1300°C.

The results shown in Figure 4.16 agree with the preceding findings that the induction period is associated with the amount of native oxide residing on the surface of silicon grains. The nitridation of silicon granules that are pretreated for 3 hours shows no induction period while granules pretreated for 1 hour show a lag time of about 10 minutes. However, the overall conversions obtained from both batches approach the same level, although the nitridation of 1-hour pretreated silicon is much slower than the nitridation of 3-hour pretreated sample.

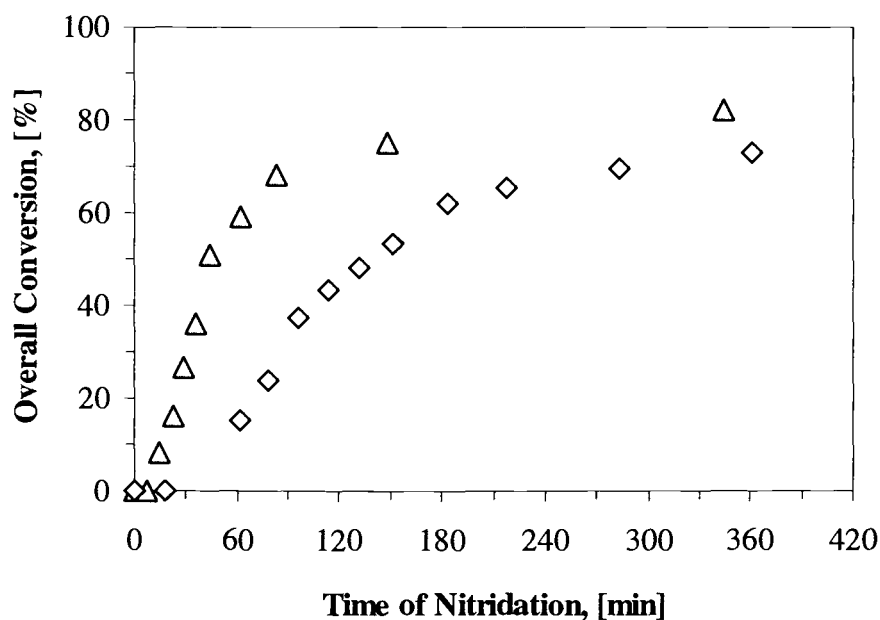


Figure 4.17 The progress of fluidized-bed nitridation at 1200 and 1300°C of samples pretreated for 1 hour at 1300°C: (◇) – nitridation at 1200°C; (△) – nitridation at 1300°C.

Figure 4.17 shows the results of the nitridation at 1200°C and 1300°C of silicon granules pretreated under the same conditions (1 hour at 1300°C). It is found that the induction period in the nitridation at 1200°C is longer than the induction period in the nitridation at 1300°C, although silicon granules in both the runs are expected to have roughly the same amount of oxide on the surface. These results also agree with the findings from the tubular flow reactor.

It should be noted that the results from the fluidized-bed reactor are slightly different from the results obtained from the tubular flow reactor. The comparison is

shown in Figure 4.18. The nitridation of 1-hour pretreated silicon granules in the tubular flow reactor shows no induction period, while silicon granules pretreated for the same time in the fluidized-bed reactor show a lag time of about 10 minutes. Moreover, the initial nitridation rate observed in the fluidized-bed reactor is lower than that observed in the tubular flow reactor, although the overall conversions after reaching the stage of very slow nitridation in both the reactors are roughly the same.

This result indicates that the removal of native oxide in the fluidized-bed reactor is not as effective as in the tubular flow reactor. As mentioned in the preceding section, the removal of oxide layer becomes possible only when the product silicon monoxide vapor is continuously removed away from the Si/SiO₂ interface and the SiO partial pressure close to the interface is maintained at a very low level (equilibrium vapor pressure of SiO at 1300°C is 1.82×10^{-3} atm or 184 Pa). In the fluidized-bed reactor, silicon monoxide generated at the bottom of the bed would be carried to the top of the bed by fluidizing gas. However, since the bed height of silicon granules in the fluidized-bed reactor is significant (8 cm), silicon monoxide partial pressure at the top of the bed might not be low enough for sustaining the SiO generation reaction (according to rough calculations, the SiO partial pressure at the top of the bed is approximately 1 order of magnitude higher than the equilibrium vapor pressure of SiO). Although silicon granules move around in the fluidized-bed, it might take a long time for the complete removal of the native oxide layer. On the contrary, in the tubular flow reactor, the thickness of the sample

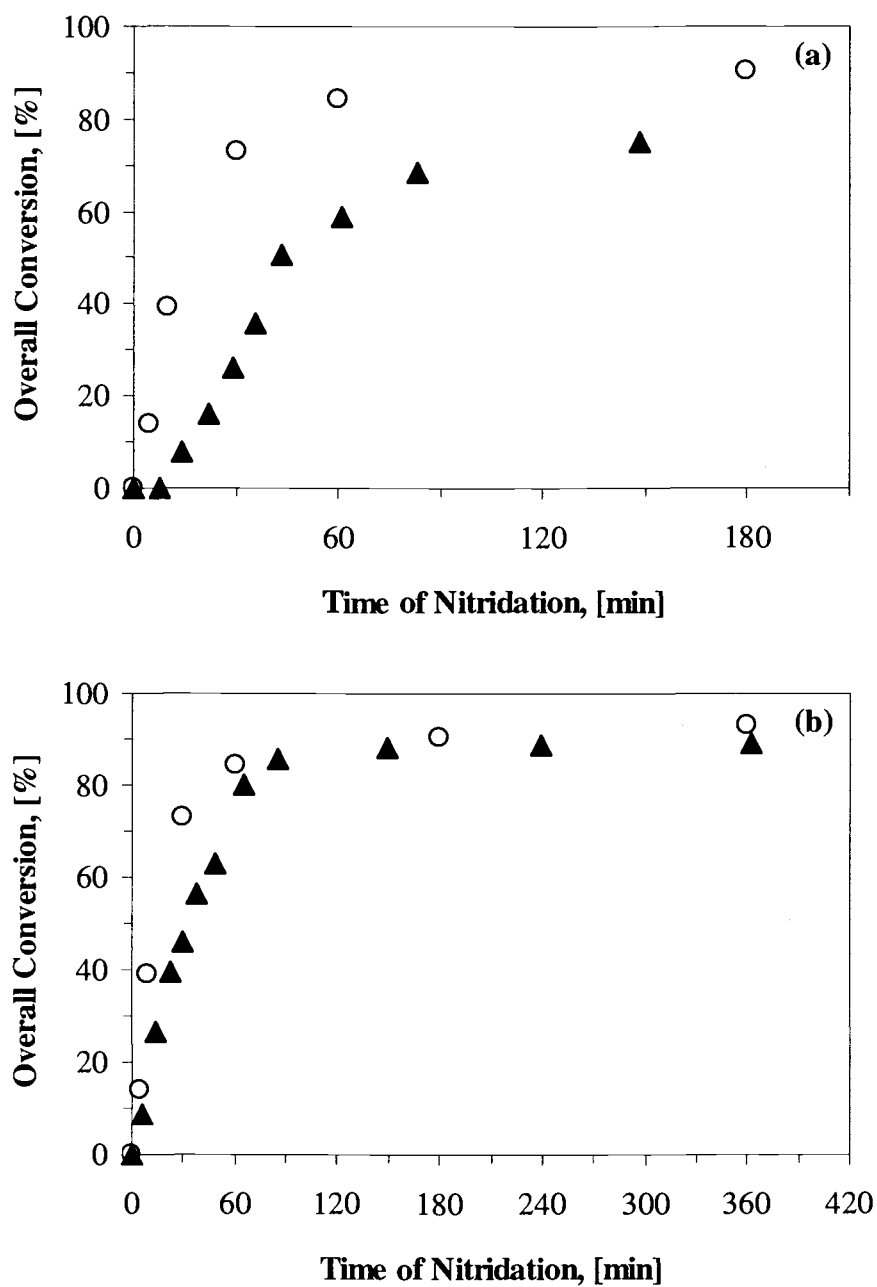


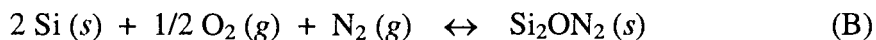
Figure 4.18 Comparison of nitridation results obtained in the fluidized-bed reactor and tubular flow reactor: (▲) – nitridation in the fluidized-bed reactor; (○) – nitridation in the tubular flow reactor. (a) display the nitridation from 0 to 3 hours. (b) display the nitridation from 0 to 6 hours.

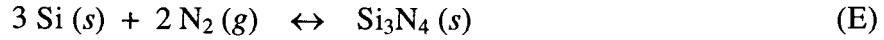
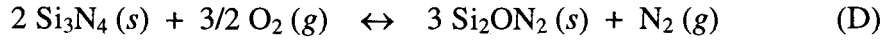
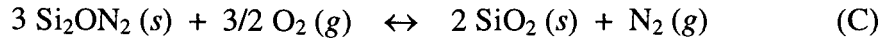
layer in the sample holder is very thin (about 2 mm). The partial pressure of silicon monoxide around and above silicon granules can be kept at a very low level as long as the flow over the sample bed is fast enough.

4.3 ROLES OF HYDROGEN

4.3.1 Phase Diagram for the Si-O-N System

Thermodynamics can be used to relate stable solid phases to the partial pressures of relevant components in the vapor phase and the temperature in an equilibrium system. A phase diagram offers a prediction for the limiting phases that can be formed under given pressure, temperature, and system composition conditions. Under the assumption that no solid solution phases are present, the stability of phases in the Si-O-N system, at temperature below the melting point of silicon, can be calculated. It is conventionally analyzed based on the following chemical reactions [Hendry, 1977]:





From Gibbs free energy change for each reaction, the equilibrium O_2 partial pressure can be calculated as a function of the N_2 pressure at any temperature. A stability field diagram is then constructed by plotting the relationship between partial pressure of O_2 and the partial pressure of N_2 in equilibrium, at any temperature, for each of the above reactions.

For example, for reaction (A), the equilibrium constant is defined as

$$K_{[\text{A}]} = \frac{1}{P_{\text{O}_2, [\text{A}]}} \quad (4.1)$$

Using thermodynamics relationship, $\Delta G^\circ = -RT \ln K$, Equation (4.1) can be rearranged as:

$$\log P_{\text{O}_2, [\text{A}]} = \left(\frac{\Delta G_{[\text{A}]}^\circ}{RT} \right) \log(e) \quad (4.2)$$

For reactions (B) to (E), the following equations are obtained.

$$\log P_{\text{O}_2, [\text{B}]} = -2 \log P_{\text{N}_2, [\text{B}]} + 2 \left(\frac{\Delta G_{[\text{B}]}^\circ}{RT} \right) \log(e) \quad (4.3)$$

$$\log P_{\text{O}_2, [\text{C}]} = \frac{2}{3} \log P_{\text{N}_2, [\text{C}]} + \frac{2}{3} \left(\frac{\Delta G_{[\text{C}]}^\circ}{RT} \right) \log(e) \quad (4.4)$$

$$\log P_{\text{O}_2, [\text{D}]} = \frac{2}{3} \log P_{\text{N}_2, [\text{D}]} + \frac{2}{3} \left(\frac{\Delta G_{[\text{D}]}^\circ}{RT} \right) \log(e) \quad (4.5)$$

$$\log P_{\text{N}_2, [\text{E}]} = \frac{1}{2} \left(\frac{\Delta G_{[\text{E}]}^\circ}{RT} \right) \log(e) \quad (4.6)$$

Thus, using Equations (4.2)-(4.6), the stability field diagram for any temperature can be drawn as shown in Figure 4.19. Note that all the free energy data are obtained from the literatures reported by Hendry [1977], Du *et al.* [1989] and Pankratz [1982], as shown in Appendix A. Data for α -phase are used for silicon nitride because of the unreliability of data differentiating α - and β -silicon nitride.

According to the stability field diagram shown in Figure 4.19, silicon nitride is stable only in the environment of an extremely low partial pressure of oxygen, on the order of $10^{-22} \sim 10^{-24}$ atm, at a rather high partial pressure of N_2 , greater than 10^{-4} atm. However, the nitridation of silicon is usually carried out using nitrogen having oxygen partial pressure on the order of 10^{-6} atm. The discrepancy between the thermodynamic calculations and the experimental findings may have resulted from the fact that the conventional calculations ignore the presence of silicon monoxide

(SiO) vapor. Lin [1975] has reported that the significant concentration of SiO is present in the gas phase during the nitridation of silicon. Silicon monoxide vapor is the result from the active oxidation of silicon [Wagner, 1958]:

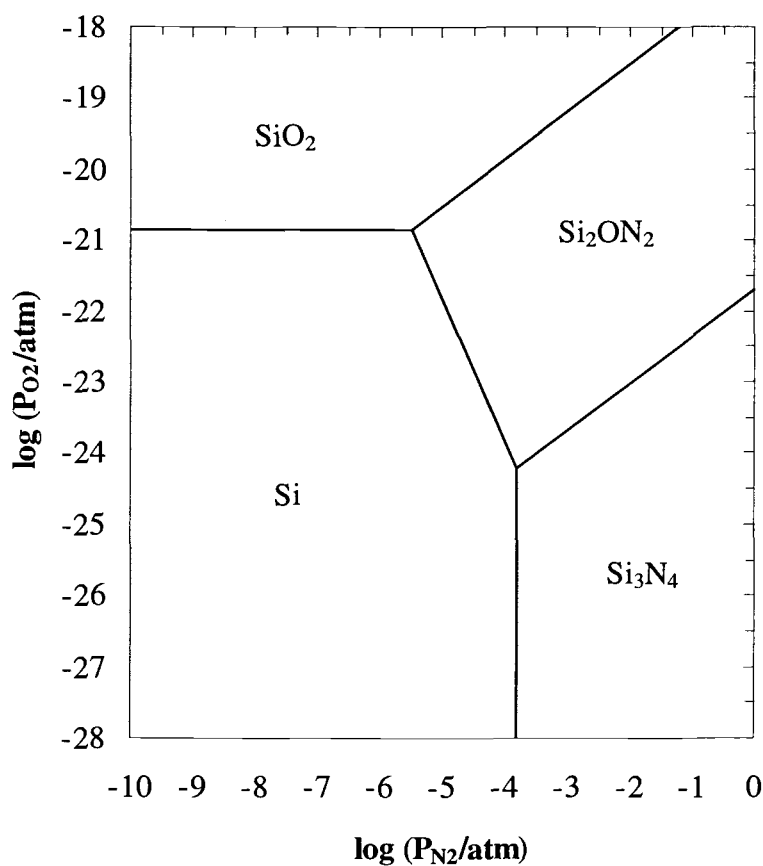
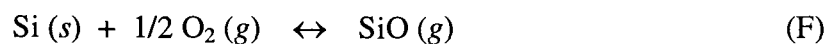
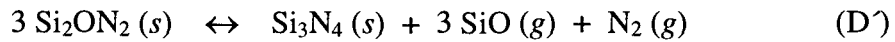
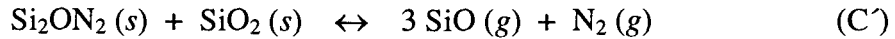
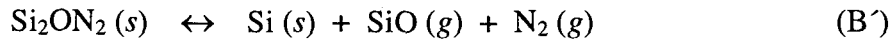
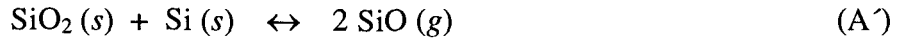
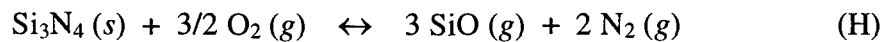
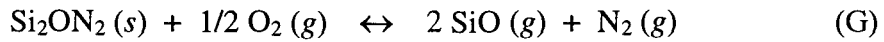


Figure 4.19 Stability-field diagram for the Si-O-N system calculated based on reaction (A)-(E) at 1300°C.

In order to incorporate the active oxidation to the calculations for the stability field diagram, Giridhar and Rose [1988] have suggested that the following reactions be included:



The combination of reactions A/A' and B/B' results in the active oxidation of silicon, as shown in Equation (F), while reactions C/C' and D/D' define the active oxidation of Si_2ON_2 and Si_3N_4 , respectively.



Giridhar and Rose [1988] have proposed that the nitridation of silicon could occur in N_2/O_2 mixtures only under conditions permitting the active oxidation. Nevertheless, the conditions that satisfy the active oxidation depend upon the

direction of reactions (A^ˆ) through (D^ˆ), since reactions (A) through (E) are always thermodynamically favored in the forward direction under reaction conditions where oxygen partial pressure is much higher than 10^{-18} atm.

By using the same calculation procedures as shown earlier for constructing the diagram presented in Figure 4.19, the relationship between the equilibrium SiO partial pressure and the equilibrium N₂ partial pressure for reactions (A^ˆ) to (D^ˆ) can be found.

$$\log P_{\text{SiO},[\text{A}^{\wedge}]} = -\frac{1}{2} \left(\frac{\Delta G_{[\text{A}^{\wedge}]}^{\circ}}{RT} \right) \log(e) \quad (4.7)$$

$$\log P_{\text{SiO},[\text{B}^{\wedge}]} = -\log P_{\text{N}_2,[\text{B}^{\wedge}]} - \left(\frac{\Delta G_{[\text{B}^{\wedge}]}^{\circ}}{RT} \right) \log(e) \quad (4.8)$$

$$\log P_{\text{SiO},[\text{C}^{\wedge}]} = -\frac{1}{3} \log P_{\text{N}_2,[\text{C}^{\wedge}]} - \frac{1}{3} \left(\frac{\Delta G_{[\text{C}^{\wedge}]}^{\circ}}{RT} \right) \log(e) \quad (4.9)$$

$$\log P_{\text{SiO},[\text{D}^{\wedge}]} = -\frac{1}{3} \log P_{\text{N}_2,[\text{D}^{\wedge}]} - \frac{1}{3} \left(\frac{\Delta G_{[\text{D}^{\wedge}]}^{\circ}}{RT} \right) \log(e) \quad (4.10)$$

However, it is very hard to measure experimentally the partial pressure of silicon monoxide. The calculations should be performed in terms of the partial pressure of oxygen, which is easy to measure. The model that relates the partial

pressure of silicon monoxide to oxygen partial pressure for the active oxidation in the viscous gas flow regime was proposed by Wagner [1958]. The model assumes that the reaction between oxygen and silicon has low activation energy and can be represented as shown in Figure 4.20:

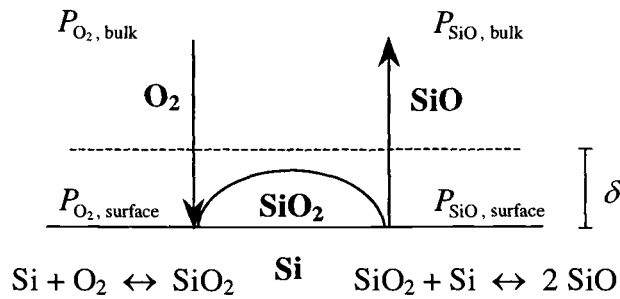


Figure 4.20 Schematic presentation of the Wagner's model.

where

$P_{O_2, \text{bulk}}$ is the partial pressure of oxygen in the bulk phase.

$P_{O_2, \text{surface}}$ is the partial pressure of oxygen at the surface.

$P_{SiO, \text{bulk}}$ is the partial pressure of silicon monoxide in the bulk phase.

$P_{SiO, \text{surface}}$ is the partial pressure of silicon monoxide at the surface.

δ is the thickness of the effective boundary layer for diffusion.

Oxygen is transported from the bulk gas phase toward the silicon surface, and silicon monoxide vapor produced is transported away from the surface. If the partial

pressure of SiO at the surface exceeds the equilibrium vapor pressure of SiO ($P_{\text{SiO,eq}}$), a protective SiO_2 film will grow laterally on the surface, in the reverse direction of reaction (A'). If $P_{\text{SiO,surface}}$ is less than $P_{\text{SiO,eq}}$, under steady state conditions, the flux of oxygen atoms toward the surface has to balance with the flux of oxygen atoms away from the surface. According to Wagner [1958], these fluxes are given by

$$j_1 = \frac{2D_{\text{O}_2}}{\delta} \left(\frac{P_{\text{O}_2,\text{bulk}}}{RT} \right) \quad (4.11)$$

$$j_2 = \frac{D_{\text{SiO}}}{\delta} \left(\frac{P_{\text{SiO,surface}}}{RT} \right) \quad (4.12)$$

where D_{O_2} and D_{SiO} are the diffusivities of O_2 and SiO, respectively. Under steady state, $j_1 = j_2$. Thus, from equation (4.11) and (4.12):

$$P_{\text{O}_2,\text{bulk}} = \frac{1}{2} \left(\frac{D_{\text{SiO}}}{D_{\text{O}_2}} \right) P_{\text{SiO,surface}} \quad (4.13)$$

Although the actual values of diffusivities of SiO and O_2 in N_2 are not known, their ratio is estimated from the molecular weights and molecular diameters of the species

to be about 0.9 for the case in which both are dilute in N_2 [Giridhar and Rose, 1988].

Thus, equation (4.13) is reduced to

$$P_{O_2, \text{bulk}} \doteq 0.45 P_{SiO, \text{surface}} \quad (4.14)$$

which relates the bulk oxygen partial pressure to the partial pressure of silicon monoxide near the reaction site. The maximum oxygen partial pressure for the active oxidation can be calculated from the equilibrium partial pressure of SiO. Consequently, under the assumption that the oxygen consumption rate due to the formation of Si_2ON_2 can be neglected compared to the total oxygen flux to silicon surface, the conditions for the active oxidation in the Si-O-N system, equation (4.6) and (4.7) to (4.10), can be displayed as shown in Figure 4.21.

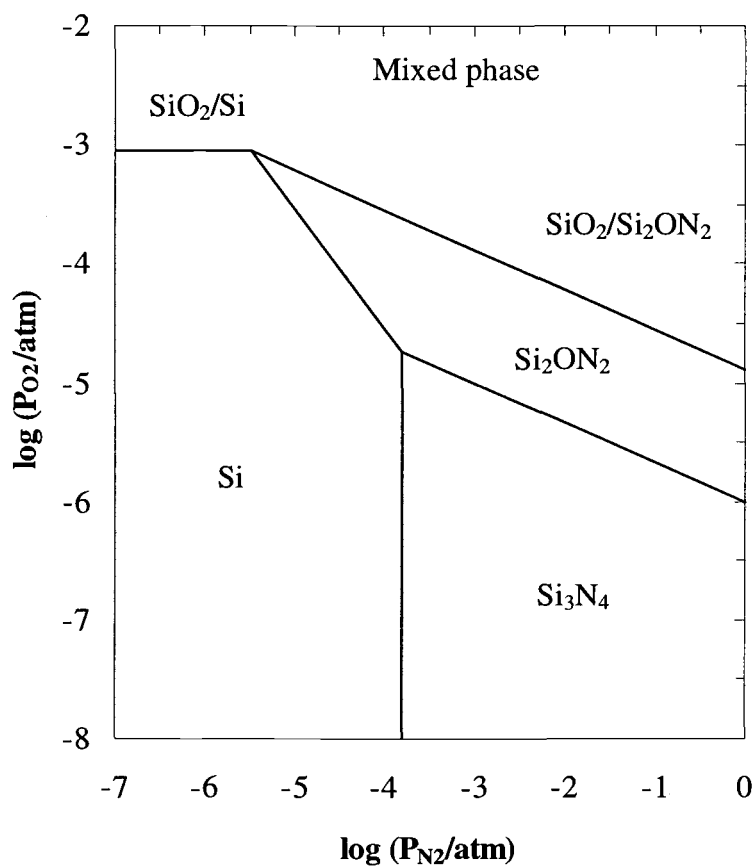


Figure 4.21 Stability-field diagram for the Si-O-N system at 1300°C with the active oxidation, i.e. reactions (A')-(D'), incorporated.

For any values of nitrogen partial pressure, the stable phase can be displayed as a function of temperature. Such a diagram for a nitrogen partial pressure of 1 atm is shown in Figure 4.22. It should be noted that both Si_2ON_2 and SiO_2 are stable in the region above the stable region for Si_2ON_2 in Figure 4.22 since reactions (A') through (D') are thermodynamically favored in the backward direction. Thus, a mixed phase between Si_2ON_2 and SiO_2 is expected.

It should be noted that the free energy data for silicon oxynitride reported from different authors are inconsistent, unlike those for silicon nitride and silicon dioxide. The values of free energy used to construct the stability field diagram shown as the solid lines in Figure 4.22 are the average values from the values reported by Hendry [1977] and Du *et al.* [1989]. Colquhoun *et al.* [1973] also reported the free energy data of silicon oxynitride, but it was shown by Hendry [1977] that the data reported by Colquhoun *et al.* [1973] was not consistent with the results reported by 3 other authors. However, if the free energy data reported by Colquhoun *et al.* [1973] is included in the calculations, the border line between Si_3N_4 and Si_2ON_2 regions in the stability field diagram will be significantly shifted, while the border line between mixed phase and Si_2ON_2 is roughly unaffected, shown as dash line in Figure 4.22. It is suggested that the prediction from the stability field diagram for the conditions close to the border line between Si_3N_4 and Si_2ON_2 may not be accurate due to the uncertainty of thermodynamics data of Si_2ON_2 .

The conditions investigated in this study are indicated by (●), i.e. at 1200, 1250, 1300 and 1350°C at a oxygen partial pressure of 5×10^{-6} atm in 1 atm nitrogen.

Figure 4.22 implies that a mixture of SiO_2 and Si_2ON_2 forms at 1200°C , Si_2ON_2 or a $\text{SiO}_2/\text{Si}_2\text{ON}_2$ mixture at 1250°C , Si_2ON_2 at 1300°C , and Si_2ON_2 or Si_3N_4 or a $\text{Si}_3\text{N}_4/\text{Si}_2\text{ON}_2$ mixture at 1350°C when the oxygen partial pressure is at the level of impurity oxygen in nitrogen.

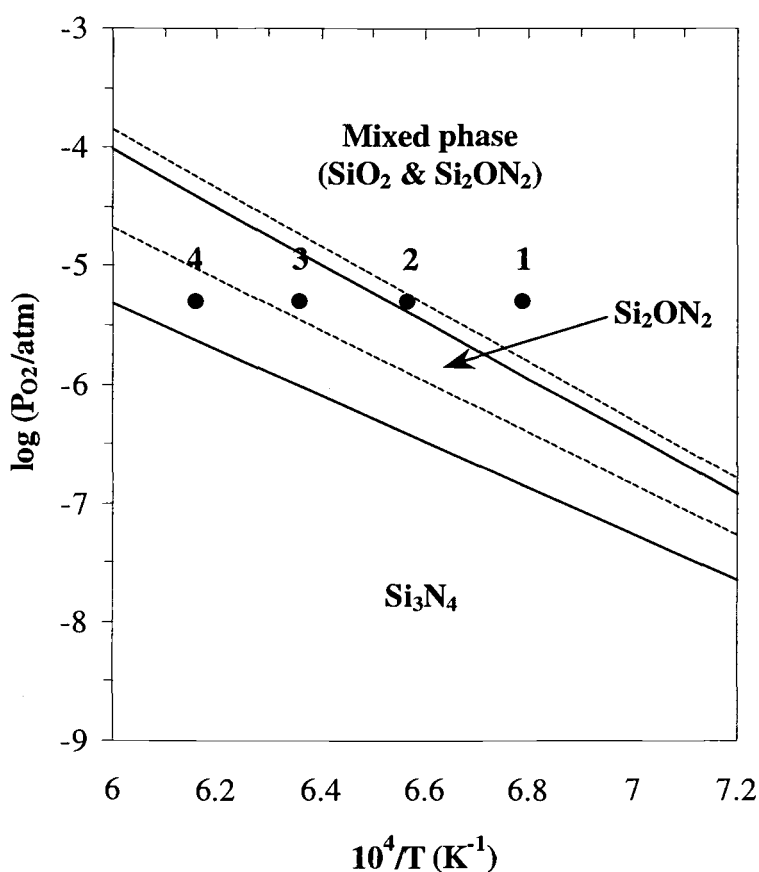


Figure 4.22 Regions of stability of different phases as a function of temperature and oxygen partial pressure in 1 atm nitrogen: (—) – the stability field diagram based on the free energy data reported by Hendry [1977] and Du *et al.* [1989]; (---) – the stability field diagram based on the free energy data reported by Hendry [1977], Du *et al.* [1989] and Colquhoun *et al.* [1973]; (●) – the conditions investigated in this work.; 1 : 1200°C , 2 : 1250°C , 3 : 1300°C and 4 : 1350°C .

4.3.2 Nitridation without Hydrogen at 1300°C

It has been known that silicon is hardly nitrided with nitrogen in the absence of hydrogen. A crucial impact from hydrogen interruption is found, as shown in Figure 4.23. When silicon granules, after removing the surface oxide by the pretreatment at 1300°C, are nitrided with nitrogen in the presence of hydrogen, the nitridation proceeds towards the completion. Although the nitridation rate gradually slows down, the overall conversion reaches roughly 90% within 3 hours. On the other hand, when uncovered silicon grains are exposed to nitrogen without hydrogen at the beginning, the subsequent nitridation becomes very slow even in the presence of hydrogen. As shown in Figure 4.23, the overall conversion reaches only about 10% in 3 hours of nitridation when only the first 5 minutes of nitridation is carried out in the absence of hydrogen. The reaction rate is so slow that the overall conversion reaches only about 50% in 9 hours of nitridation. From the shape of the conversion curve, it is apparent that the kinetics of the subsequent nitridation is altered when no hydrogen is present in the initial stage. Further nitridation is diminished and can not be recovered even though hydrogen is resumed. It is thus implied that a thin layer of material has formed on the silicon surface when uncovered silicon is exposed to nitrogen without hydrogen. This layer protects silicon from being further nitrided.

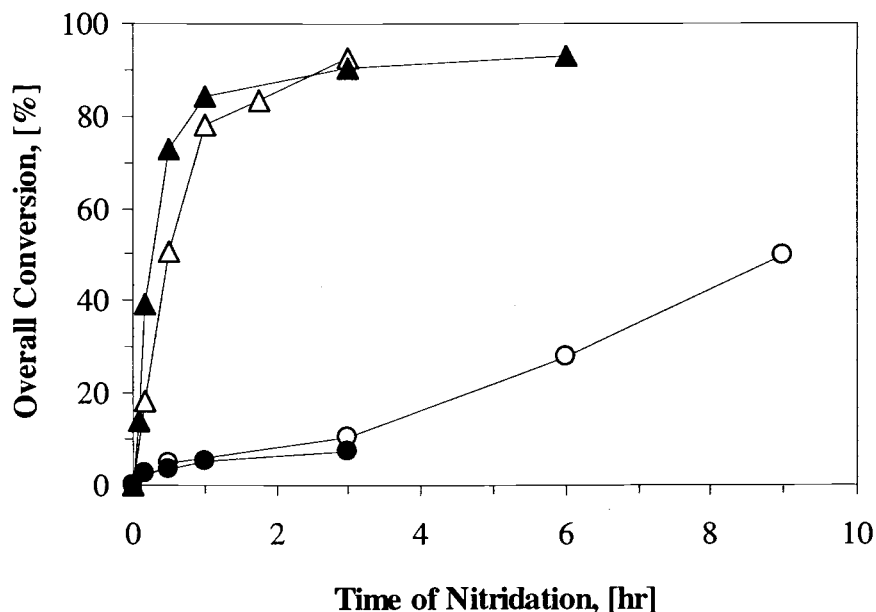


Figure 4.23 Progress of nitridation at 1300°C under various reaction conditions:
 (O) – 6-hr pretreatment, 5-min H₂ deficiency at the beginning;
 (Δ) – 6-hr pretreatment, nitridation with uninterrupted hydrogen;
 (●) – 1-hr pretreatment, nitridation with 100% nitrogen;
 (▲) – 1-hr pretreatment, nitridation with uninterrupted hydrogen.

It is also found that the concentration of hydrogen needed to sustain a high level of conversion in the nitridation of silicon is not necessarily high. Figure 4.24 compares the 3-hour conversion of nitridation at 1300°C at various hydrogen concentrations during the first 5 minutes, followed by the same nitridation with 90% nitrogen and 10% hydrogen. All the samples were pretreated for 6 hours at 1300°C, so the effect from the surface oxide was minimized. It should be noted that the flow rate of the reactant gas mixture for all the runs were kept constant by using argon as an inert balance.

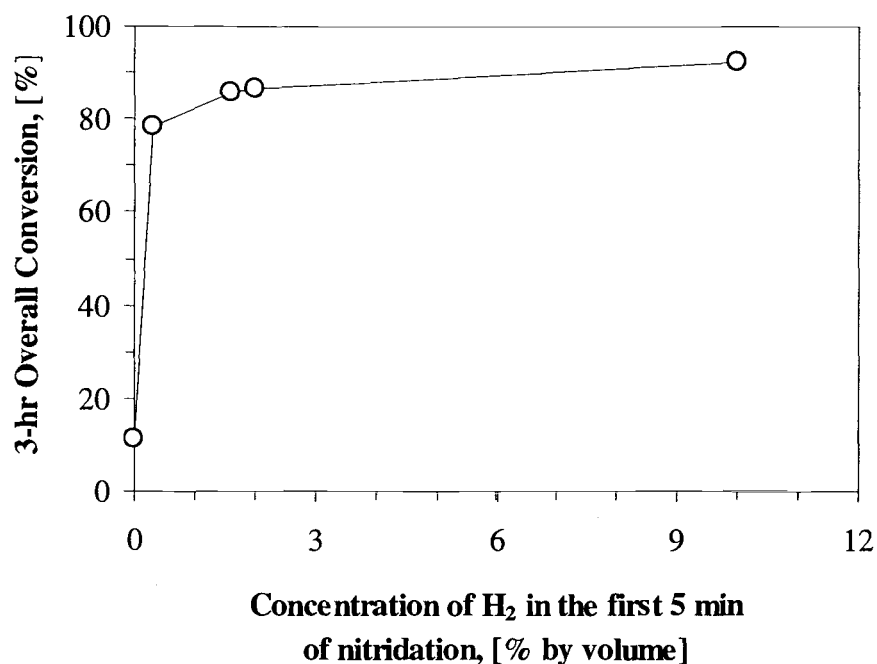


Figure 4.24 Effects of hydrogen concentration.

The subsequent nitridation becomes extremely slow after the uncovered silicon granules are exposed to nitrogen without hydrogen (0% hydrogen in Figure 4.24), even for only 5 minutes. The overall conversion reaches only 11.5% in 3 hours. On the contrary, if hydrogen is contained in the reaction gas mixture, only by 0.3% or higher, the following nitridation proceeds smoothly, reaching 80 to 90% in 3 hours. Thus, it is indicated that a high conversion can be achieved within a relatively short time as long as hydrogen is maintained in the nitridation environment.

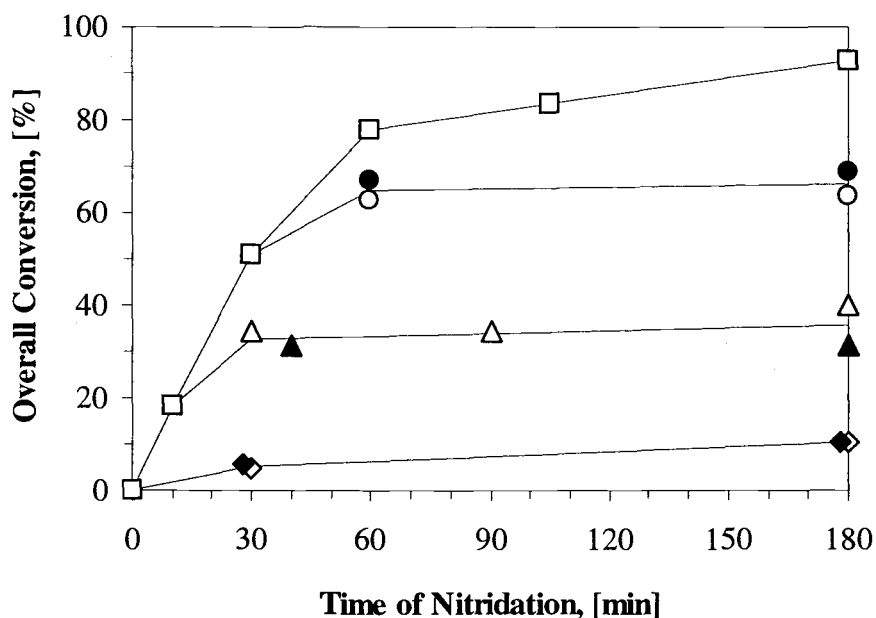


Figure 4.25 Progress of nitridation when hydrogen was interrupted during the reaction:

- (\square) – nitridation without H_2 deficiency;
- (\diamond) – 5-min H_2 deficiency at the beginning of nitridation;
- (\blacklozenge) – 10-min H_2 deficiency at the beginning of nitridation;
- (\triangle) – 5-min H_2 deficiency after 10-min nitridation;
- (\blacktriangle) – 10-min H_2 deficiency after 10-min nitridation;
- (\circ) – 5-min H_2 deficiency after 30-min nitridation;
- (\bullet) – 10-min H_2 deficiency after 30-min nitridation.

Figure 4.25 shows the results from the nitridation at 1300°C of 6-hour pretreated silicon granules. The hydrogen supply was stopped for 5 or 10 minutes at various points during the course of the nitridation. The results indicate that the effect of hydrogen interruption at the beginning of the nitridation is slightly different from the effect of hydrogen interruption after silicon is partly nitrided, although the extents of the subsequent nitridation in both the cases are limited. When silicon is

exposed to nitrogen without hydrogen immediately after the surface oxide is removed, the following nitridation with hydrogen proceeds very slowly, reaching a level of conversion slightly higher than 10% in 3-hour. However, when silicon is exposed to nitrogen without hydrogen after it is partly nitrided in the nitridation gas mixture containing hydrogen, the extent of conversion increases about 15% in 20-30 minutes after the hydrogen interruption period, after which the nitridation almost completely ceases. There seems to be a difference in the protective layers, which have formed during the hydrogen interruption period, depending on either before or after the nitridation. The surface of granules after the nitridation is more complex than the surface of granules before the nitridation, being implied from the SEM pictures of silicon-wafers specimens before and after the nitridation.

As mentioned in the prior section, SEM pictures of silicon-wafer specimens nitrided under the same conditions as silicon granules are used to observe the surface of silicon and nitrided products. SEM pictures of silicon-wafer specimen exposed to nitrogen with and without hydrogen for 5 minutes at 1300°C are shown in Figure 4.26 and Figure 4.27, respectively.

SEM pictures of silicon-wafer specimen right after the 5-minute nitridation with hydrogen, shown in Figure 4.26, clearly indicate that the surface of silicon is significantly different from the surface of the wafer specimen before being nitrided (Figure 4.15). The surface of silicon after the 6-hour pretreatment (before exposed to nitrogen) is generally smooth, although scattered surface defects are found. The energy dispersive X-ray (EDX) analysis reveals that the surface consists of only

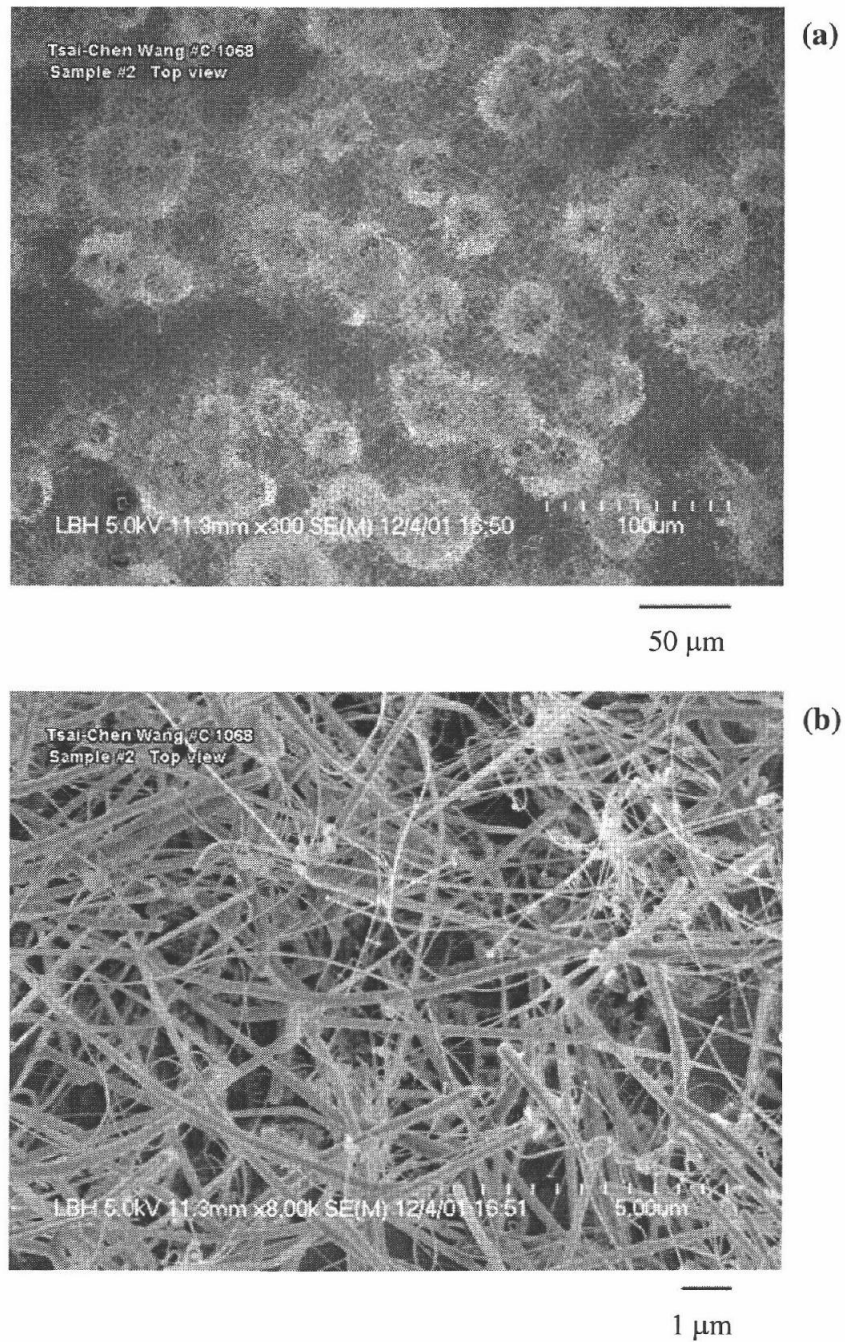


Figure 4.26 SEM pictures of silicon-wafer specimen after 6-hour pretreatment, followed by 5-minute nitridation with hydrogen at 1300°C.
(a) Surface at low magnification.
(b) Surface at high magnification.

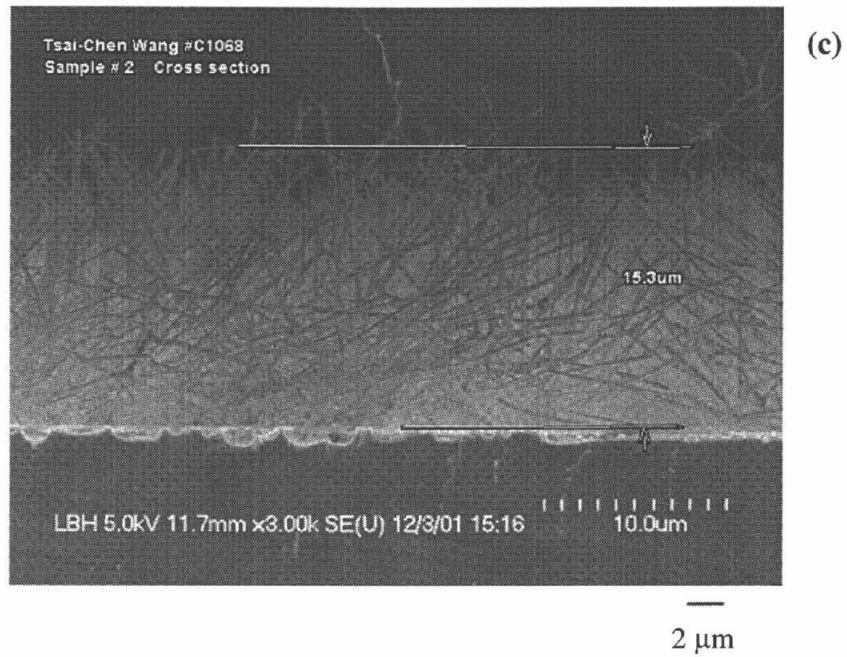


Figure 4.26(c) SEM picture of silicon-wafer specimen after 6-hour pretreatment, followed by 5-minute nitridation with hydrogen at 1300°C: Cross sectional view.

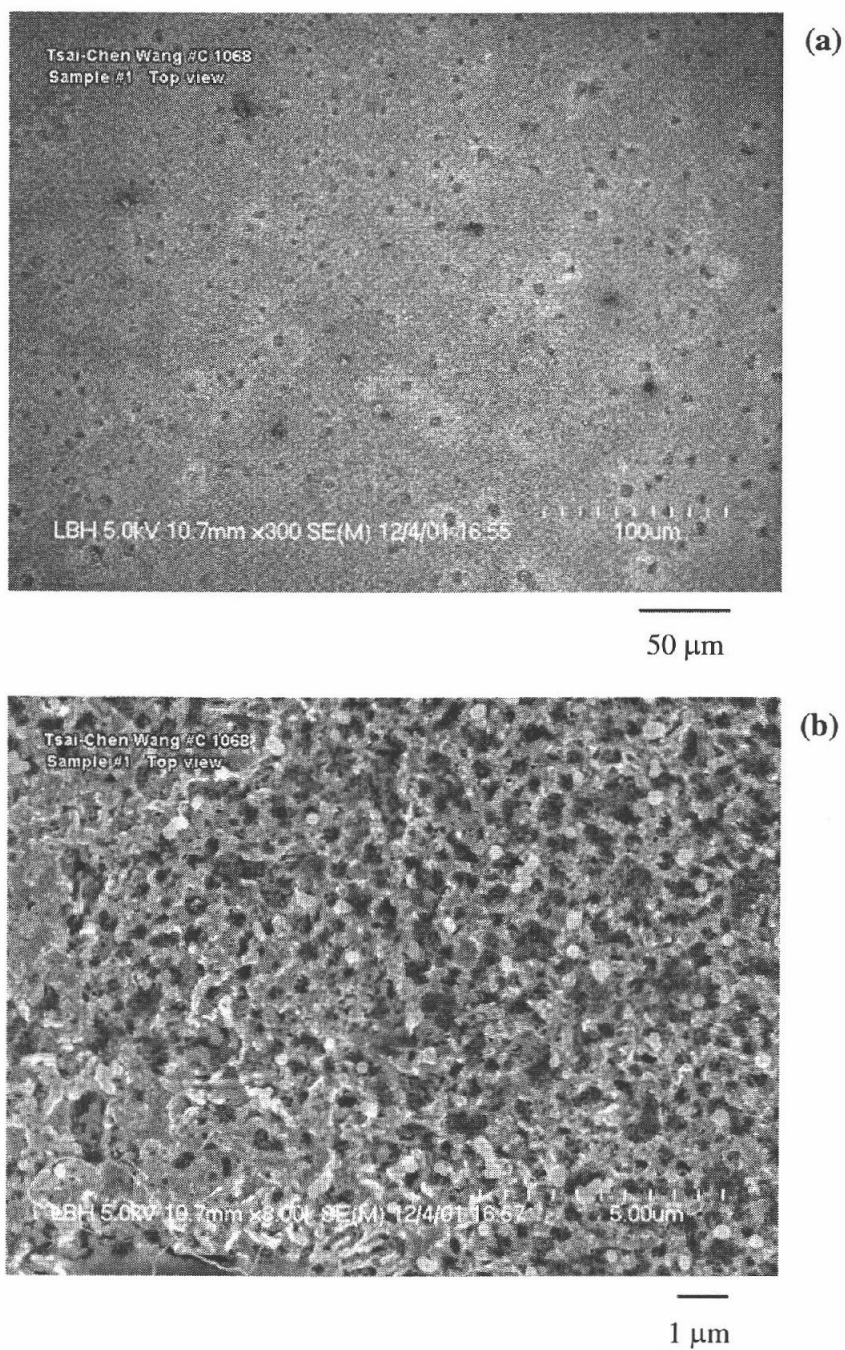


Figure 4.27 SEM pictures of silicon-wafer specimen after 6-hour pretreatment, followed by 5-minute nitridation without hydrogen at 1300°C.
(a) Surface at low magnification.
(b) Surface at high magnification.

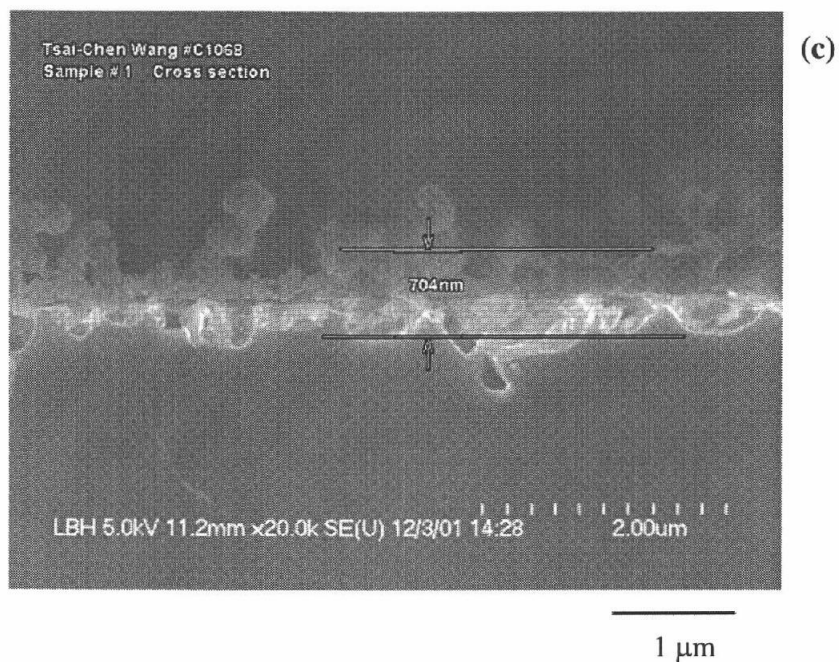


Figure 4.27(c) SEM picture of silicon-wafer specimen after 6-hour pretreatment, followed by 5-minute nitridation without hydrogen at 1300°C: Cross sectional view.

silicon with trace amount of oxygen (the ratio of Si peak height : O peak height is roughly 1:0.015). On the other hand, after the exposure to nitrogen with 10% hydrogen for only 5 minutes, the surface is clearly altered. Some regions are covered by a layer of fibers, as thick as 15 μm . The diameter of these fibers ranges from approximately 50 nm to 0.3 μm . It seems that the fibers are localized around defects on the surface of wafer, which are observed after the pretreatment. The cross sectional view of the wafer reveals that the surface underneath fibers is rough. The EDX analysis shows that the fibers contain Si, O and N (the ratio of peak-heights of Si:O:N is roughly 1:0.1:0.2), while the rugged surface contains mainly silicon with small amounts of oxygen and nitrogen (the ratio of peak-heights of Si:O:N is roughly 1:0.05:0.05).

On the other hand, no fiber is found on the surface of silicon-wafer specimen exposed to nitrogen without hydrogen for 5 minutes. The whole surface of the wafer is covered with a thin layer of coral-like structure (Figure 4.27). The thickness of the covering layer is found to be roughly 0.3 μm . The surface of silicon underneath is rugged and it is revealed by the EDX analyzer that it consists of silicon and small amounts of oxygen and nitrogen (the ratio of peak-heights of Si:O:N is roughly 1:0.06:0.03). Unfortunately, the EDX analysis of the covering layer failed.

More SEM pictures were taken from silicon-wafers specimens nitrided for 3 hours at 1300°C, after 1-hour pretreatment at the same temperature. The surface of the wafer that is nitrided in the presence of hydrogen is completely covered by a thick layer (roughly 150 μm thick) of very long fibers, as shown in Figure 4.28. On

the contrary, fibers are hardly found on the surface of wafer that is nitrided without hydrogen for 5 minutes, followed by the nitridation with hydrogen for 3 hours. The whole surface of the wafer that experienced 5-minute hydrogen deficiency is covered with a dense coral-like structure (Figure 4.29). The EDX analysis indicates that this dense layer consists of silicon with small amounts of oxygen and nitrogen (the ratio of peak-heights of Si:O:N is roughly 1:0.2:0.1).

It is clear that the surface of silicon is fully covered after being exposed to nitrogen without hydrogen, even for a very short period. This coating, formed during the hydrogen interruption period in the nitridation, may hinder further nitridation. The presence of hydrogen in the nitridation gas mixture prevents the formation of this protective coating. However, once the protective layer is formed, it can not be removed even in the presence of hydrogen.

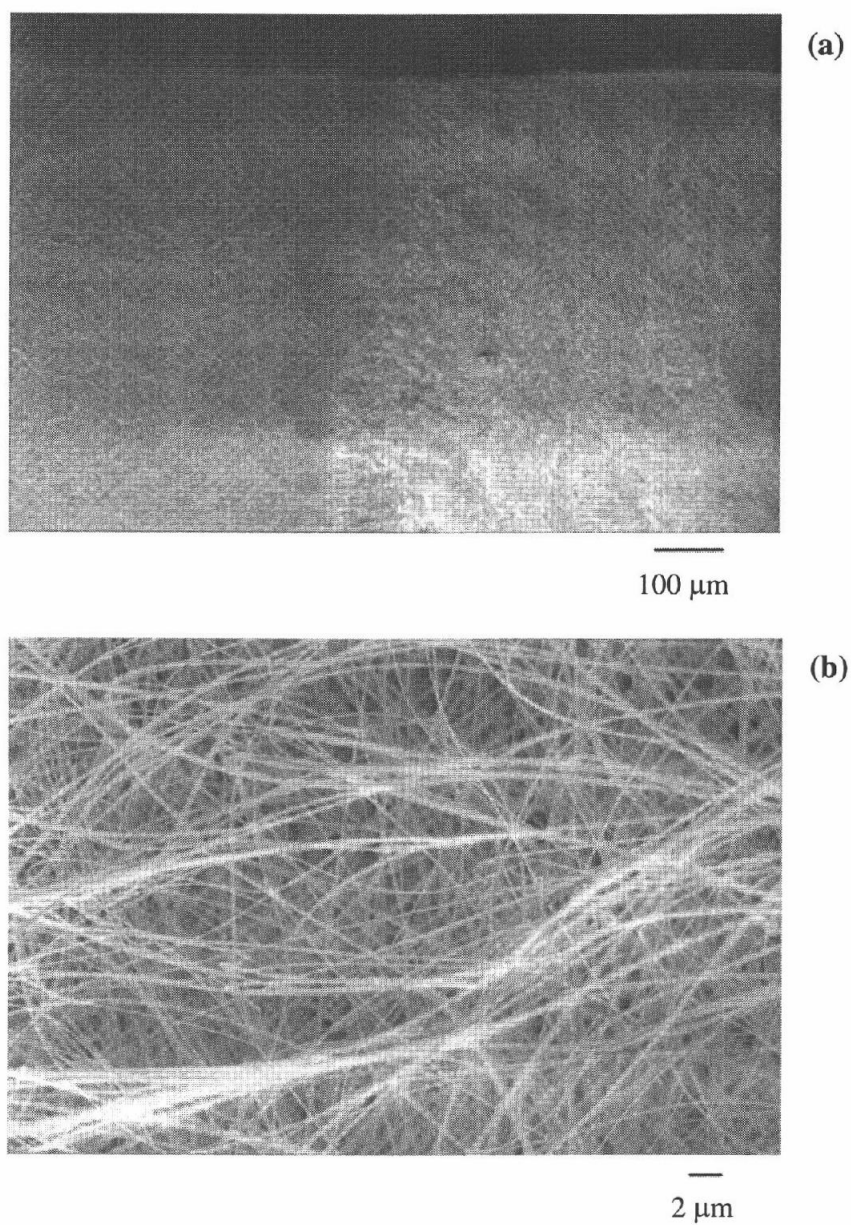


Figure 4.28 SEM pictures of silicon-wafer specimen after 1-hour pretreatment, followed by 3-hour nitridation with hydrogen at 1300°C.
(a) Surface at low magnification.
(b) Surface at high magnification.

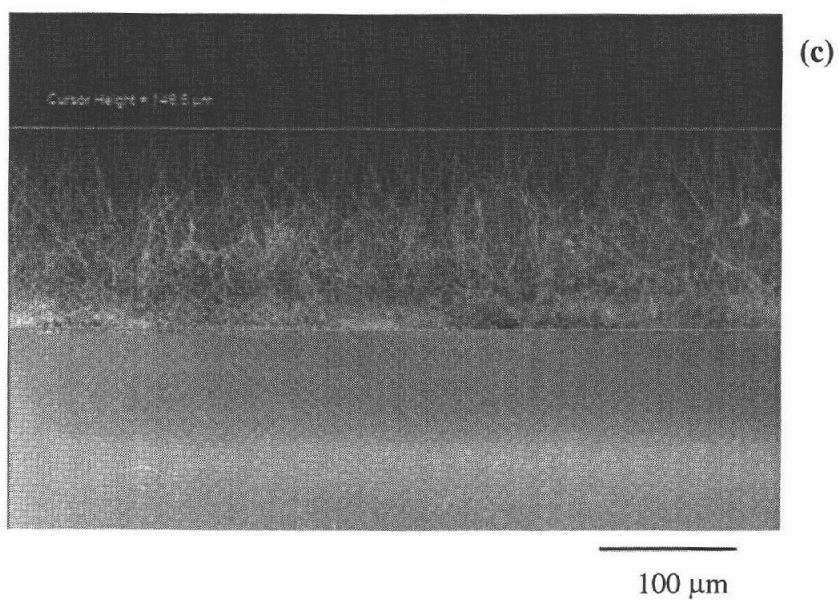


Figure 4.28(c) SEM picture of silicon-wafer specimen after 1-hour pretreatment, followed by 3-hour nitridation with hydrogen at 1300°C: Cross sectional view.

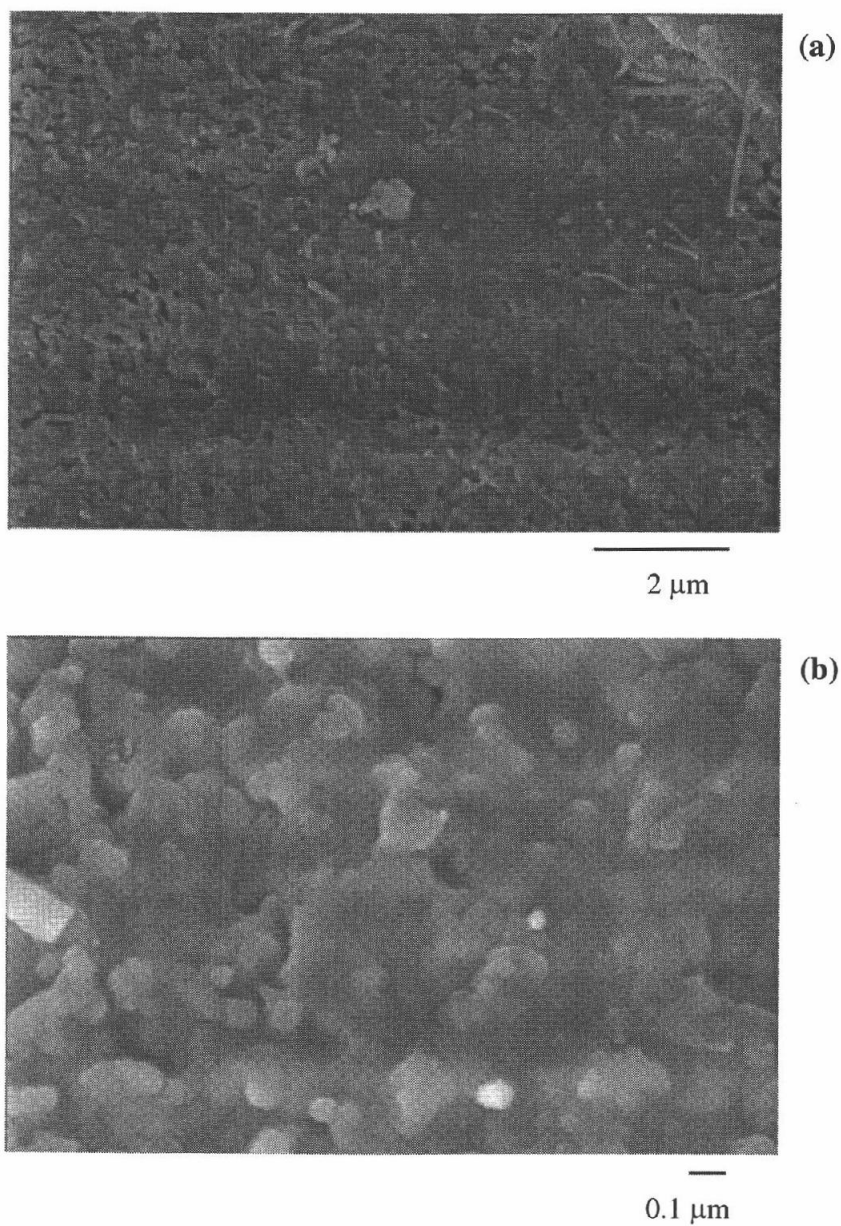


Figure 4.29 SEM pictures of silicon-wafer specimen exposed to nitrogen without hydrogen for 5 minutes after 1-hour pretreatment, followed by 3-hour nitridation with hydrogen at 1300°C.
(a) Surface at low magnification.
(b) Surface at high magnification.

4.3.3 Nitridation without Hydrogen at Different Temperatures

As discussed in the prior section, exposing silicon granules to nitrogen without hydrogen at 1300°C, even for a short period of time, results in a dramatic decrease in the conversion of subsequent nitridation. Nevertheless, it is found, as shown in Figure 4.30, that the effect of hydrogen interruption varies depending on the reaction temperature. Figure 4.30 compares the 3-hour conversion achieved in the nitridation with continuous supply of hydrogen with that in the 3-hour nitridation with 5-minute hydrogen interruption at the beginning at different temperatures. Silicon granules were all pretreated for 6 hours at 1300°C.

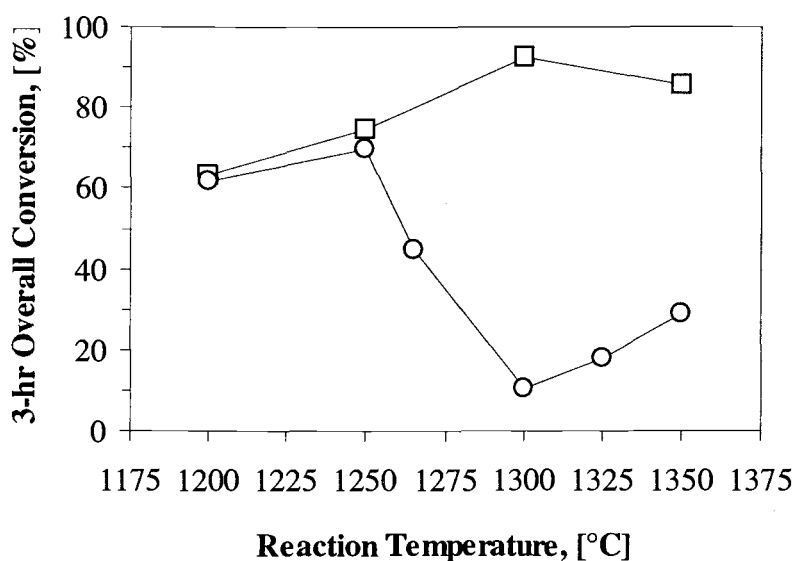


Figure 4.30 Effects of hydrogen interruption at different temperatures:
(○) – nitridation with 5-min H₂ deficiency at the beginning;
(□) – nitridation with uninterrupted H₂.

When the nitridation temperature is 1250°C or lower, the 5-minute hydrogen interruption does not significantly affect the following nitridation. The 3-hour conversions obtained from the nitridation with a 5-minute hydrogen interruption at 1200 and 1250°C are roughly the same as those from the nitridation in the presence of hydrogen at all time.

However, when the reaction temperature is 1300°C or higher, the exposure of silicon granules to nitrogen without hydrogen considerably affects the nitridation that follows. The subsequent nitridation is hindered, especially at 1300°C. The 3-hour conversion obtained from the nitridation with a 5-minute hydrogen interruption is less than one-third of that obtained from the regular nitridation (with hydrogen). Note that the 3-hour overall conversion from the nitridation with hydrogen interruption during the first 5 minutes at 1350°C is higher than that at 1300°C. Higher temperature may accelerate the transport of reactive species through the protective film by simply enhancing the diffusion or by a more complex mechanism. As seen from SEM pictures, the protective film becomes denser after the subsequent nitridation with hydrogen for 3 hours. Since the thickness of this film remains roughly unchanged after the 3-hour nitridation, the stress inside the film should have built up as the reaction progresses. If the temperature is high enough, the subsequent reaction might be enhanced and result in higher stress within the protective film until the film cracks, providing easy paths for the reactant species to go through. However, further study is needed to clarify the mechanism.

More experiments were focused on the effect of temperature at which the protective film is formed. The results are shown in Table 4.1. Note that all samples were pretreated for 6 hours before being exposed to reactant gas.

Table 4.1 Effects of temperature at which the protective film is formed.

Exposure to N ₂ without H ₂ , after pretreatment	Subsequent nitridation with H ₂	3-hour overall conversion (%)
5 min at 1300°C	3 hr at 1300°C	10.47
5 min at 1300°C	3 hr at 1200°C	13.83
5 min at 1200°C	3 hr at 1300°C	80.27
5 min at 1200°C	3 hr at 1200°C	61.80
-	3 hr at 1300°C	92.40
-	3 hr at 1200°C	63.21

The results indicate different inhibiting characteristics of the protective film formed during the nitridation without hydrogen, depending on temperatures. When the film is formed at high temperature (1300°C), the subsequent nitridation, even

with hydrogen, is prohibited. The conversion obtained in 3 hours is very low. However, if the film is formed at low temperature (1200°C), a high conversion can be achieved in the subsequent nitridation, especially when the temperature of the subsequent nitridation with hydrogen is high (1300°C). It seems that the transport of reactive species through this protective film at high temperature is more effective than at low temperature. The conversion obtained in 3 hours, when the temperature of the subsequent nitridation with hydrogen is 1300°C, is much higher than that when the temperature of the subsequent nitridation is 1200°C (80.27% compared to 61.80%). Nevertheless, it is still significantly lower than the conversion obtained in the nitridation with uninterrupted supply of hydrogen (92.40%). These results confirm the formation of protective film when silicon is exposed to nitrogen without hydrogen, even at 1200°C. Furthermore, it is evident that the film, formed during the exposure of uncovered silicon to nitrogen without hydrogen at 1200°C, still has a hindering effect on the nitridation that follows.

4.3.4 Infrared Spectrophotometry Analysis

Infrared (IR) analysis was also used to identify the composition of nitridation products. IR transmittance measurements were performed with a Nicolet 510P Fourier Transform Infrared Spectrometer. The measurements were conducted on thin disks prepared from thoroughly mixed power of sample and dry potassium

bromide (KBr). The IR spectra of the raw material and products from the nitridation at 1300°C are shown in Figure 4.31.

It is clear that the product from the 3-hour nitridation with hydrogen after 6 hours of pretreatment is mainly silicon nitride. The main strong absorption band near 950 cm^{-1} is a fundamental vibration due to the Si-N-Si antisymmetrical stretching mode and the absorption at 495 cm^{-1} is the symmetrical stretching mode for the Si-N-Si molecular group [Luongo, 1983]. The absorption bands at 957, 941, 906, 893, 871, 854, 684, 600, 495, 460 and 406 cm^{-1} appear as distinct strong sharp bands, while the absorption bands at 578 cm^{-1} and 443 cm^{-1} are indistinct, indicating that the sample contains mainly α -phase silicon nitride with only small amount of β -phase [Luongo, 1983].

On the other hand, no distinct bands corresponding to the absorption from silicon nitride is found in the product from 3-hour nitridation, in which the reaction gas during the first 5 minutes contains no hydrogen. The result agrees with the finding from the X-ray diffraction analysis that product is mainly unreacted silicon. However, absorption bands around 1100 cm^{-1} and 485 cm^{-1} , which are corresponding to stretching mode of Si-O bonding in SiO_2 [Lippincott, *et al.*, 1958], are clearly observed. Moreover, unidentified absorption bands are observed at 889, 850, 569 and 430 cm^{-1} . Since the absorption bands corresponding to silicon dioxide do not appear in the product from the 3-hour nitridation with uninterrupted hydrogen, it is suggested that silicon dioxide may be responsible for the low conversion observed in the nitridation with a 5-minute hydrogen interruption. However, according to

Schalch *et al.* [1987], silicon oxynitride with a high oxygen-to-nitrogen ratio also expresses absorption at wave numbers very close to those of silicon dioxide. Thus, it is suggested that the protective film that is formed during the nitridation without hydrogen at 1300°C might be either silicon oxynitride or silicon dioxide.

The IR spectra of the product in the nitridation at 1200°C with a 5-minute hydrogen interruption period is shown in Figure 4.32. All absorption bands observed match the bands from the product of 3-hour nitridation with uninterrupted hydrogen, which agrees with the results from the X-ray diffraction analysis. No absorption band corresponding to Si-O bonding is found.

According to the results shown earlier in Figure 4.30, 3-hour conversions from the nitridation with continuous supply of hydrogen or with a 5-minute hydrogen interruption at 1200°C are not significantly different. Hence, no protective film or very thin layer of protective film is expected to form during the hydrogen interruption period. The findings from the IR analysis also support this conclusion.

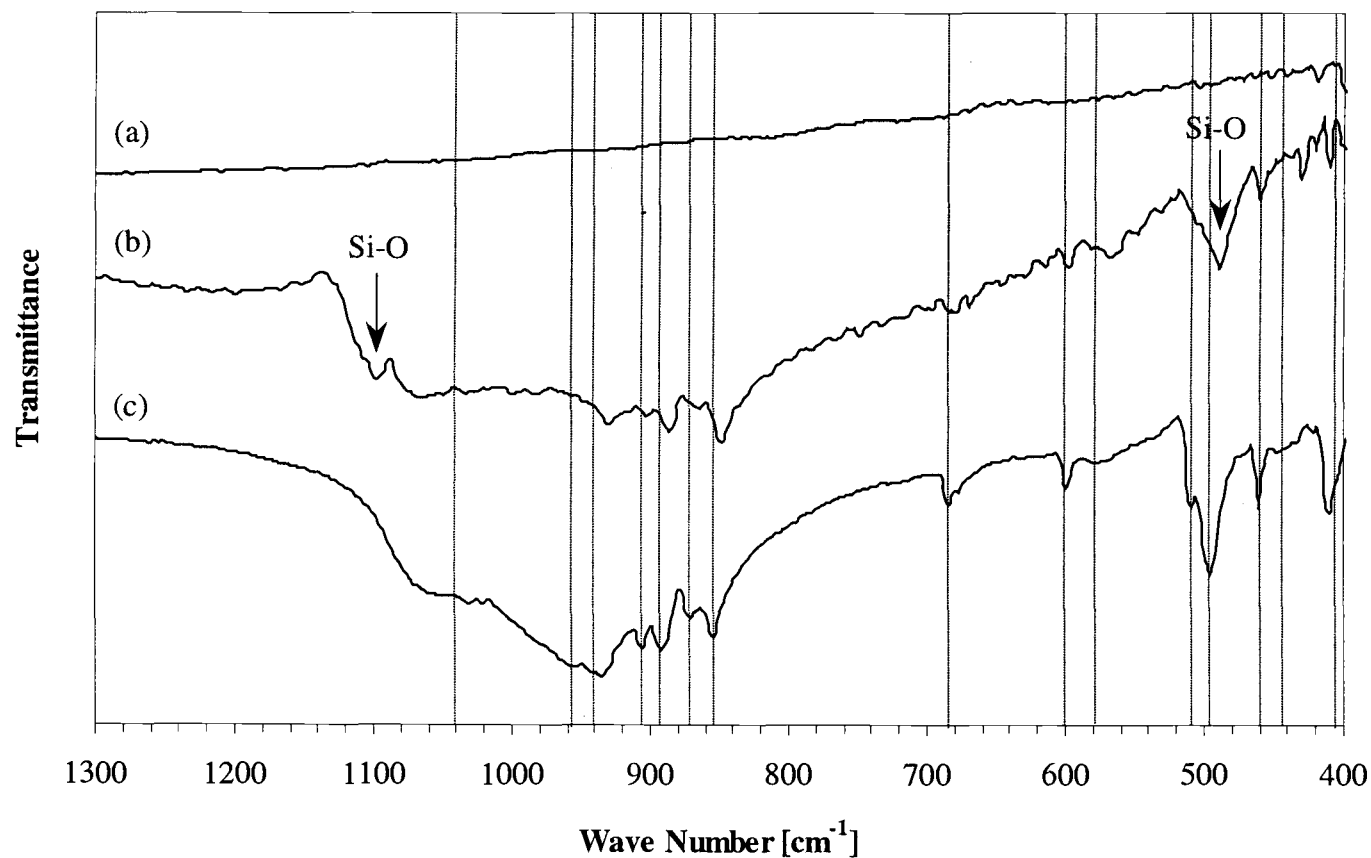


Figure 4.31 IR spectra of products in the nitridation at 1300°C: (—) – absorption bands for Si₃N₄.
 (a) raw material; (b) 3-hr nitridation with 5-min H₂ deficiency at the beginning; (c) 3-hr nitridation with H₂.

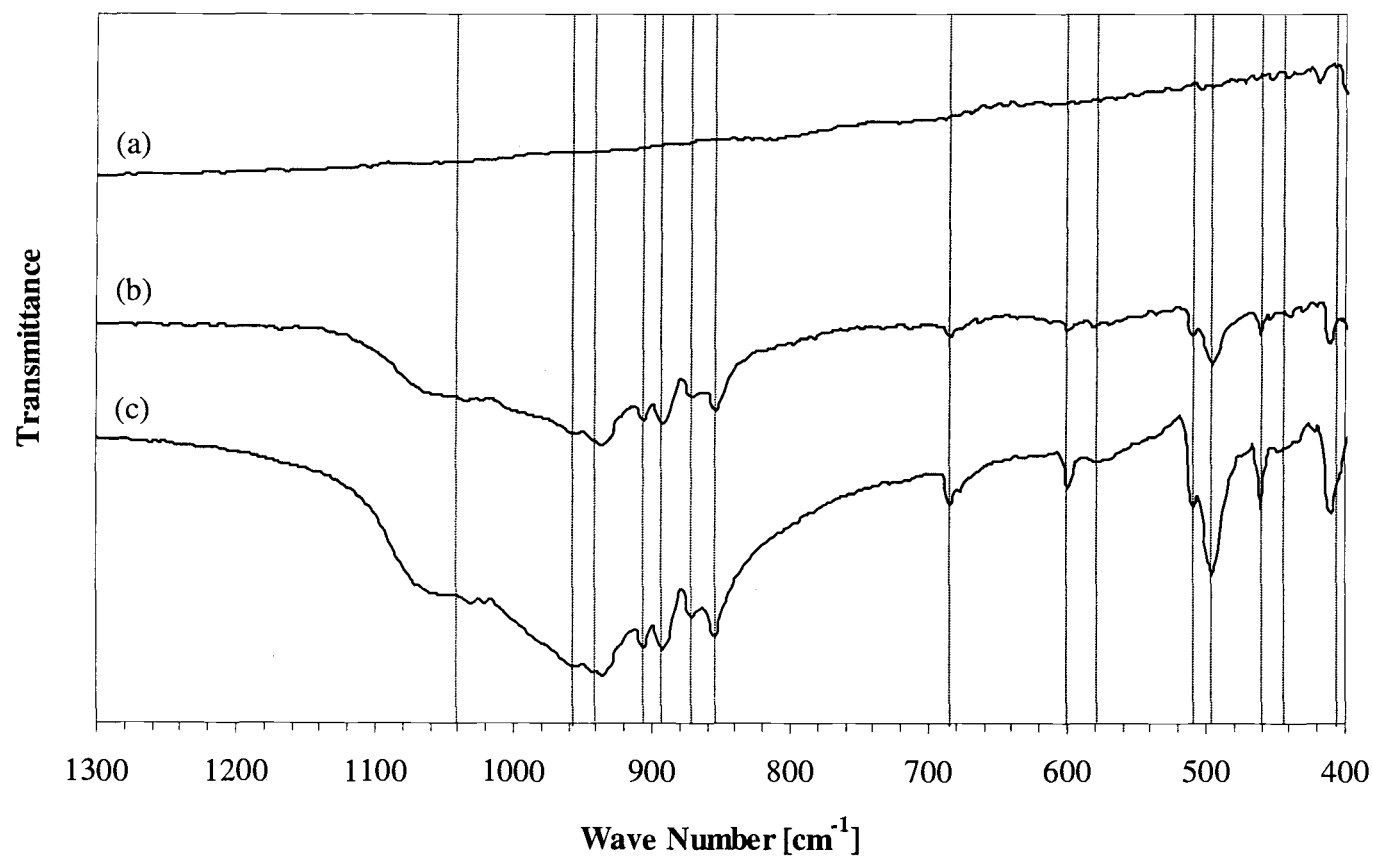


Figure 4.32 IR spectra of products in the nitridation at 1200 and 1300°C: (—) – absorption bands for Si_3N_4 .
 (a) raw material; (b) 3-hr nitridation at 1200°C with 5-min H_2 deficiency at the beginning; (c) 3-hr nitridation at 1300°C with H_2 .

4.3.5 Formation of Protective Film

The observations described in the preceding sections imply that a thin protective film is formed when uncovered silicon grains are exposed to nitrogen without hydrogen. This film can not be removed even in the presence of hydrogen and hinders the subsequent nitridation.

The major difference between the nitridation with and the nitridation without hydrogen is the oxygen partial pressure. The oxygen concentration in the nitrogen gas used for this study is about 5 ppm, measured by a Portable Trace Oxygen Analyzer, Teledyne Analytical Instruments Model #311. In the presence of 10% hydrogen, the oxygen partial pressure drops to a level on the order of magnitude of 10^{-12} atm because of the reaction between oxygen and hydrogen to form water vapor. According to the stability field diagram (Figure 4.22), at a nitrogen partial pressure around 1 atm and this low level of oxygen partial pressure, silicon nitride is always the stable phase at all temperatures investigated in this study.

However, when there is no hydrogen in the reaction gas, the oxygen partial pressure is that of impurity oxygen, on the order of magnitude of 10^{-6} atm. It is then suspected that the formation of the protective film is attributed to the impurity oxygen in the nitrogen. The results from both the EDX and IR analyses also indicate the presence of oxygen in the solid products of nitridation without hydrogen. The stability field diagram suggests that the stable equilibrium phase at this level of oxygen partial pressure varies with temperature, i.e. a mixed phase of silicon dioxide

and silicon oxynitride at temperature lower than 1250°C, silicon oxynitride at 1300°C and silicon nitride or silicon oxynitride or a silicon nitride/silicon oxynitride mixture at 1350°C.

When uncovered silicon granules are exposed to nitrogen without hydrogen at 1200°C or 1250°C, a mixed phase of silicon dioxide and silicon oxynitride is predicted to form on the surface of silicon. Grain boundaries between silicon dioxide and silicon oxynitride may provide easy path for transport of nitrogen to react with silicon underneath in the following nitridation. Then, with grain boundaries present in the layer formed during the hydrogen interruption, the spallation of the nitrided layer formed in the subsequent nitridation is possible, which is proposed to be a key for the nitridation process [Koike and Kimura, 1996]. Moreover, since the temperature is low, the formation of the protective film may not reach an effective thickness within a short period of time. Consequently, the subsequent nitridation can proceed smoothly, resulting in a 3-hour conversion that is not significantly different from that in the nitridation with uninterrupted hydrogen.

On the other hand, when silicon granules are exposed to nitrogen without hydrogen at 1300°C or 1350°C, only silicon oxynitride is expected to grow on the surface of silicon. Due to its denser atomic structure, silicon oxynitride has been shown to be a superior diffusion barrier than silicon dioxide [Du, *et al.*, 1989; Ito, *et al.*, 1980]. During the oxidation of silicon nitride, a thin layer of silicon oxynitride is found in between the silicon nitride and external silicon dioxide layers and it is believed to attribute to the superior oxidation resistance of silicon nitride [Du, *et al.*,

1989]. The diffusivity of oxygen in silicon oxynitride ($9.27 \times 10^{-11} \text{ cm}^2/\text{s}$, at 1300°C) is at least two order of magnitude smaller than the diffusivity of oxygen in silicon dioxide at the same temperature ($5.00 \times 10^{-8} \text{ cm}^2/\text{s}$, at 1300°C) [Du, *et al.*, 1989].

Although there is no report on either the diffusivity of nitrogen in silicon oxynitride or the diffusivity of oxygen in silicon nitride, it is likely that the diffusivity of nitrogen in silicon nitride ($3.82 \times 10^{-8} \text{ cm}^2/\text{s}$, at 1300°C) [Kijima and Shirasaki, 1976] is much larger than the diffusivity in silicon oxynitride, being implied by the observation that the diffusion rates of oxygen and nitrogen in silica are on the same order of magnitude [Barrer, 1934]. It should be noted that Kijima and Shirasaki [1976] reported two values of diffusivity of nitrogen in silicon nitride, i.e. for the diffusion along grain boundaries of polycrystalline silicon nitride and/or the diffusion in the bulk of single crystal, while values reported by Du *et al.* [1989] are for bulk silicon oxynitride which is not single crystal. The diffusivity for polycrystalline is used in the comparison described earlier, because it is unlikely for a single crystal to form in the present study.

Thus, it is implied that the diffusion of nitrogen during the subsequent nitridation is limited due to the presence of silicon oxynitride layer. Moreover, if silicon oxynitride forms as a protective thin layer on the silicon surface, the nitrided product can not build up to the thickness that is thick enough to have high stress for the outer shell to peel off, as described in the spallation process [Koike and Kimura, 1996]. Therefore, the subsequent nitridation becomes an extremely slow process and

the 3-hour conversion is much lower than that from the nitridation with uninterrupted hydrogen.

However, for the reaction at 1350°C which is located close to the Si_3N_4 - Si_2ON_2 boundary in the stability field diagram than 1300°C, the protective layer may contain a small amount of silicon nitride grains which consequently create grain boundaries, leading to the faster subsequent nitridation, as indicated by the higher 3-hour overall conversion from the reaction at 1350°C (Figure 4.30).

4.4 EFFECTS OF OXIDE LAYER IN THE ABSENCE OF HYDROGEN

4.4.1 Effects of Oxide Layer in the Nitridation without Hydrogen at 1300°C

As discussed in the preceding section, a protective layer is formed during the exposure of uncovered silicon granules to nitrogen without hydrogen.

Characteristics of this layer depend upon the temperature of its formation. At 1300°C, the protective film is suspected to be silicon oxynitride which is a stronger diffusion barrier than silicon dioxide. However, it is also found that the hindering effect of the protective layer varies with pretreatment conditions, i.e. an amount of native oxide layer on the surface of silicon (Figure 4.33). In Figure 4.33, silicon granules pretreated for various periods of time at 1300°C were exposed to nitrogen

without hydrogen, followed by the 3 hours of nitridation at 1300°C with 10% hydrogen.

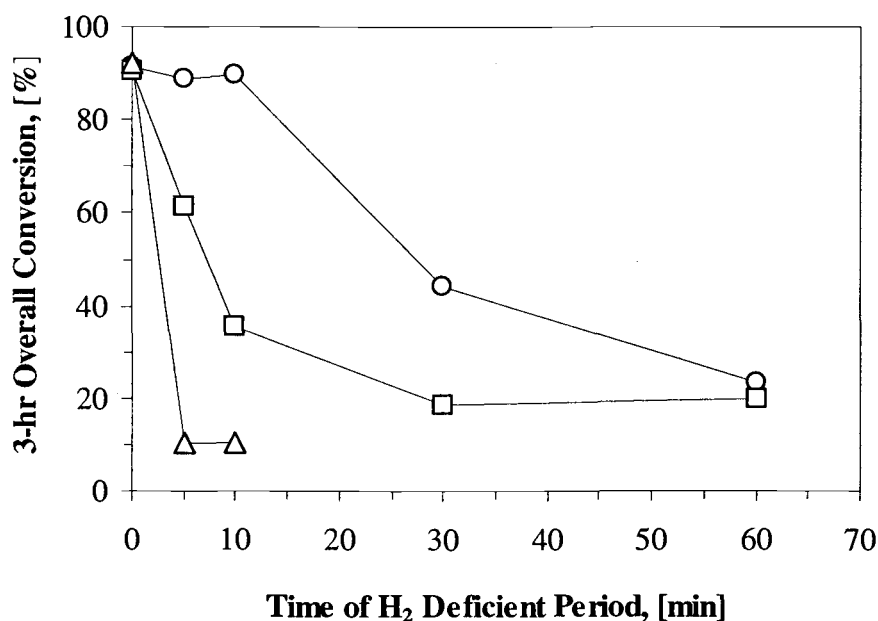


Figure 4.33 Effects of hydrogen interruption at 1300°C under different pretreatment conditions: (O) – no pretreatment; (□) – 1-hr pretreatment; (Δ) – 6-hr pretreatment.

When silicon grains are first exposed to nitrogen without hydrogen at 1300°C for only 5 minutes, the subsequent nitridation is effectively inhibited if the silicon granules have been pretreated for 6 hours. However, no such effect is observed when untreated silicon granules are used. The 3-hour overall conversion from a sample which has experienced no pretreatment is roughly the same as that from the nitridation with uninterrupted hydrogen (time of H₂ deficient period of 0 minute).

Nevertheless, when the length of hydrogen interruption is increased beyond 10 minutes, a decrease in the 3-hour conversion from the untreated sample is eventually observed. The longer the hydrogen interruption period, the lower the conversion achieved.

The results shown in Figure 4.33 suggest that the native oxide layer may inhibit (or interfere with) the formation of the protective layer during the no-hydrogen period. As discussed earlier, the removal of native oxide, as described by reaction (A'), should be patch-wise. During the pretreatment, the native oxide layer is reduced into islands of silicon dioxide, revealing silicon surface underneath. As the pretreatment progresses, the size of the oxide islands decreases, and finally all oxide is removed after a long enough pretreatment time. The longer the pretreatment period, the smaller the area covered with the native oxide. Because the native oxide occupies part of particle surface and may act like a diffusion barrier to the reactive species transport, the protective layer would form on the uncovered surface first. If the hydrogen interruption period is short, the native oxide islands remain un-removed. Then, during the subsequent nitridation with hydrogen, the native oxide is removed in the presence of hydrogen in the nitridation gas mixture as described in the preceding section, revealing the silicon surface underneath, and the nitridation continues. However, since the removal of oxide layer depends only on the partial pressure of SiO close to Si/SiO_2 interface, the native oxide can be removed in nitrogen during the hydrogen interruption period as well. Thus, if the hydrogen depletion period is long enough, the native oxide is removed and

uncovered silicon surface comes into direct contact with nitrogen without hydrogen, resulting in the formation of the protective layer.

4.4.2 Effects of Oxide Layer in the Nitridation without Hydrogen at Different Temperature

Effects of hydrogen interruption and oxide layer at different reaction temperatures are shown in Figures 4.34 to 4.37. The hydrogen feed was stopped for 5 minutes after the 6-hour pretreatment. The pretreatment temperature for all runs is fixed at 1300°C. Only the reaction temperature is changed.

The results shown in Figure 4.34 and Figure 4.35 agree with the findings in the preceding section. The effect from hydrogen interruption at low temperature (1200 and 1250°C) is generally not as vital as that at high temperature. Although slight decrease in the 3-hour overall conversion is observed, the levels of conversion in the nitridation with a 5-minute hydrogen interruption are relatively close to those in the nitridation with uninterrupted supply of hydrogen, especially at 1200°C, regardless of the pretreatment conditions.

On the other hand, the effectiveness of the protective layer formed during the 5-minute exposure to nitrogen without hydrogen at high temperatures (1300 and 1350°C) varies with pretreatment conditions. The more oxide on the surface, the less

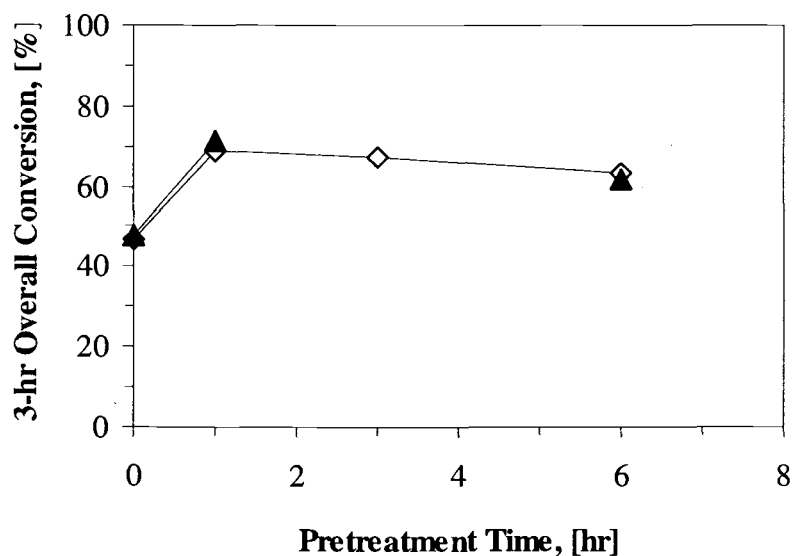


Figure 4.34 Effects of hydrogen interruption in the nitridation at 1200°C with various pretreatment times: (▲) – nitridation with 5-min H₂ deficiency; (◇) – nitridation with uninterrupted H₂.

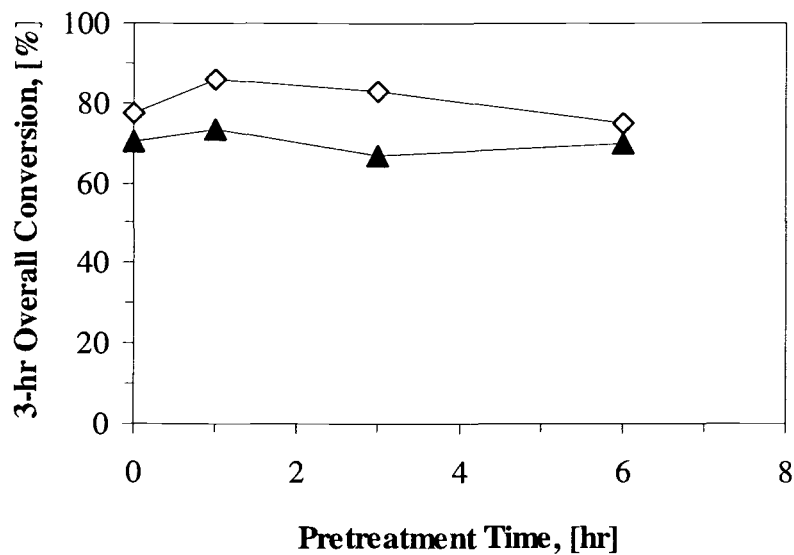


Figure 4.35 Effects of hydrogen interruption in the nitridation at 1250°C with various pretreatment times: (▲) – nitridation with 5-min H₂ deficiency; (◇) – nitridation with uninterrupted H₂.

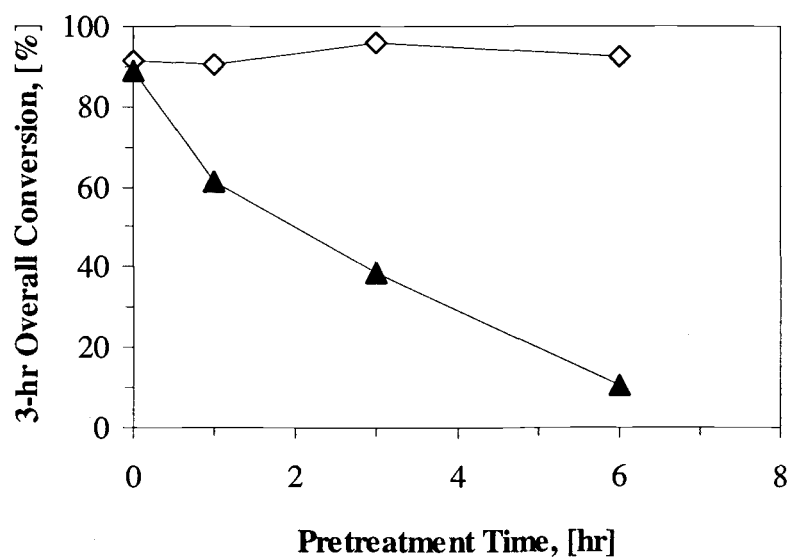


Figure 4.36 Effects of hydrogen interruption in the nitridation at 1300°C with various pretreatment times: (▲) – nitridation with 5-min H₂ deficiency; (◇) – nitridation with uninterrupted H₂.

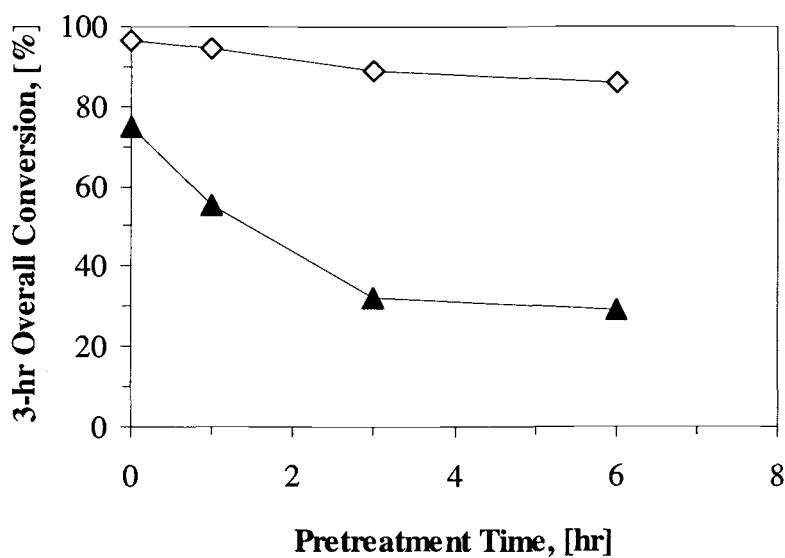


Figure 4.37 Effects of hydrogen interruption in the nitridation at 1350°C with various pretreatment times: (▲) – nitridation with 5-min H₂ deficiency; (◇) – nitridation with uninterrupted H₂.

effective for inhibiting the further nitridation. The masking effect by the native oxide is suggested. As seen in Figure 4.36 and Figure 4.37, for both 1300 and 1350°C, the conversions obtained from untreated samples are much higher than those from pretreated samples. The conversion obtained from the nitridation at 1300°C with hydrogen interruption of untreated silicon is approximately the same as that from the nitridation with uninterrupted hydrogen. It should be noted that, in case of the reaction at 1350°C using untreated silicon, the conversion obtained from the nitridation with hydrogen interrupted is quite lower than the conversion obtained from the nitridation with uninterrupted hydrogen because some native oxide could be removed during the heating up process from the pretreatment temperature (1300°C) to the reaction temperature (1350°C). The protective film can form on the surface that is partly uncovered during the heating-up and inhibits the subsequent nitridation to greater extent than that at 1300°C.

For pretreated samples, once the native oxide is partially removed by the pretreatment, the protective layer is easily formed during the nitridation without hydrogen because the reaction of silicon with nitrogen and oxygen at these high temperature is more spontaneous. The protective film can build up within a short period of time. As the results, the following nitridation, after silicon is exposed to nitrogen without hydrogen, is limited and the 3-hour conversion observed is low.

The results can also be displayed as a function of temperature, in the same fashion as shown earlier in Figure 4.30. In Figure 4.38, 3-hour overall conversions are plotted against the reaction temperature, in which the nitridation of silicon

granules pretreated at 1300°C were carried out after exposing them to nitrogen without hydrogen for 5 minutes.

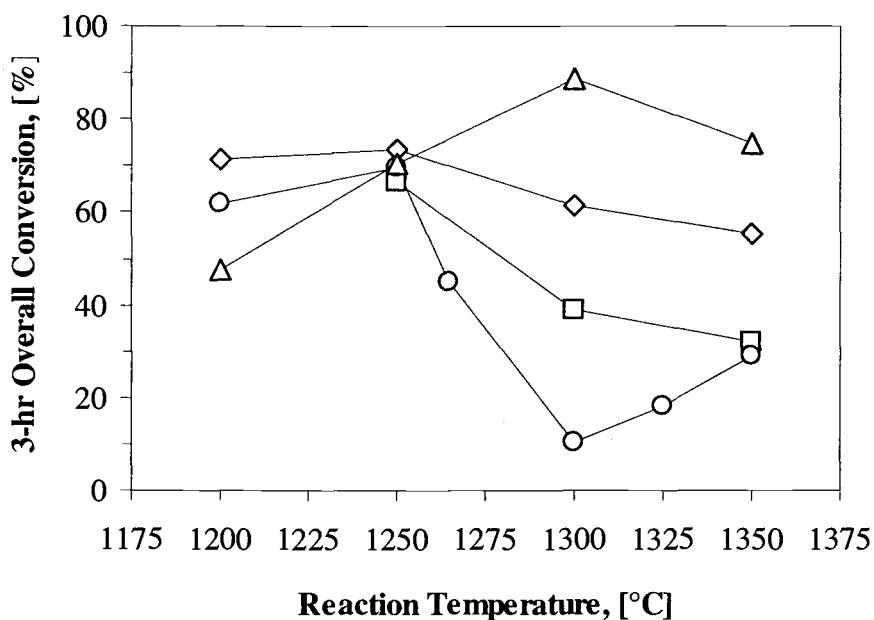


Figure 4.38 Effects of hydrogen interruption at different temperatures under different pretreatment conditions:
 (Δ) – no pretreatment; (◇) – 1-hr pretreatment; (□) – 3-hr pretreatment; (○) – 6-hr pretreatment.

For untreated samples, majority of the surface is still covered with the native oxide which masks the formation of the protective layer. Thus, the protective layer forms on only small portion of the surface, i.e. in cracks or defects on the surface. Once the hydrogen is resumed, the native oxide that covers majority of the surface is removed and the subsequent nitridation can smoothly continue. The higher the

reaction temperature, the more efficient the removal of the native oxide, resulting in a higher conversion in the subsequent nitridation at higher temperature. However, when the reaction temperature is 1350°C, some oxide may be removed during the heating-up process from the pretreatment temperature (1300°C) to the reaction temperature. Hence, more surface is covered with the protective layer and less conversion, compared to that from the reaction at 1300°C, is achieved.

For samples having experienced 1-hour pretreatment, a less amount of native oxide remains on the surface after the pretreatment, compared to untreated samples. Thus, a bigger area is covered by the layer of product formed during the hydrogen interruption period. Because the product formed when silicon is exposed to nitrogen (and oxygen) without hydrogen at 1200 and 1250°C does not effectively hinder the further nitridation, and because less native oxide is left on the surface, a higher conversion is achieved in the subsequent nitridation at low temperatures than that of untreated samples. However, at high reaction temperatures (1300 and 1350°C), the product formed during the hydrogen interruption period is a very strong diffusion barrier. The subsequent nitridation at 1300 and 1350°C is more difficult than the case of untreated samples, especially for the reaction at 1350°C where the formation of the protective layer is more spontaneous, resulting in a decrease in the conversion achieved. Nevertheless, the 3-hour conversions are not very low because part of silicon surface is covered with the native oxide which is then removed during the subsequent nitridation, providing fresh silicon for the nitridation.

For samples having experienced 3-hour pretreatment, the results indicate that there is native oxide remaining. Thus, it is the same scenario as the case of 1-hour pretreatment. The only difference is that the amount of native oxide on the surface is less than that after 1-hour pretreatment. So, bigger part of the surface is covered by the protective film, resulting in a lower conversion achieved at high temperatures.

For the samples with 6-hour pretreatment, all or almost all of the native oxide is expected to be removed. The extent of nitridation after 5-minute exposure to nitrogen without hydrogen depends on the nature of the product formed during that 5-minute exposure, as discussed in more detail in the preceding section.

Finally, it is found that the effect of the exposure to nitrogen without hydrogen increases with exposure time, until 30 minutes. For all temperatures investigated, the hydrogen interruption period longer than 30 minutes does not result in a lower conversion than the conversion from the nitridation with 30-minute no-hydrogen period. The results are shown in Figure 4.39. All samples were pretreated at 1300°C for 1 hour.

At high reaction temperature (1350°C), a very abrupt decrease in the achieved conversion, compared to the run with uninterrupted supply of hydrogen (0-minute hydrogen interruption period), is observed when hydrogen is interrupted for only 3 minutes. However, the damage from a long hydrogen interruption period is roughly the same as that from the 3-minute no-hydrogen period. This result confirms that the formation of the protective film during the exposure of silicon to nitrogen without hydrogen at 1350°C is faster than at other temperatures. However,

since the conversion stays at a high level even though the hydrogen interruption period is extended to 60 minutes, it is suggested that the thickness of the protective film remains unchanged after the film is formed. During the subsequent nitridation with hydrogen, the native oxide layer is removed and the nitridation progresses.

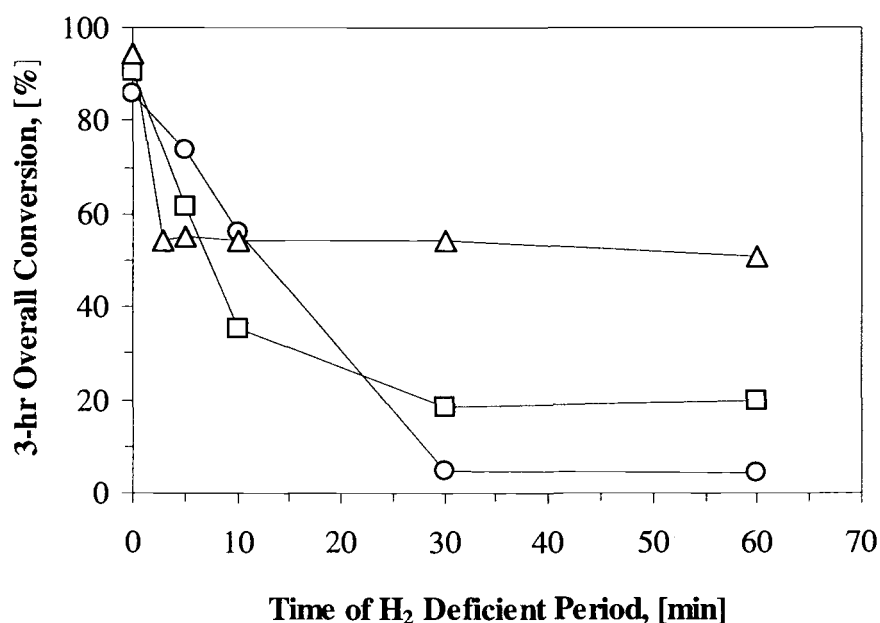


Figure 4.39 Effects of hydrogen interruption time at various temperatures under different pretreatment conditions: (Δ) – nitridation at 1350°C; (□) – nitridation at 1300°C; (○) – nitridation at 1250°C.

For the reaction at 1250°C, the 3-hour conversion slowly decreases as the hydrogen interruption period is extended. These results suggest that the formation of protective layer from the exposure of silicon to nitrogen without hydrogen at 1250°C is slow. The longer the hydrogen interruption period, the thicker the protective film and the lower conversion achieved.

4.5 CATALYTIC EFFECTS OF METALS

As mentioned earlier, one of the purposes of this work was to achieve high content of α -silicon nitride in the product from the direct nitridation of silicon. One of the most apparent factors that affect α -/ β -phase formation is the presence of metals in silicon. In this section, the effects of various transition metals on the nitridation of silicon are investigated, using a tubular flow reactor operated at three temperatures, i.e. 1200°C, 1250°C and 1300°C. The nitridation was conducted for 3 hours in a stream of nitrogen with 10% hydrogen, after 1 hour of pretreatment in a stream of argon with 10% hydrogen at the same temperature as the reaction temperature. The metals that enhanced the content of α -phase in the product were further studied under extended reaction conditions.

4.5.1 Calcium

Figure 4.40 indicates that an addition of a small amount of calcium, as low as 0.125%, significantly promotes the conversion of silicon to α -silicon nitride at 1300°C and suppresses the conversion of silicon to β -silicon nitride. The contents of β -silicon nitride in the products obtained from the nitridation of calcium-impregnated granules were too small to be detected from the XRD patterns in the majority of cases studied. However, the overall conversion decreases when the content of calcium increases to 1% or higher.

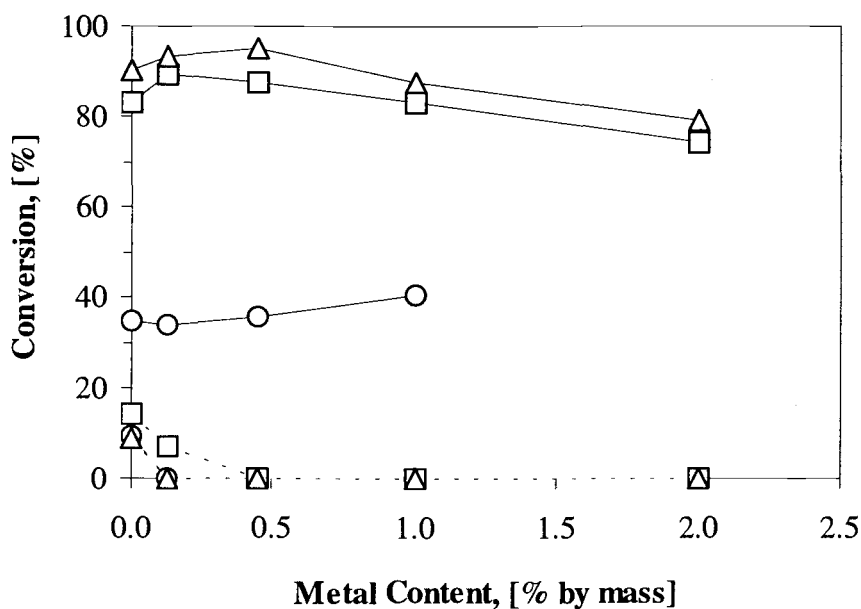


Figure 4.40 Nitridation of calcium impregnated silicon:
 (O) – nitridation at 1200°C; (□) – nitridation at 1250°C;
 (Δ) – nitridation at 1300°C; (—) – conversion to α -phase;
 (---) – conversion to β -phase.

The nitridation of bare silicon granules at 1300°C reaches a stage of very slow progress in about 3 hours [Jovanovic, *et al.*, 1994]. The same phenomena are also observed in the nitridation of calcium-impregnated silicon granules. The overall conversion slightly increases when the reaction time is extended from 3 hours to 6 hours, while the content of β -silicon nitride remains undetectable (Figure 4.41).

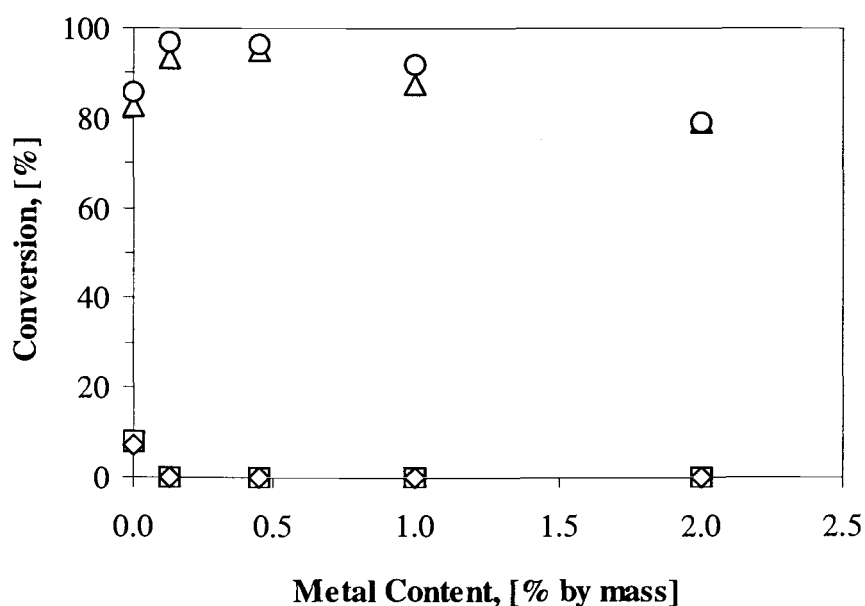


Figure 4.41 Nitridation at 1300°C of calcium impregnated silicon for 3 and 6 hours:
 (Δ) – conversion to α -phase from 3-hr nitridation;
 (\square) – conversion to β -phase from 3-hr nitridation;
 (\circ) – conversion to α -phase from 6-hr nitridation;
 (\diamond) – conversion to β -phase from 6-hr nitridation.

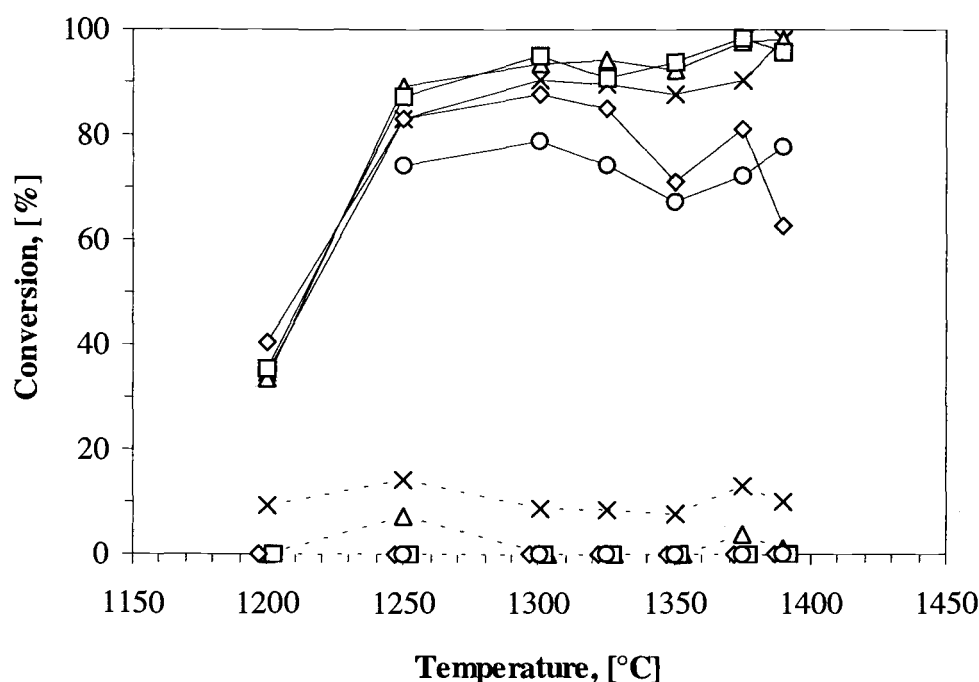


Figure 4.42 Nitridation of calcium impregnated silicon as a function of temperature: (X) – bare silicon; (Δ) – 0.125% Ca; (□) – 0.45% Ca; (◇) – 1.0% Ca; (○) – 2.0% Ca; (—) – conversion to α -phase (----) – conversion to β -phase. Noted that some data points are intentionally shifted in X-direction for clarity.

Because calcium was found to be effective in terms of enhancing the formation of α -silicon nitride, the range of reaction temperature coverage was extended to 1390°C for further investigating its behavior. The results shown in Figure 4.42 indicates that the fraction of β -phase in the product silicon nitride stays at negligibly low level, for the whole range of reaction temperature and calcium content investigated. However, the overall conversion of silicon varies with the reaction temperature and calcium content. Raising the reaction temperature with an

addition of 0.125-0.45% calcium is still effective in both the aspects of promoting the overall conversion toward 100% and suppressing the formation of β -silicon nitride. An addition of higher amounts of calcium presents adverse effects on the progress of nitridation.

Calcium is the metal, among all the metals investigated, that enhances only the formation of α -silicon nitride. Although almost pure α -silicon nitride can be obtained by impregnating silicon with a very small amount of calcium (0.125%), there may be degradation in the high-temperature strength of sintered silicon nitride parts. It was found that an addition of CaO significantly increased the amount of non-elastic deformation occurring prior to fracture and decreased the flexural strength at elevated temperature (1400°C) of hot-pressed silicon nitride, even though it had no apparent effect on the room temperature mechanical properties [Iskoe, *et al.*, 1976]. It has also been reported that the subcritical crack-growth resistance as well as the creep resistance of silicon nitride doped with small amounts of calcium (80-450 ppm) is significantly reduced [Tanaka, *et al.*, 1995]. Further study is needed to verify the usefulness of silicon nitride containing calcium.

4.5.2 Yttrium

Figure 4.43 indicates that yttrium is another metal that suppresses the β -silicon nitride formation. β -silicon nitride is hardly detected from the X-ray

diffraction patterns of products obtained when silicon granules impregnated with 1% yttrium of higher are nitrided at 1300°C. However, the overall conversion of yttrium-impregnated silicon is always lower than that of bare silicon. The more yttrium added, the lower the overall conversion at any temperature investigated.

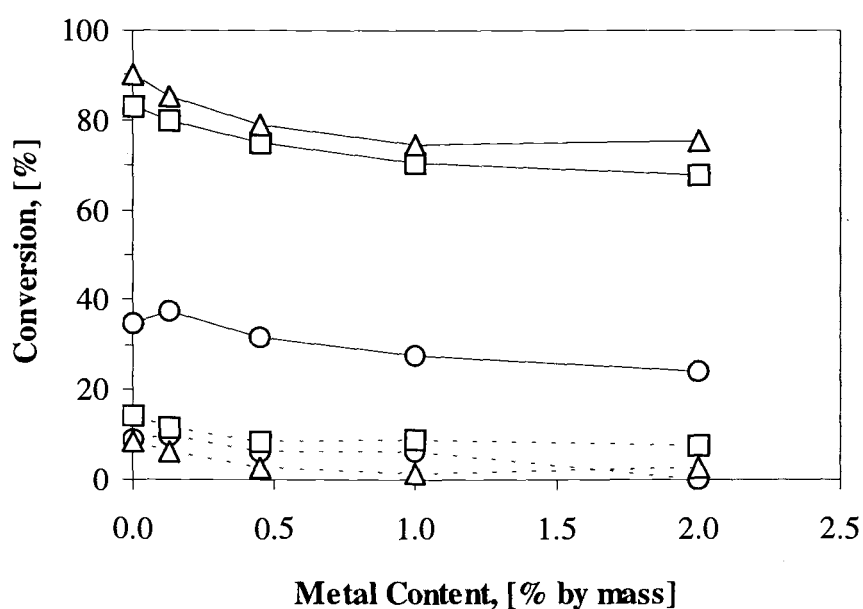


Figure 4.43 Nitridation of yttrium impregnated silicon:
 (○) – nitridation at 1200°C; (□) – nitridation at 1250°C;
 (△) – nitridation at 1300°C; (—) – conversion to α-phase;
 (---) – conversion to β-phase.

A longer reaction time of 6 hours was used to investigate any change in α- and β-silicon nitride contents in the product obtained from yttrium impregnated silicon as well. Figure 4.44 shows that the conversion after 6 hours of reaction is

slightly higher than the conversion obtained in 3 hours, while the content of α -silicon nitride does not change appreciably.

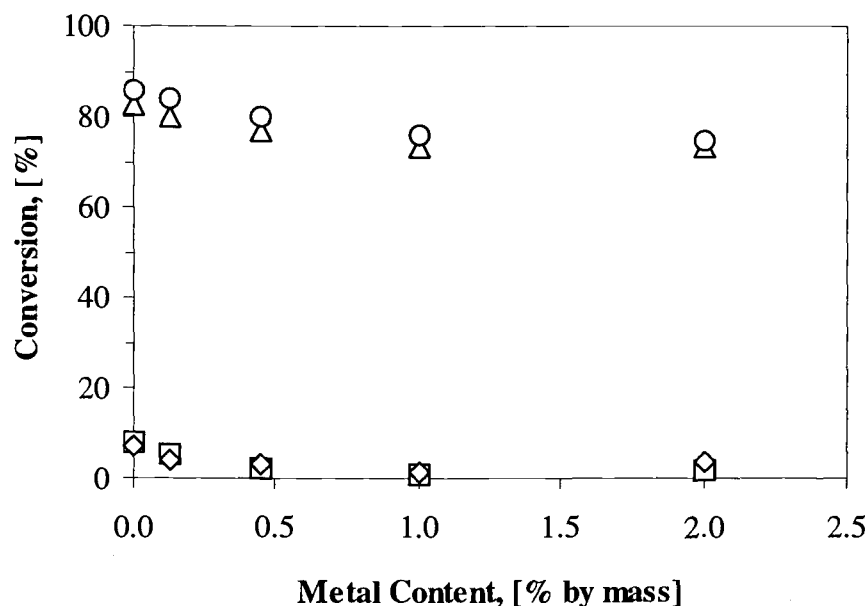


Figure 4.44 Nitridation at 1300°C of yttrium impregnated silicon for 3 and 6 hours:
 (\triangle) – conversion to α -phase from 3-hr nitridation;
 (\square) – conversion to β -phase from 3-hr nitridation;
 (\circ) – conversion to α -phase from 6-hr nitridation;
 (\diamond) – conversion to β -phase from 6-hr nitridation.

The range of the reaction temperature coverage was extended to 1390°C for further study of the behavior of yttrium, since yttrium could suppress the formation of β -silicon nitride. The results show that the overall conversion of silicon impregnated with yttrium follows the behavior of the bare silicon nitridation. The

overall conversion tends to decrease around 1350°C, above which it increases with temperature. The conversions achieved from yttrium impregnated silicon are lower than that of bare silicon for all temperatures investigated. The tendency of decreasing overall conversion with an increase in the amount of yttrium addition becomes insignificant at high yttrium contents as the temperature goes higher. Nevertheless, the fraction of β -phase remains at low levels and decreases roughly with the yttrium content.

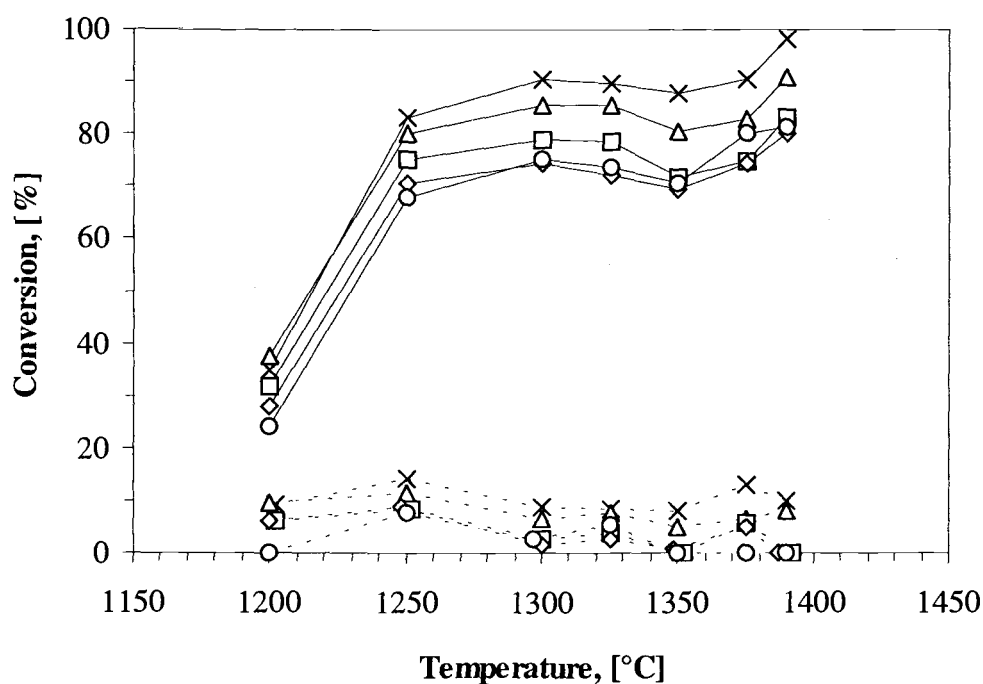


Figure 4.45 Nitridation of yttrium impregnated silicon as a function of temperature: (X) – bare silicon; (Δ) – 0.125% Y; (□) – 0.45% Y; (◇) – 1.0% Y; (○) – 2.0% Y; (—) – conversion to α -phase (---) – conversion to β -phase. Noted that some data points are intentionally shifted in X-direction for clarity.

Because yttria (Y_2O_3) is a common sintering aid for silicon nitride, yttrium unlikely causes deterioration in the physical properties of sintered products. However, further study is needed to investigate effects of yttrium on physical properties of sintered products.

4.5.3 Iron

The yield of β -silicon nitride from iron impregnated silicon is higher than that from silicon impregnated with other metals investigated, which agrees with the previous finding by Pigeon *et al.* [1993]. It is obvious that iron enhances the β -silicon nitride formation, and with an increase in iron the content of β -silicon nitride becomes as high as double the content of β -phase in the product from bare silicon at 1300°C. The increase in β -phase formation with iron, when the addition of iron is less than 1% agrees with the results obtained in the same range by Boyer and Moulson [1978]. However, this study indicates that the yield of β -silicon nitride levels off for iron contents higher than 1%.

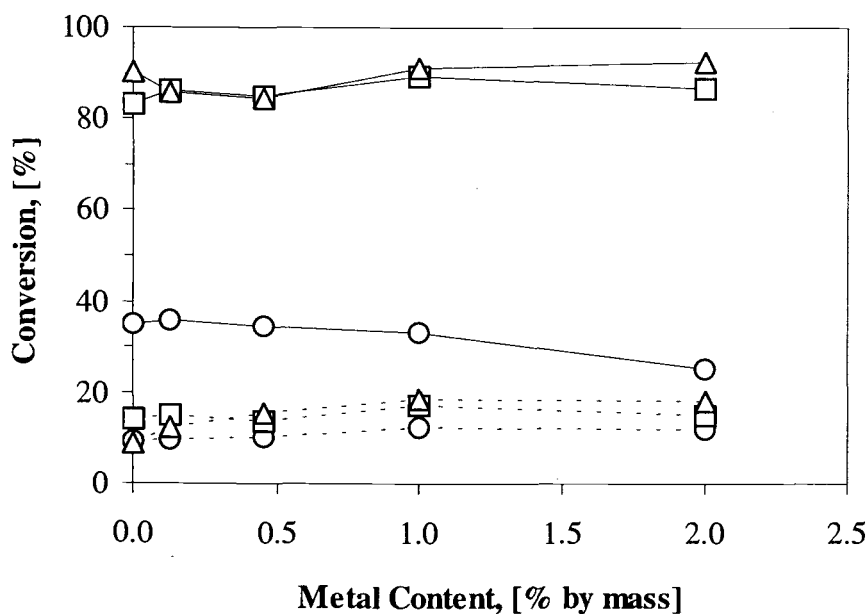


Figure 4.46 Nitridation of iron impregnated silicon:
 (○) – nitridation at 1200°C; (□) – nitridation at 1250°C;
 (△) – nitridation at 1300°C; (—) – conversion to α -phase;
 (----) – conversion to β -phase.

4.5.4 Copper

None of the metals discussed above is effective in enhancing the nitridation at low temperature. On the other hand, the impregnation with copper significantly increases the overall conversion at low temperature. Copper is the metal, among all the metals investigated, that enables the nitridation of silicon at 1150°C. No silicon nitride was found from 3-hour nitridation of bare silicon at 1150°C, while α -silicon nitride about 35% by mass was found from copper impregnated samples. Moreover,

as shown in Figure 4.47, the nitridation of silicon with 0.125% copper at 1200°C yields an overall conversion as high as almost double that from bare silicon. The overall conversion at 1200°C also increases with the copper content and approaches the conversion level achieved in the nitridation of bare silicon at 1250°C. In addition to the enhancement of the nitridation, the formation of β -silicon nitride is also suppressed when silicon granules with a high amount of copper are nitrided at 1200°C.

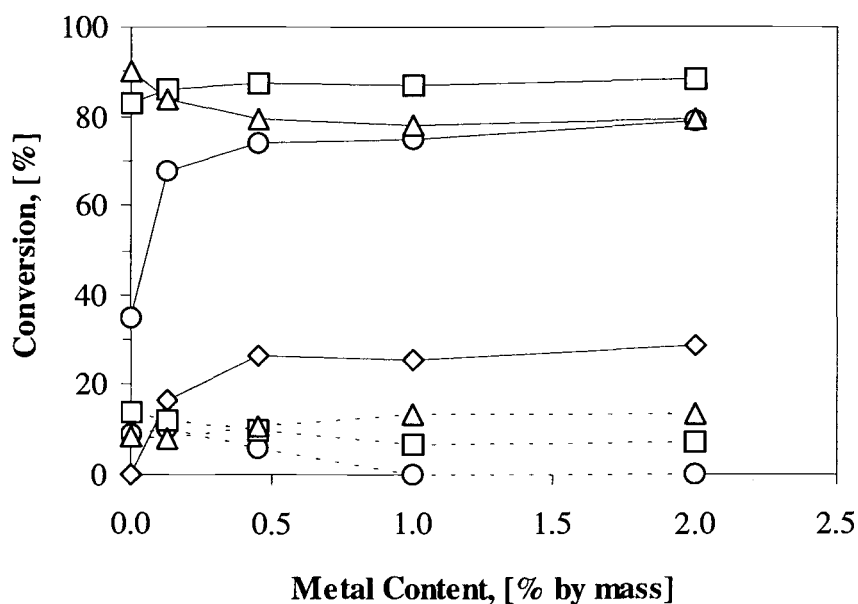


Figure 4.47 Nitridation of copper impregnated silicon:
 (\diamond) – nitridation at 1150°C; (\circ) – nitridation at 1200°C;
 (\square) – nitridation at 1250°C; (\triangle) – nitridation at 1300°C;
 (—) – conversion to α -phase; (---) – conversion to β -phase.

The enhancement of nitridation by copper decreases with temperature. The overall conversion of silicon as well as the yield of α -silicon nitride at 1250°C is only slightly higher than the observations in the bare silicon nitridation. At 1300°C, the overall conversion is even lower than that from bare silicon. Copper also tends to enhance the growth of β -silicon nitride at 1300°C while it suppresses the β -phase formation at 1200°C.

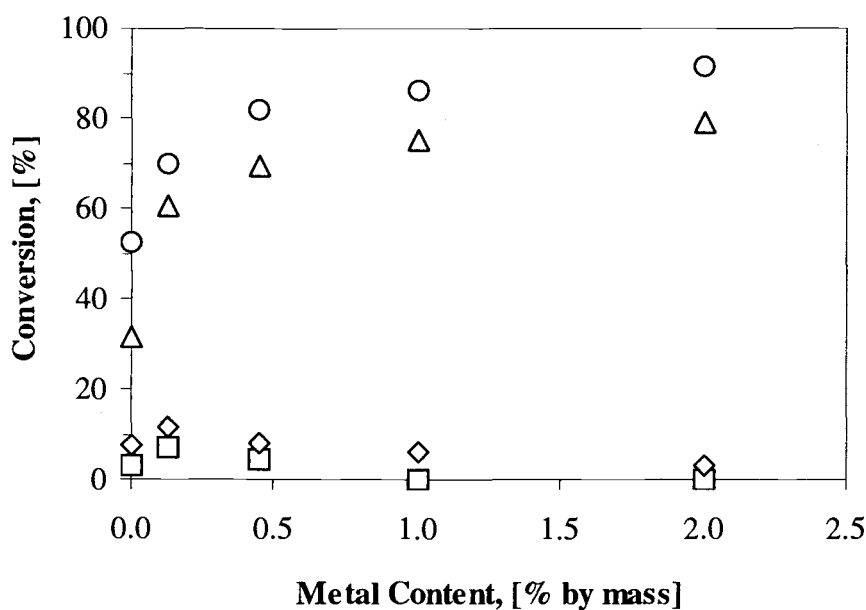


Figure 4.48 Nitridation at 1200°C of copper impregnated silicon for 3 and 6 hours:
 (Δ) – conversion to α -phase from 3-hr nitridation;
 (\square) – conversion to β -phase from 3-hr nitridation;
 (\circ) – conversion to α -phase from 6-hr nitridation;
 (\diamond) – conversion to β -phase from 6-hr nitridation.

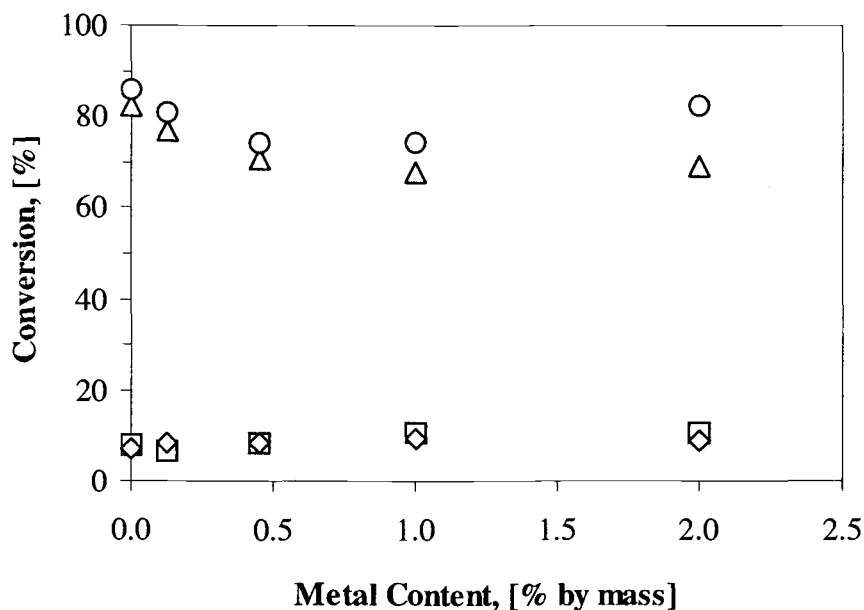


Figure 4.49 Nitridation at 1300°C of copper impregnated silicon for 3 and 6 hours:
 (Δ) – conversion to α -phase from 3-hr nitridation;
 (\square) – conversion to β -phase from 3-hr nitridation;
 (\circ) – conversion to α -phase from 6-hr nitridation;
 (\diamond) – conversion to β -phase from 6-hr nitridation.

When the reaction time is extended from 3 hours to 6 hours, the overall conversion of copper impregnated silicon at 1200°C increases by about 15% in the additional 3-hour nitridation, reaching as high as about 95%. Although the product obtained in the 3-hour nitridation is of almost 100% α -form, β -silicon nitride has been formed by 3.2% in the additional 3-hour nitridation. For the reaction at 1300°C, no significant change in conversion was observed from the additional 3-

hour nitridation, except when copper content is 2% in which the overall conversion increases by about 12%. Nevertheless, the conversion of 6-hour nitridation of 2% copper impregnated silicon is approximately the same as the conversion of 3-hour nitridation of bare silicon.

Copper has demonstrated most complex catalytic effects on the silicon nitridation. High level copper impregnation is very effective for the nitridation at low temperature in terms of achieving a high overall conversion and suppressing the β -phase formation. However, the effects of adding copper up to 2% on the properties of sintered silicon nitride parts are unknown. Further study is necessary.

4.5.5 Palladium

The effects of palladium on the nitridation of silicon are very similar to those of copper. It was found that the impregnation with palladium also considerably increases the overall conversion at low temperature, like the impregnation with copper, but the enhancement from palladium is not as much as copper. The overall conversions at 1200°C obtained from palladium impregnated samples are about 15% lower than the conversions obtained from the impregnation with copper with the same metal contents. However, the addition of palladium does not affect the content of α - or β -phase in the product silicon nitride. The phase composition of the silicon

nitride products obtained from palladium impregnated silicon is roughly the same as the product from bare silicon.

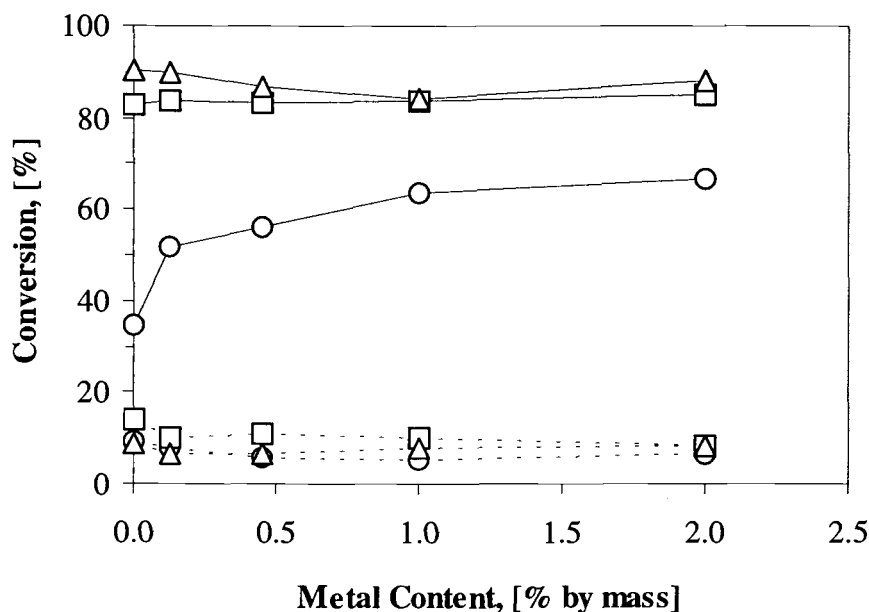


Figure 4.50 Nitridation of palladium impregnated silicon:
 (○) – nitridation at 1200°C; (□) – nitridation at 1250°C;
 (△) – nitridation at 1300°C; (—) – conversion to α-phase;
 (---) – conversion to β-phase.

The enhancement of nitridation by palladium also decreases with temperature, the same as in the case of copper. The overall conversion of palladium impregnated silicon at 1250°C is roughly the same as that from bare silicon, while the overall conversion at 1300°C is lower than that from bare silicon.

4.5.6 Chromium, Tungsten and Silver

Figures 4.51 to 4.53 indicate that tungsten and silver do not significantly influence the progress of silicon nitridation at all of the temperatures investigated while chromium demonstrates different behaviors depending on nitridation temperature. It should be noted that an addition of chromium at high content tends to decrease the fraction of α -silicon nitride at higher temperature, while the other two metals do not indicate such a tendency. The effects of these three metals will be discussed further in more detail in a later section.

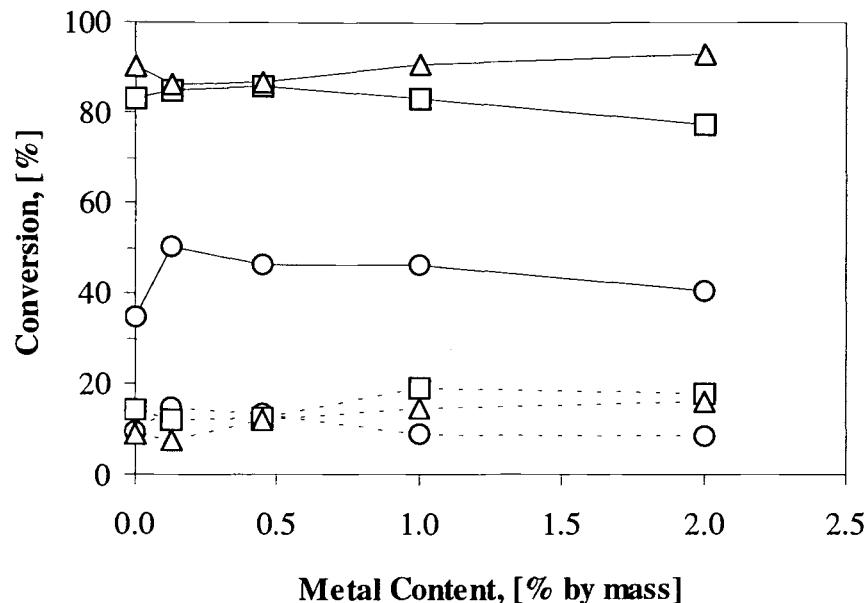


Figure 4.51 Nitridation of chromium impregnated silicon:
 (○) – nitridation at 1200°C; (□) – nitridation at 1250°C;
 (△) – nitridation at 1300°C; (—) – conversion to α -phase;
 (---) – conversion to β -phase.

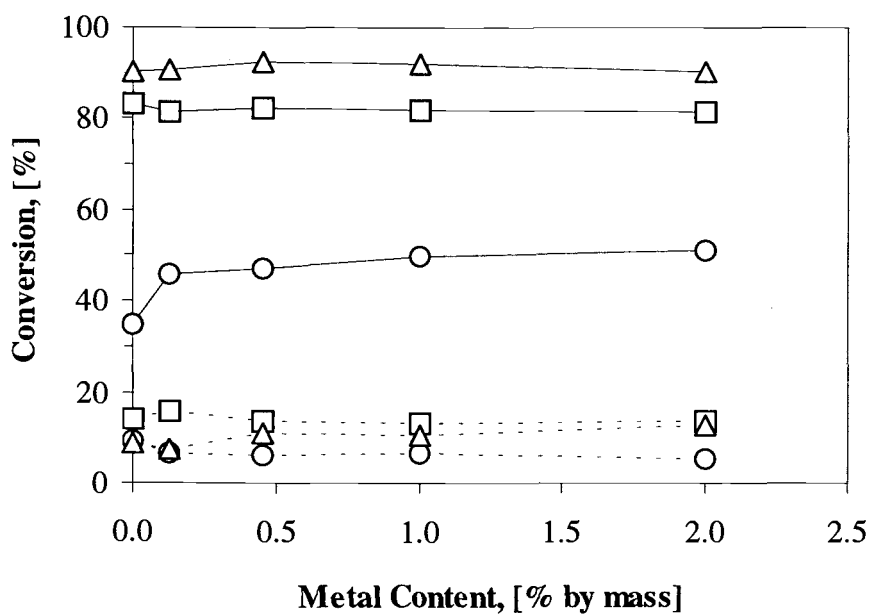


Figure 4.52 Nitridation of tungsten impregnated silicon:
 (○) – nitridation at 1200°C; (□) – nitridation at 1250°C;
 (△) – nitridation at 1300°C; (—) – conversion to α -phase;
 (---) – conversion to β -phase.

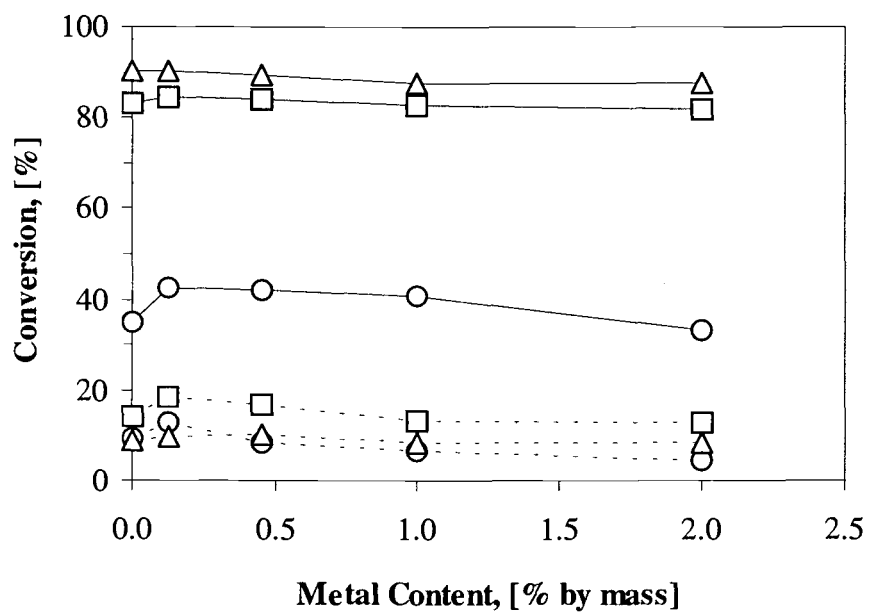


Figure 4.53 Nitridation of silver impregnated silicon:
 (O) – nitridation at 1200°C; (□) – nitridation at 1250°C;
 (Δ) – nitridation at 1300°C; (—) – conversion to α -phase;
 (---) – conversion to β -phase.

4.5.7 Summary for Catalytic Effects of Metals

Silicon granules impregnated with copper, calcium, iron, yttrium, palladium, chromium, tungsten and silver were nitrided in a stream of 90% nitrogen with 10% hydrogen at temperatures in the range of 1200-1300°C to investigate the catalytic effects of each metal on the direct nitridation of silicon. Only copper and palladium have shown a significant enhancement of the nitridation at 1200°C. The nitridation of silicon impregnated with copper or palladium at 1200°C yields the overall conversion that is almost double the conversion achieved by bare silicon. The formation of β -silicon nitride is also suppressed with an addition of copper, but no change in the α -/ β -phase content in the silicon nitride product is observed when palladium is added.

The comparison of the effects of each metal on the overall conversion and fraction of α -phase in the product obtained at 1250 and 1300°C are presented in Figure 4.54 and 4.55. Calcium enhances the formation of α -silicon nitride while it suppresses the formation of β -silicon nitride at negligibly low levels. Yttrium does not enhance the formation of α -phase, but it is effective in terms of suppressing the formation of β -silicon nitride when yttrium content is higher than 1%. Iron and chromium tend to enhance the formation of β -silicon nitride, especially at 1300°C and high metal content. Copper no longer enhances the nitridation at 1300°C. The overall conversion is lower than the conversion achieved by bare silicon and the

fraction of β -phase is increased. Silver, tungsten and palladium do not significantly influence the nitridation at 1250 and 1300°C.

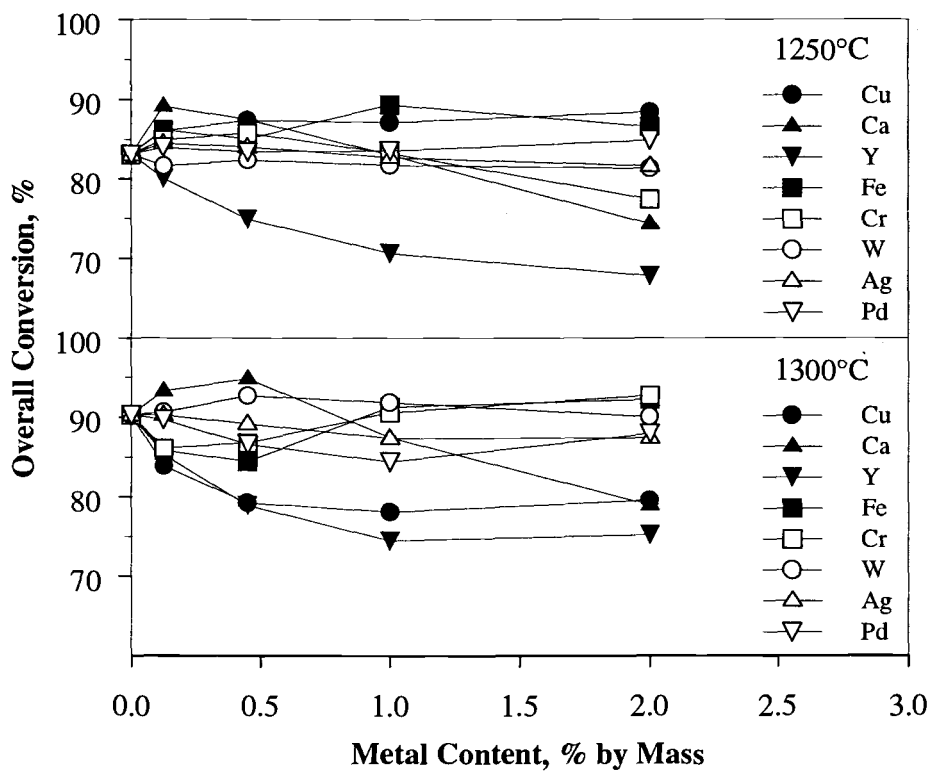


Figure 4.54 Comparison of overall conversions in the nitridation of silicon impregnated with various kind of metals.

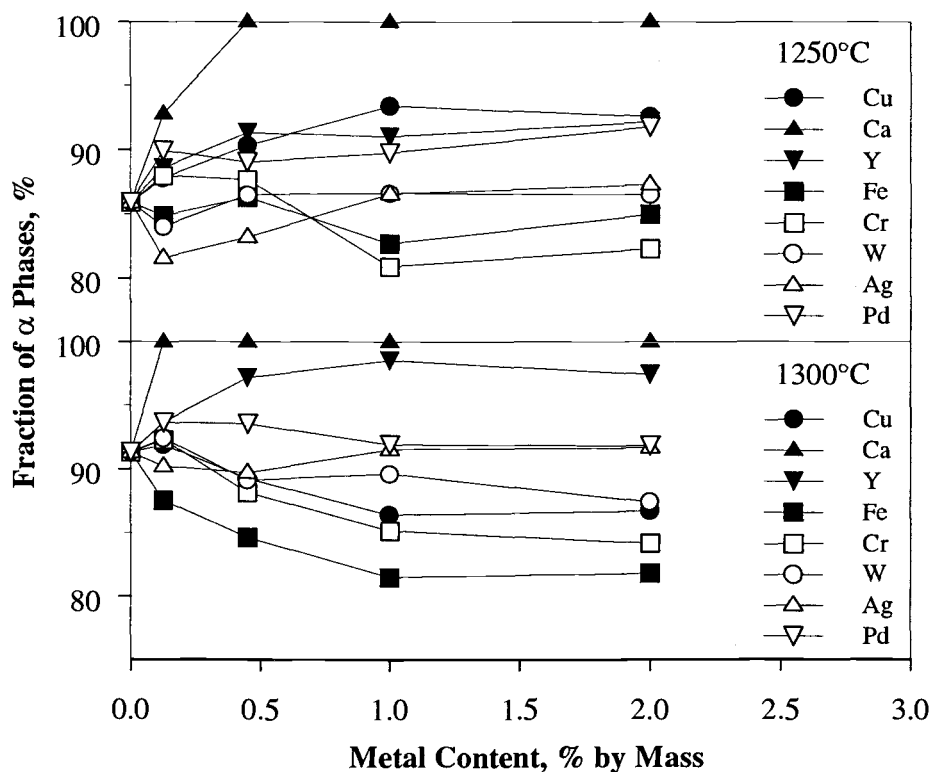


Figure 4.55 Comparison of the fraction of α -phase in the product from the nitridation of silicon impregnated with various kind of metals.

Both the X-ray and IR analyses for the products from the nitridation of silicon impregnated with metals in the range of 0.125 to 2.0% did not reveal the presence of any other compounds, beside silicon nitride. Since the amount of metal added to the granules is small, it is possible that the intensity of signals from any compounds formed (if formed) on the surface of silicon grains is too low to be detected. However, when the content of metal added to silicon is increased to a very

high level (up to 20%), extra peaks, other than those from silicon nitride, are detected. Nevertheless, it can not be concluded whether the compound attributed to those extra peaks will form on the surface of silicon grains when the content of the metal added to silicon granules is low. The results of study using high contents of metals are shown in Appendix B.

The X-ray photoelectron spectroscopy (XPS) was also used to characterize the surface of the product obtained from the nitridation of silicon granules impregnated with 1.0% yttrium. However, because no yttrium was detected on the surface, further analysis of other samples was not conducted. It is suspected that yttrium remains in the silicon phase, covered with the nitride phase which is thick enough so that yttrium is not detected by XPS. Further study is needed to identify where yttrium is actually located and in what form it is present.

4.5.8 Effects of Liquid Phase

As discussed earlier, various metals show different catalytic effects on the α - and β -silicon nitride formation. There is a hypothesis that the enhancement of α - or β -phase formation results from the liquid phase of melted alloys of silicon and metal impurities. As shown in Table 4.2, the reaction temperatures covered in this study (1200-1390°C) are in the range of the eutectic points of silicon-yttrium (1215-1710°C), silicon-iron (1200-1410°C) and silicon-palladium (821-1394°C) systems

[Massalski, 1986]. Hence, the presence of liquid phases depends on the concentration of metal in the alloy. Since the distribution of yttrium, iron or palladium in silicon grains is not known, it is not certain whether a liquid phase is present.

Table 4.2 Melting points and eutectic points for metal-silicon binary systems [Massalski, 1986].

Metal	Melting point of metal [°C]	Range of eutectic point [°C]
Silicon	1410	-
Calcium	842	792 - 1268
Chromium	1863	1305 - 1705
Copper	1084.87	802 - 859
Iron	1538	1200 - 1410
Palladium	1555	821 - 1394
Silver	961.93	835
Tungsten	3422	1390 - 2180
Yttrium	1522	1215 - 1710

In order to avoid the uncertainty regarding the presence of liquid phases, the nitridation of silicon impregnated with calcium, chromium, copper, silver and tungsten at 1300°C may be compared. This reaction temperature is higher than any of the eutectic points of calcium-, copper- and silver-silicon systems. On the contrary, this reaction temperature is lower than any of the eutectic points in the systems of chromium- and tungsten-silicon. Therefore, liquid phases are likely present in calcium-, copper- or silver-impregnated silicon while no liquid phase is expected in chromium- or tungsten-impregnated silicon.

The yields of α -silicon nitride from silver-impregnated silicon are roughly the same as those from tungsten-impregnated silicon, though a liquid phase may have occurred only in the silver-silicon system. The results imply that the presence of liquid phases may not be the dominant contributor to the enhancement of the α -silicon nitride formation. It has been shown earlier in this study that copper discourages the formation of α -silicon nitride at 1300°C, a much higher temperature than the eutectic points of copper-silicon alloys. These observations contrast the conclusion by Pigeon *et al.* [1993], based on the iron- and calcium-silicon systems with 0.3 atomic % metals, that liquid phases are significant contributors to the production of silicon vapor reacting with nitrogen to form α -silicon nitride, which is the dominant mode of the α -phase formation. This study implies that the characteristics of individual metals rather than the formation of liquid phases dominate the formation of α - or β -silicon nitride.

The results obtained in this study also suggest that the production of β -silicon nitride is not limited to the presence of liquid phases, as was postulated by Boyer and Moulson [1978], based on their results obtained when silicon with 0.0055 to 0.5% iron was nitrated at 1350°C. The enhancement of the β -silicon nitride formation is observed in the nitridation of chromium impregnated silicon while no β -silicon nitride is found in the product from calcium impregnated silicon, though a liquid phases is possible only in the calcium-silicon system.

The enhancement of α - and β -phase formation may need to be investigated in view not only of the presence of liquid phases by also of the formation of intermediate transition metal nitrides which may assist in the silicon nitridation. Also the distribution of metal atoms on as well as in silicon needs to be investigated, which may be different depending on metals. Transmission electron microscope analysis may be useful. The distribution of metal atoms will suggest not only the location of reaction but also silicon-metal forms active as a catalyst. The phase diagram may also be affected by the presence of nitrogen. Further study is needed.

4.5.9 Operation with Programmed Temperature

Although calcium and yttrium suppress the β -silicon nitride formation, the achievable overall conversion of silicon is not high enough even at 1300°C. In case

of the nitridation of 1% yttrium-impregnated silicon for 6 hours at 1300°C, for instance, over 20% by mass of silicon still remains unreacted in the final product.

The nitridation of silicon, impregnated with calcium or yttrium, was tested using a step-wise increase in the reaction temperature from 1300°C to 1390°C, as suggested elsewhere [Jovanovic, *et al.*, 1994]. The reaction was carried out at 1300°C for one hour, followed by the nitridation at 1390°C for two hours. Figure 4.56 shows that the nitridation can be completed with no β -silicon nitride formation when silicon is impregnated with calcium. A significantly improved conversion over 98% is achieved with an α -phase content higher than 97% in the 2% yttrium-silicon system. These results are clearly different from those obtained from the nitridation at a constant temperature. Thus, when the reaction temperature is maintained at 1390°C from the beginning throughout the nitridation for 3 hours, the overall conversion of calcium or yttrium impregnated silicon remains low, as illustrated in Figure 4.56 and 4.57. The higher the content of these metals, the lower the overall conversion, when the nitridation temperature is held constant.

In either case of calcium or yttrium, a step-wise increase in the reaction temperature from 1300°C to 1390°C has not caused an appreciable decrease in the fraction of α -silicon nitride. The results in Figure 4.56 and 4.57, indicate that an addition of a small amount of calcium helps suppress the formation of β -silicon nitride, while the content of yttrium needs to be high to maintain a high fraction of α -silicon nitride, when the reaction temperature is increased during the nitridation

process. The content of α -silicon nitride decreases when bare silicon is nitrided in the step-wise temperature-increase mode, as also shown elsewhere [Jovanovic, *et al.*, 1994]. The step-wise increase in the reaction temperature is effective in the catalytic nitridation of silicon for achieving a high overall conversion in a short time without decreasing the fraction of α -silicon nitride.

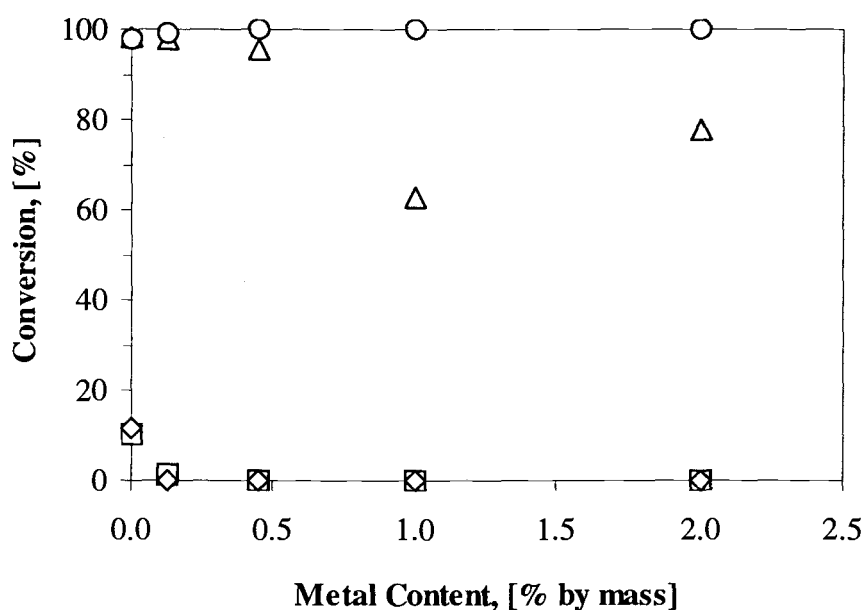


Figure 4.56 Comparison of the nitridation of calcium impregnated silicon with a step-wise increase in temperature to the nitridation at 1390°C:
 (Δ) – overall conversion, nitridation at 1390°C;
 (□) – conversion to β -phase, nitridation at 1390°C;
 (O) – overall conversion, nitridation with temperature program;
 (◇) – conversion to β -phase, nitridation with temperature program.

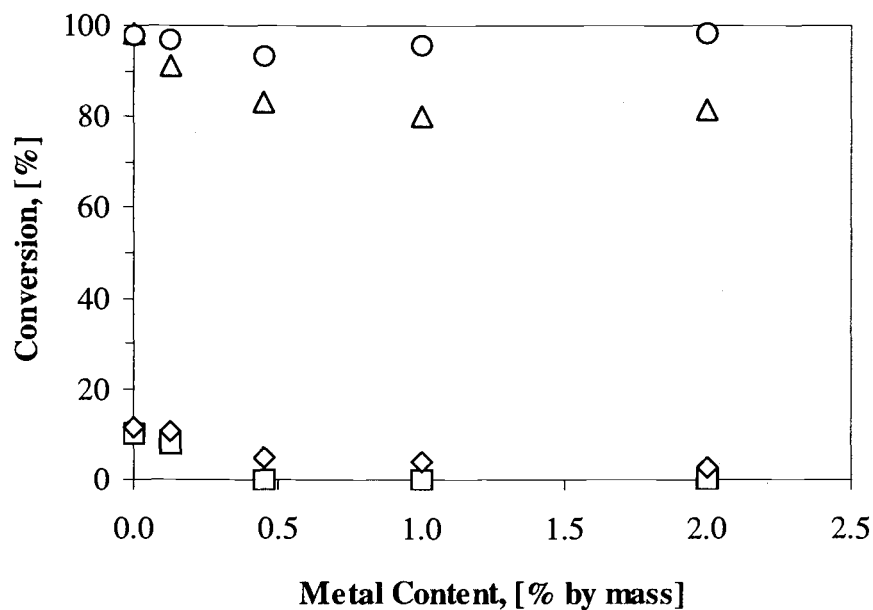


Figure 4.57 Comparison of the nitridation of yttrium impregnated silicon with a step-wise increase in temperature to the nitridation at 1390°C:
 (Δ) – overall conversion, nitridation at 1390°C;
 (\square) – conversion to β -phase, nitridation at 1390°C;
 (\circ) – overall conversion, nitridation with temperature program;
 (\diamond) – conversion to β -phase, nitridation with temperature program.

5. CONCLUSIONS AND RECOMMENDATIONS

5.1 CONCLUSIONS

The factors influencing the direct nitridation of silicon were studied in a tubular flow reactor and a fluidized-bed reactor at temperatures in the range from 1150 to 1350°C. The effects of the native oxide layer covering the surface of silicon raw materials, the effects of hydrogen contained in the nitridation atmosphere and the effects of metals added to silicon on the nitridation of silicon were investigated. The results are summarized in the following sections.

5.1.1 Effects of the Native Oxide Layer

- (1) Silicon covered with native oxide can not be nitrified. The nitridation process does not start until the covering native oxide layer is removed.
- (2) Native oxide is suspected to be removed by the reaction between silicon and silicon dioxide to form silicon monoxide vapor. It is found that hydrogen contained in argon during the pretreatment or in the nitridation gas mixture assists the native oxide removal.

- (3) The induction period in the nitridation, during which no nitridation takes place, is associated with the presence of the native oxide on the surface of silicon. The length of the induction time depends on the nitridation temperature as well as the amount of oxide remaining on the surface. No induction time is observed when silicon grains are pretreated at 1300°C for 1 hour or longer.

5.1.2 Roles of Hydrogen

- (1) Once pretreated silicon grains are exposed to nitrogen without hydrogen, for as short as 5 minutes, the subsequent nitridation becomes very slow even in the presence of hydrogen.
- (2) A high conversion in the nitridation can be achieved within a relatively short time if hydrogen is maintained in the nitridation environment, as low as 0.3%.
- (3) A protective barrier forms on the surface of silicon when silicon grains are exposed to nitrogen without hydrogen. The protective film is suspected to be the product from the reaction of silicon with oxygen and nitrogen, i.e. silicon oxynitride, a mixture of silicon dioxide and silicon oxynitride, or a mixture of silicon oxynitride and silicon nitride, depending on the temperature of its formation.
- (4) The formation of the protective film at low temperature is less spontaneous and a longer hydrogen interruption period is needed to reach an effective inhibiting

thickness, after which the following nitridation is inhibited. At higher temperature, the formation of the protective film is more spontaneous, but it may be easier for reactive species to transport to the reaction site, during the subsequent nitridation.

- (5) The role of hydrogen is to maintain oxygen partial pressure to a low level so that only silicon nitride is formed.

5.1.3 Combined Effect of Hydrogen Interruption and Native Oxide

- (1) The native oxide layer can mask the formation of the protective film during the hydrogen interruption period.
- (2) During the subsequent nitridation, the protective film is not removed, but the native oxide is removed and the nitridation takes place at the exposed surface.

5.1.4 Catalytic Effects of Metals

- (1) The formation of β -silicon nitride is significantly suppressed by adding a small amount of calcium or yttrium in the nitridation at 1300°C, or copper at 1200°C. An addition of calcium as small as 0.125% could eliminate the formation of β -

silicon nitride, and only a small amount of β -silicon nitride was detected in the product from the nitridation of 1% yttrium impregnated silicon at 1300°C.

- (2) Iron enhances the formation of β -silicon nitride at all temperatures investigated, while the addition of chromium, tungsten, silver or palladium does not significantly affect the fraction of α -/ β -phase in the silicon nitride product.
- (3) The addition of copper or palladium significantly enhances the nitridation at 1200°C. The overall conversion achieved from the nitridation of copper- or palladium-impregnated silicon is almost double of that from non-impregnated silicon.
- (4) Raising the reaction temperature stepwise from 1300°C to 1390°C accelerates, toward the complete conversion, the nitridation of calcium- or yttrium-impregnated silicon without promoting the formation of β -silicon nitride.
- (5) It is difficult to state that the formation of liquid phases of silicon-metal alloys has the dominant effect on the α - or β -silicon nitride formation.

5.2 RECOMMENDATIONS FOR FUTURE WORK

The direct nitridation of silicon is one of the most commonly used process for the mass production of silicon nitride. There are many critical factors involved in this process that have not been fully investigated. Detailed investigation of these

factors can lead to more efficient process and improve the quality of the product.

Some recommendations for future work are listed as follows:

- (1) Although the presence of the protective layer formed during the exposure of silicon granules to nitrogen without hydrogen is observed, the actual morphology and composition of the protective film have never been studied. The microscopic study using high-resolution instruments such as a transmission electron microscope (TEM) and a high-resolution electron microscope (HREM) should be used to study the boundary between the protective layer and the silicon underneath.
- (2) The kinetics of the native oxide removal, the kinetics of the protective film formation as well as the kinetics of the nitridation of silicon impregnated with metals should be investigated.
- (3) The nitridation should be studied *in situ* by using high temperature X-ray diffraction. Moreover, the composition of the reactant gas mixture should be constantly monitored at the inlet and outlet of the reactor.
- (4) The mechanism for the nitridation of silicon impregnated with metals is not clear. The actual distribution of metals on the surface of silicon grains and the concentration of metals inside the grains should be investigated. Surface study using the X-ray photoelectron spectroscopy (XPS) is suggested.
- (5) Although it is found that an addition of calcium, yttrium or copper enhances the formation of α -silicon nitride. The physical properties of the products from the

nitridation of silicon impregnated with metals (calcium, yttrium or copper) have never been tested. The physical and mechanical properties, as well as the sinterability of the product should be investigated.

BIBLIOGRAPHY

- Atkinson, A. and A. J. Moulson, "Some Important Variables Affecting the Course of the Reaction between Silicon Powder and Nitrogen," *Science of Ceramics*, **8**, 111-121 (1976).
- Atkinson, A., A. J. Moulson and E. W. Roberts, "Nitridation of High-Purity Silicon," *Journal of the American Ceramic Society*, **59** [7-8], 285-289 (1973).
- Ault, N. N. and R. L. Yeckley, "Silicon Nitride," *American Ceramic Society Bulletin*, **73** [6], 129-133 (1994).
- Barrer, R. M., "The Mechanism of Activated Diffusion Through Silica Glass," *Journal of the Chemical Society*, **136**, 378-386 (1934).
- Barsoum, M., P. Kangutkar and M. J. Koczak, "Nitridation Kinetics and Thermodynamics of Silicon Powder Compacts," *Journal of the American Ceramic Society*, **74** [6], 1248-1253 (1991).
- Boyer, S. M. and A. J. Moulson, "A Mechanism for the Nitridation of Fe-Contaminated Silicon," *Journal of Materials Science*, **13** [8], 1637-1646 (1978).
- Cambier, F. and A. Leriche, "Silicon Nitride: Relations between Powder Characteristics and Sinterability", The Physics and Chemistry of Carbides, Nitrides and Borides, edited by R. Freer, Kluwer Academic Publishers, Netherlands, 13-28 (1990).
- Campos-Loriz, D. and F. L. Riley, "Factors Affecting the Formation of the α - and β -Phases of Silicon Nitride," *Journal of Materials Science*, **13**, 1125-1127 (1978).
- Cofer, C. G. and J. A. Lewis, "Chromium Catalysed Silicon Nitridation," *Journal of Materials Science*, **29** [22], 5880-5886 (1994).

- Colquhoun I., S. Wild, P. Grieveson and K. H. Jack, "Thermodynamics of the Silicon-Nitrogen-Oxygen System," *Proceedings of the British Ceramic Society*, **22**, 207-227 (1973).
- Deckwerth, M. and C. Rüssel, "A New Polymeric Route to Silicon Carbide and Silicon Nitride using Elementary Silicon as Starting Material," *Journal of Materials Science*, **29** [17], 4500-4504 (1994).
- Dervišbegovic, H. and F. L. Riley, "The Role of Hydrogen in the Nitridation of Silicon Powder Compacts," *Journal of Materials Science*, **16**, 1945-1955 (1981).
- Du, H., R. E. Tressler, K. E. Spear and C. G. Pantano, "Oxidation Studies of Crystalline CVD Silicon Nitride," *Journal of the Electrochemical Society*, **136** [5], 1527-1536 (1989).
- Du, H., R. E. Tressler and K. E. Spear, "Thermodynamics of the Si-N-O System and Kinetic Modeling of Oxidation of Si_3N_4 ," *Journal of the Electrochemical Society*, **136** [11], 3210-3215 (1989).
- Evans, J. W. and S. K. Chatterji, "Kinetics of the Oxidation and Nitridation of Silicon at High Temperatures," *Journal of Physical Chemistry*, **62**, 1064-1067 (1958).
- Geldart, D. and A. R. Abrahamsen, "Homogeneous Fluidization of Fine Powders using Various Gases and Pressures," *Powder Technology*, **19**, 133-136 (1978).
- Giridhar, R. V. and K. Rose, "Conditions for Thermal Nitridation of Si and $\text{N}_2\text{-O}_2$ Mixtures," *Journal of the Electrochemical Society*, **135** [11], 2803-2807 (1988).
- Hendry, A., "Thermodynamics of Silicon Nitride and Oxynitride", Nitrogen Ceramics, edited by F. L. Riley, Noordoff International, Manchester, (1977).

- Hüttinger, K. J. and T. W. Pieschnick, "A Synthesis of Mono-Crystalline Silicon Nitride Filaments," *Journal of Materials Science*, **29** [11], 2879-2883 (1994).
- Iskoe, J. L., F. F. Lange and E. S. Diaz, "Effect of Selected Impurities on the High Temperature Mechanical Properties of Hot-Pressed Silicon Nitride," *Journal of Materials Science*, **11** [5], 908-912 (1976).
- Ito, T., T. Nozaki and H. Ishikawa, "Direct Thermal Nitridation of Silicon Dioxide Films in Anhydrous Ammonia Gas," *Journal of the Electrochemical Society*, **127** [9], 2053-2057 (1980).
- JANAF Tables, *Journal of Physical and Chemical Reference Data* **14**, Supplements 1, (1985).
- Jennings, H. M. and M. H. Richman, "Structure, Formation Mechanisms and Kinetics of Reaction-Bonded Silicon Nitride," *Journal of Materials Science*, **11**, 2087-2098 (1976).
- Jennings, H. M., "Review on Reactions between Silicon and Nitrogen : Part 1 Mechanisms," *Journal of Materials Science*, **18**, 951-967 (1983).
- Jovanovic, Z. R., "Kinetic Study on the Production of Silicon Nitride by Direct Nitridation of Silicon in a Fluidized Bed: Experiment and Modeling", Ph.D. Dissertation. Oregon State University, Corvallis, OR, (1994).
- Jovanovic, Z. and S. Kimura, "Use of Two-Phase Standards of Unknown Compositions to Determine Calibration Constants for Powder XRD by Linear Regression," *Journal of the American Ceramic Society*, **77** [8], 2226-2228 (1994).
- Jovanovic, Z., S. Kimura and O. Levenspiel, "Effects of Hydrogen and Temperature on the Kinetics of the Fluidized-Bed Nitridation of Silicon," *Journal of the American Ceramic Society*, **77** [1], 186-192 (1994).

- Kijima, K. and S. Shirasaki, "Nitrogen Self-Diffusion in Silicon Nitride," *The Journal of Chemical Physics*, **65** [7], 2668-2671 (1976).
- Koike, J. and S. Kimura, "Mechanism of Nitridation of Silicon Powder in a Fluidized-Bed Reactor," *Journal of the American Ceramic Society*, **79** [2], 365-370 (1996).
- Lange, F. F., "Fracture Toughness of Si_3N_4 as a Function of the Initial α -Phase Content," *Journal of the American Ceramic Society*, **62** [7-8], 428-430 (1979).
- Lin, S.-S., "Comparative Studies of Metal Additives on the Nitridation of Silicon," *Journal of the American Ceramic Society*, **60** [1-2], 78-81 (1977).
- Lin, S.-S., "Mass Spectrometric Studies of the Nitridation of Silicon," *Journal of The American Ceramic Society*, **58** [7-8], 271-273 (1975).
- Lindley, M. W., D. P. Elias, B. F. Jones and K. C. Pitman, "The Influence of Hydrogen in the Nitriding Gas on the Strength, Structure and Composition of Reaction-Sintered Silicon Nitride," *Journal of Materials Science*, **14**, 70-85 (1979).
- Lippincott, E. R., A. V. Valkenburg, C. E. Weir and E. N. Bunting, "Infrared Studies on Polymorphs of Silicon Dioxide and Germanium Dioxide," *Journal of Research of the National Bureau of Standards*, **61** [1], 61-70 (1958).
- Liu, Y. D., "Fluidized-Bed Nitridation of Silicon-Direct Use of Very Fine Powder for α -silicon Nitride Production", Ph.D. Dissertation. Oregon State University, Corvallis, OR, (1996).
- Liu, Y.-D. and S. Kimura, "Fluidized-Bed Nitridation of Fine Silicon Powder," *Powder Technology*, **106**, 160-167 (1999).

- Luongo, J. P., "Infrared Characterization of α - and β -Crystalline Silicon Nitride," *Journal of the Electrochemical Society*, **130** [7], 1560-1562 (1983).
- Maalmi, M. and A. Varma, "Intrinsic Nitridation Kinetics of High-Purity Silicon Powder," *AIChE Journal*, **42** [12], 3477-3483 (1996).
- Massalski, T. B., "Binary Alloy Phase Diagrams", American Society for Metals, Metals Park, OH, (1986).
- McCusker, L. B., R. B. V. Dreele, D. E. Cox, D. Louer and P. Scardi, "Rietveld Refinement Guidelines," *Journal of Applied Crystallography*, **32**, 36-50 (1999).
- Messier, D. R., F. L. Riley and R. J. Brook, "The α/β Silicon Nitride Phase Transformation," *Journal of Materials Science*, **13**, 1199-1205 (1978).
- Messier, D. R. and P. Wong, "Kinetics of Nitridation of Si Powder Compacts," *Journal of the American Ceramic Society*, **56** [9], 480-485 (1973).
- Mitomo, M., "Effect of Fe and Al Additions on Nitridation of Silicon," *Journal of Materials Science*, **12** [2], 273-276 (1977).
- Moulson, A. J., "Reaction-Bonded Silicon Nitride: Its Formation and Properties," *Journal of Materials Science*, **14**, 1017-1051 (1979).
- Mukerji, J. and S. K. Biswas, "Effect of Iron, Titanium, and Hafnium on Second-Stage Nitriding of Silicon," *Journal of the American Ceramic Society*, **64** [9], 549-552 (1981).
- Nemetz, J. A. and R. E. Tressler, "Thermal Nitridation of Silicon and Silicon Dioxide for Thin Gate Insulators," *Solid State Technology*, **26** [2], 79-85 (1983).
- Pankratz, L. B., "Thermodynamic Properties of Elements and Oxides", Bureau of Mines Bulletin 672, United States Department of the Interior (1982).

- Parr, N. L., R. Sands, P. L. Pratt, E. R. W. May, C. R. Shakespeare and D. S. Thompson, "Structural Aspects of Silicon Nitride," *Powder Metallurgy*, **8**, 152-163 (1961).
- Pavarajarn, V and S. Kimura, "Catalytic Effects of Metals on Direct Nitridation of Silicon," *Journal of the American Ceramic Society*, **84** [8], 1669-1674 (2001).
- Pigeon, R. G. and A. Varma, "Quantitative Kinetic Analysis of Silicon Nitridation," *Journal of Materials Science*, **28**, 2999-3013 (1993).
- Pigeon, R. G., A. Varma and A. E. Miller, "Some Factors Influencing the Formation of Reaction-Bonded Silicon Nitride," *Journal of Materials Science*, **28** [7], 1919-1936 (1993).
- Pompe, R., L. Hermansson, T. Johansson, E. Djurle and M. E. Hatcher, "Characterization of Silicon Powders for the Production of Si_3N_4 ," *Materials Science and Engineering*, **71**, 355-362 (1985).
- Popper, P. and S. N. Ruddlesden, "The Preparation, Properties and Structure of Silicon Nitride," *Transactions of the British Ceramic Society*, **60**, 603-625 (1961).
- Rahaman, M. N. and A. J. Moulson, "The Removal of Surface Silica and Its Effect on the Nitridation of High-Purity Silicon," *Journal of Materials Science*, **19**, 189-194 (1984).
- Raider, S. I., R. A. Gdula and J. R. Petrak, "Nitrogen Reaction at a Silicon-Silicon Dioxide Interface," *Applied Physics Letters*, **27** [3], 150-151 (1975).
- Riley, F. L., "Silicon Nitride and Related Materials," *Journal of the American Ceramic Society*, **83** [2], 245-265 (2000).
- Ruddlesden, S. N. and P. Popper, "On the Crystal Structure of the Nitrides of Silicon and Germanium," *Acta Crystallographica*, **11** [7], 465-468 (1958).

- Sanyal, A. S., J. Mukerji and S. Bandyopadhyay, "Mössbauer Study of the Influence of Fe-Si-N Liquid in the Synthesis of β -Si₃N₄ from Silica," *Journal of the American Ceramic Society*, **74** [9], 2312-2314 (1991).
- Schalch, D., A. Scharmann and R. Wolfrat, "IR Transmittance Studies of Hydrogen-Free and Hydrogenated Silicon Nitride and Silicon Oxynitride Films Deposited by Reactive Sputtering," *Thin Solid Films*, **155**, 301-308 (1987).
- Segal, D. L., "Developments in the Synthesis of Silicon Nitride," *Chemistry and Industry*, [16], 544-545 (1985).
- Shaw, N. J., "The Combined Effects of Fe and H₂ on the Nitridation of Silicon," *Journal of Materials Science Letters*, **1** [8], 337-340 (1982).
- Suematsu, H., M. Mitomo, T. E. Mitchell, J. J. Petrovic, O. Fukunaga and N. Ohashi, "The α - β Transformation in Silicon Nitride Single Crystals," *Journal of the American Ceramic Society*, **80** [3], 615-620 (1997).
- Tanaka, I., K. Igashira, T. Okamoto, K. Niihara and R. M. Cannon, "High-Temperature Fracture Mechanism of Low-Ca-Doped Silicon Nitride," *Journal of the American Ceramic Society*, **78** [3], 673-679 (1995).
- Thompson, D. S. and P. L. Pratt, "The Structure of Silicon Nitride," *Science of Ceramics*, **3**, 33-51 (1967).
- Varma, A., R. G. Pigeon and A. E. Miller, "Kinetics of α - and β -Si₃N₄ Formation from Oxide-Free High-Purity Si Powder," *Journal of Materials Science*, **26**, 4541-4544 (1991).
- Wagner, C., "Passivity during the Oxidation of Silicon at Elevated Temperature," *Journal of Applied Physics*, **29** [9], 1295-1297 (1958).
- Wang, C.-M., X. Pan and M. Ruhle, "Review Silicon Nitride Crystal Structure and Observations of Lattice Defects," *Journal of Materials Science*, **31**, 5281-5298 (1996).

Yamada, T., "Preparation and Evaluation of Sinterable Silicon Nitride Powder by Imide Decomposition Method," *American Ceramic Society Bulletin*, **72** [5], 99-106 (1993).

Zerr, A., G. Miehe, G. Serghioum, M. Schwarz, E. Kroke, R. Riedel, H. Fueb, P. Kroll and R. Boehler, "Synthesis of Cubic Silicon Nitride," *Nature*, **400**, 340-342 (1999).

APPENDICES

APPENDIX A

THERMODYNAMICS DATA

The following thermodynamics data are used in the calculation of the stability field diagram. It should be noted that the unit of the free energy, ΔG° , is converted to kJ/mol and temperature, T , is in K.

- The free energy of formation of silicon dioxide:

$$\text{Du } et al. [1989]: \quad \Delta G^\circ = -897.05 + 0.1699T$$

$$\text{Hendry [1977]:} \quad \Delta G^\circ = -940.0 + 0.20T$$

$$\text{Colquhoun } et al. [1973]: \quad \Delta G^\circ = -902.07 + 0.1736T$$

- The free energy of formation of α -silicon nitride:

$$\text{Du } et al. [1989]: \quad \Delta G^\circ = -740.15 + 0.3276T$$

$$\text{Hendry [1977]:} \quad \Delta G^\circ = -1167.3 + 0.594T$$

$$\text{Colquhoun } et al. [1973]: \quad \Delta G^\circ = -820.06 + 0.3598T$$

- The free energy of formation of silicon oxynitride:

$$\text{Du } et al. [1989]: \quad \Delta G^{\circ} = -935.96 + 0.2732T$$

$$\text{Hendry [1977]:} \quad \Delta G^{\circ} = -658.3 + 0.131T$$

$$\text{Colquhoun } et al. [1973]: \quad \Delta G^{\circ} = -882.82 + 0.2845T$$

- The free energy of formation of silicon monoxide:

Pankratz. [1982]:

$$\Delta G^{\circ} = -97.006 + 6.222 \times 10^{-3} T \ln T + 1.088 \times 10^{-6} T^2 - \frac{92.466}{T} - 0.133T$$

- The free energy of formation of water vapor, according to JANAF table:

$$\text{at } 1200^{\circ}\text{C:} \quad \Delta G^{\circ} = -165.910 \text{ kJ/mol}$$

$$\text{at } 1250^{\circ}\text{C:} \quad \Delta G^{\circ} = -163.048 \text{ kJ/mol}$$

$$\text{at } 1300^{\circ}\text{C:} \quad \Delta G^{\circ} = -160.179 \text{ kJ/mol}$$

APPENDIX B

THE NITRIDATION OF SILICON IMPREGNATED WITH HIGH-CONTENT OF METAL

As discussed earlier, no extra peaks were detected in the X-ray and IR analyses of the product from the nitridation of silicon impregnated with metal in the range of 0.125 to 2.0%. It is possible that the amount of any compound, other than silicon nitride, formed during the nitridation process is too small to be detected because the amount of metal added to the granules is small. Thus, very high content of metal (20% by mass) was used to intensify the signal. Although it is not necessary that same compound found from the nitridation with very high metal content will be present when the metal content is low, the results can be used as the preliminary data for future study.

The investigation focuses on the metals that suppress the formation of β -silicon nitride, i.e. calcium, yttrium and copper. The nitridation was conducted for 3 hours in the tubular flow reactor at 1300°C, after 1-hour pretreatment at the same temperature. The products after heating-up, the product after 1-hour pretreatment and the products after 3-hour nitridation are analyzed by using X-ray diffraction and IR analysis.

CALCIUM

The X-ray diffraction patterns of the products from each step of the nitridation process are shown in Figure B1. It is indicated a foreign compound(s), other than silicon, is found from the product after heating-up from room temperature to 1300°C. The extra peaks are located at 2θ of 32.2°, 32.8°, 41.3° and 45.6°. This compound(s) remains unreacted throughout the pretreatment. However, after the nitridation (with 90% N₂/10% H₂), the peaks corresponding to that compound(s) disappear. New extra peaks, compared with the product from the nitridation of non-impregnated silicon, are observed at 2θ of 26.3°, 26.8°, 30.3° and 38.3°. It is implied that the intermediate compound(s) that forms during the heating-up process reacts to form new compound(s).

The results from IR analysis also confirm the presence of additional compound(s), other than silicon nitride in the product of the nitridation (Figure B2). The main strong absorption band near 950 cm⁻¹ broadens dramatically. Moreover, the extra absorption bands are found around 1482, 1639 and 1735 cm⁻¹.

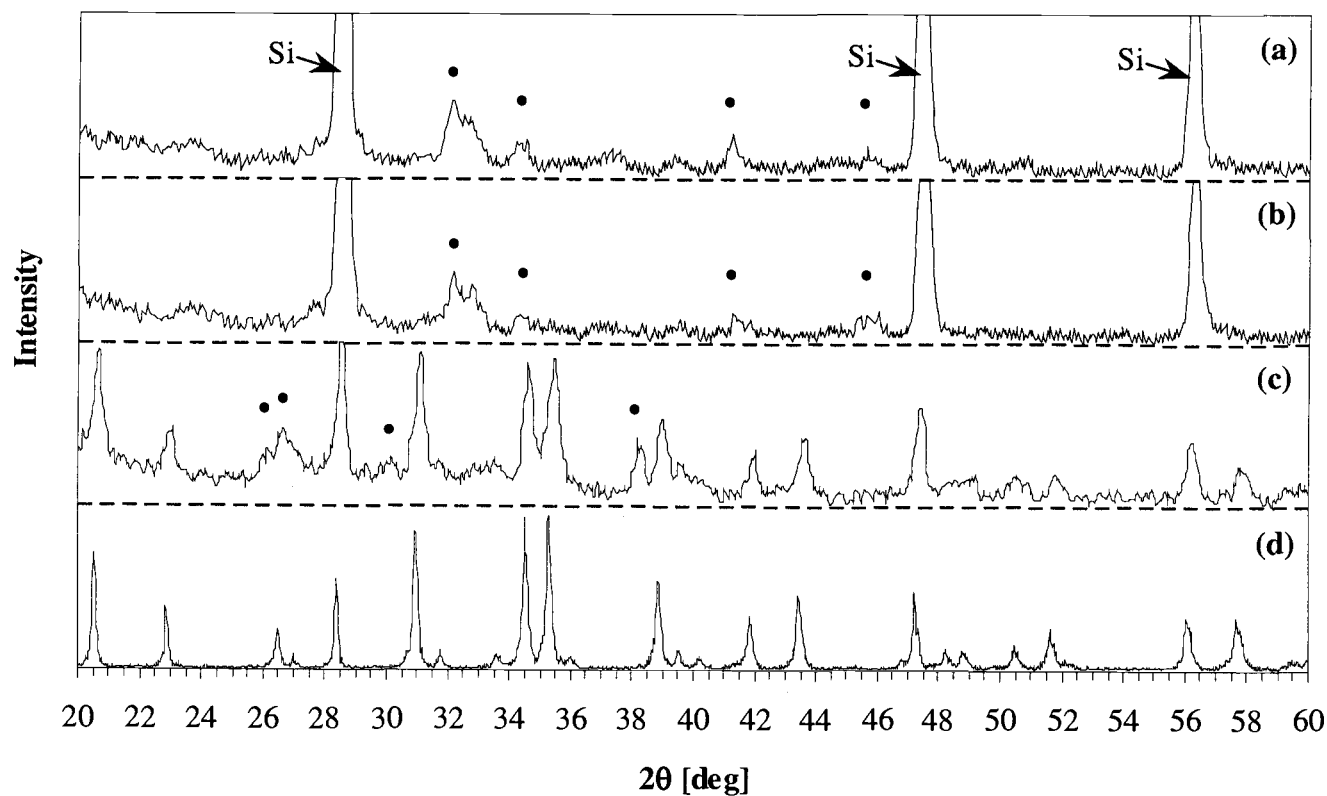


Figure B1 XRD patterns of the products from the nitridation of 20% calcium-impregnated silicon: (a) after heating-up; (b) after 1-hour pretreatment; (c) after 3-hour nitridation; (d) product from the nitridation of bare silicon.

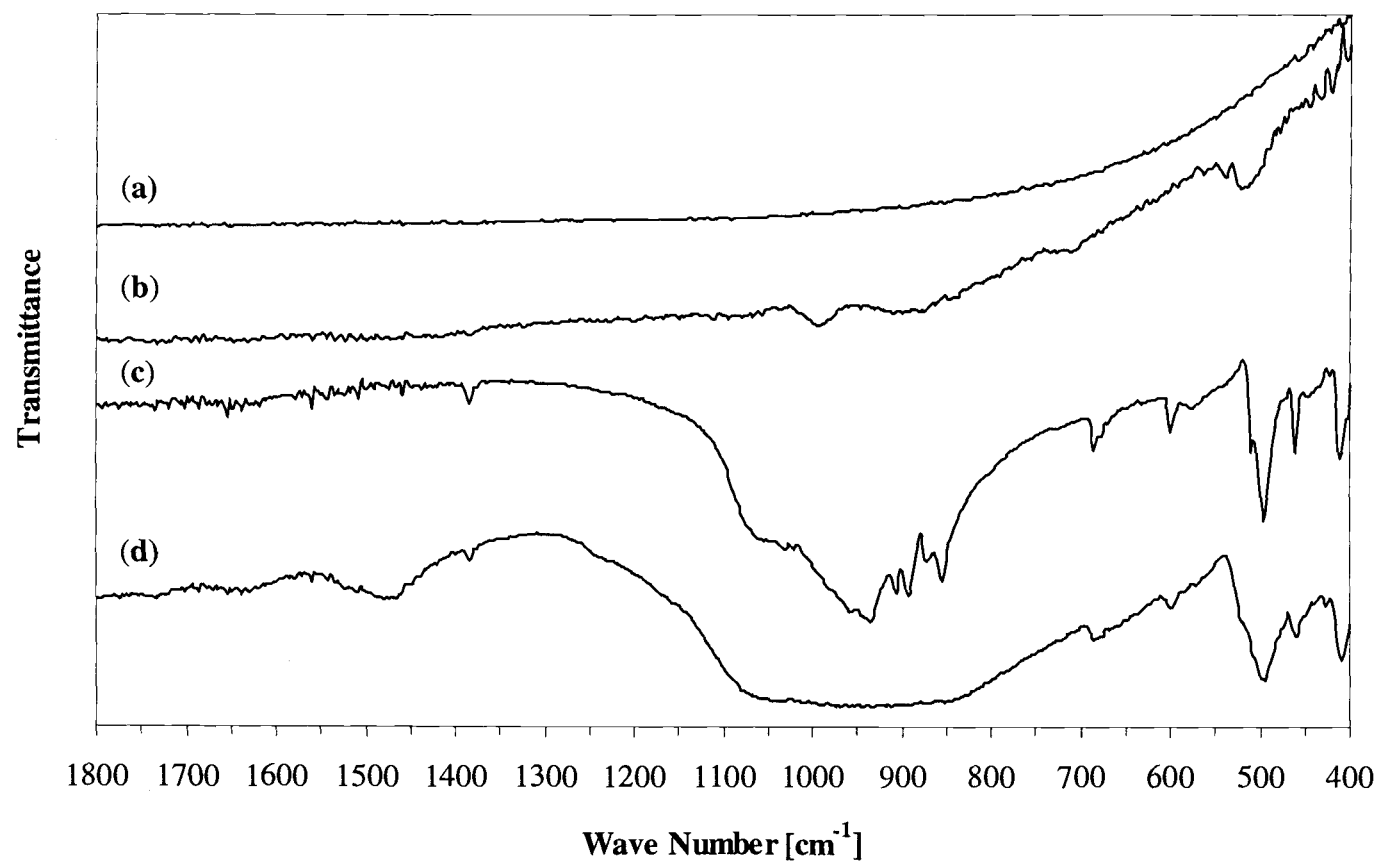


Figure B2 IR spectra of the products from the nitridation of 20% calcium-impregnated silicon compared to that from bare silicon: (a) bare silicon, after 1-hour pretreatment; (b) 20% Ca impregnated silicon, after 1-hour pretreatment; (c) bare silicon, after 3-hour nitridation; (d) 20% Ca impregnated silicon, after 3-hour nitridation.

YTTRIUM

The extra peaks are found at 2θ of 29.3° , 31.2° , 32.7° , 33.9° , 48.8° and 57.8° after silicon granules impregnated with 20% yttrium is heated to 1300°C , as shown in Figure B3. The intensity of the peaks at 32.7° and 33.9° decrease after 1-hour pretreatment and disappear after the nitridation, while new extra peaks at 27.9° , 31.5° , 44.6° and 45.8° is found. It is found that the extra peaks, compared with the peaks from the nitridation of bare silicon, are located very close to 2θ that are corresponding to $\text{Y}_6\text{Si}_3\text{O}_9\text{N}_4$. Thus, it is implied that yttrium compound forms during the heating-up process. It is reduced (or reacted) during the pretreatment and then forms new compound with nitrogen during the nitridation.

The results from IR analysis are shown in Figure B4. No significant different absorption band is detected when yttrium is added to silicon. However, small broad bands are found around 550 , 900 and 1000 cm^{-1} after the sample is pretreated.

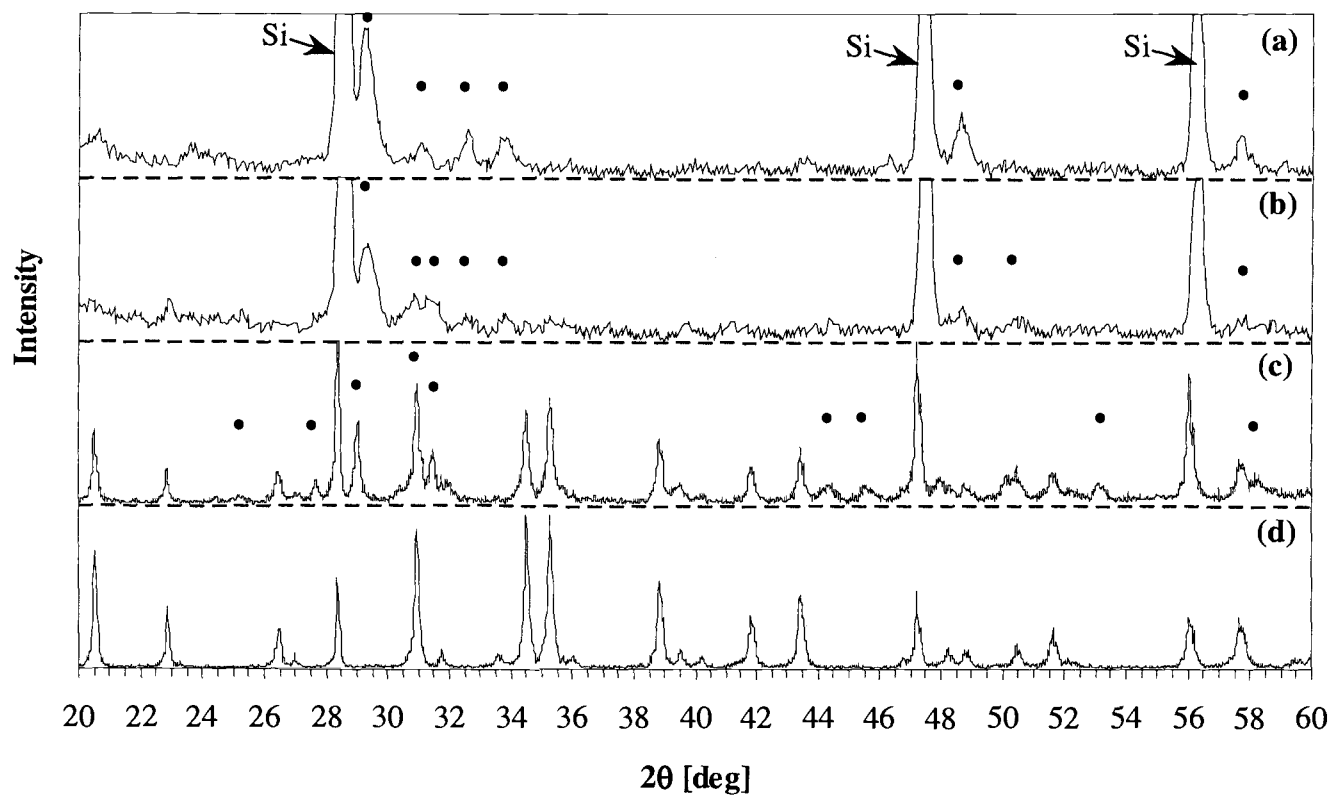


Figure B3 XRD patterns of the products from the nitridation of 20% yttrium-impregnated silicon: (a) after heating-up; (b) after 1-hour pretreatment; (c) after 3-hour nitridation; (d) product from the nitridation of bare silicon.

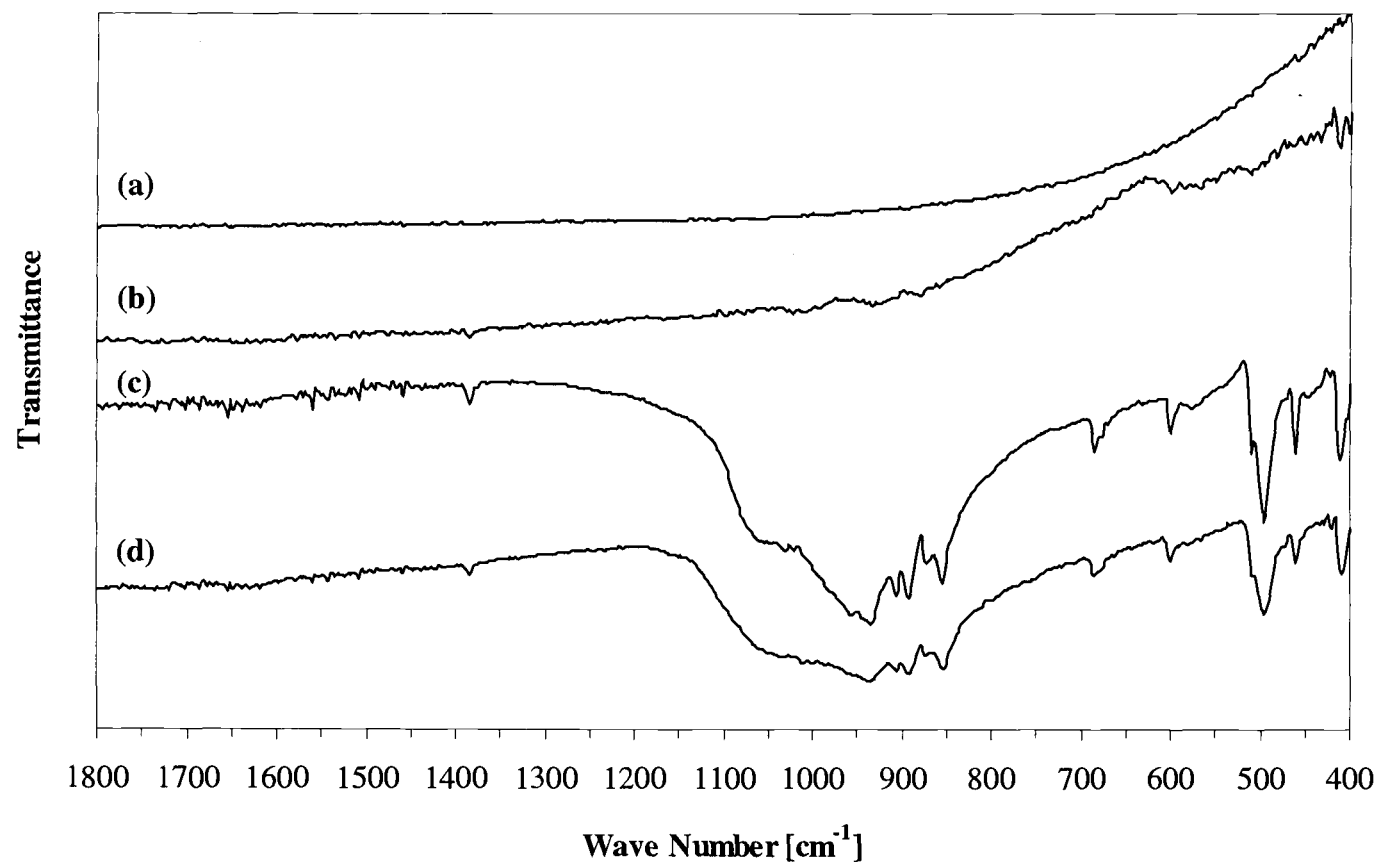


Figure B4 IR spectra of the products from the nitridation of 20% yttrium-impregnated silicon compared to that from bare silicon: (a) bare silicon, after 1-hour pretreatment; (b) 20% Y impregnated silicon, after 1-hour pretreatment; (c) bare silicon, after 3-hour nitridation; (d) 20% Y impregnated silicon, after 3-hour nitridation.

COPPER

The XRD patterns of the products from the nitridation of 20% copper impregnated silicon show extra peaks, other than those from silicon and silicon nitride, at 2θ of 44.7° and 45.2° , as shown in Figure B5. These two peaks are found from the product after heating-up from room temperature to 1300°C . They are also detected after the nitridation. No other extra peak is found. Thus, it is implied that this copper compound(s) forms during the heating-up process and remains unchanged throughout the nitridation process.

The IR spectra shown in Figure B6 indicate small extra absorption bands around 500 and 1100 cm^{-1} after 1-hour pretreatment. After the nitridation, the main strong absorption band for Si-N bonding near 950 cm^{-1} slightly broadens, but no extra band is observed.

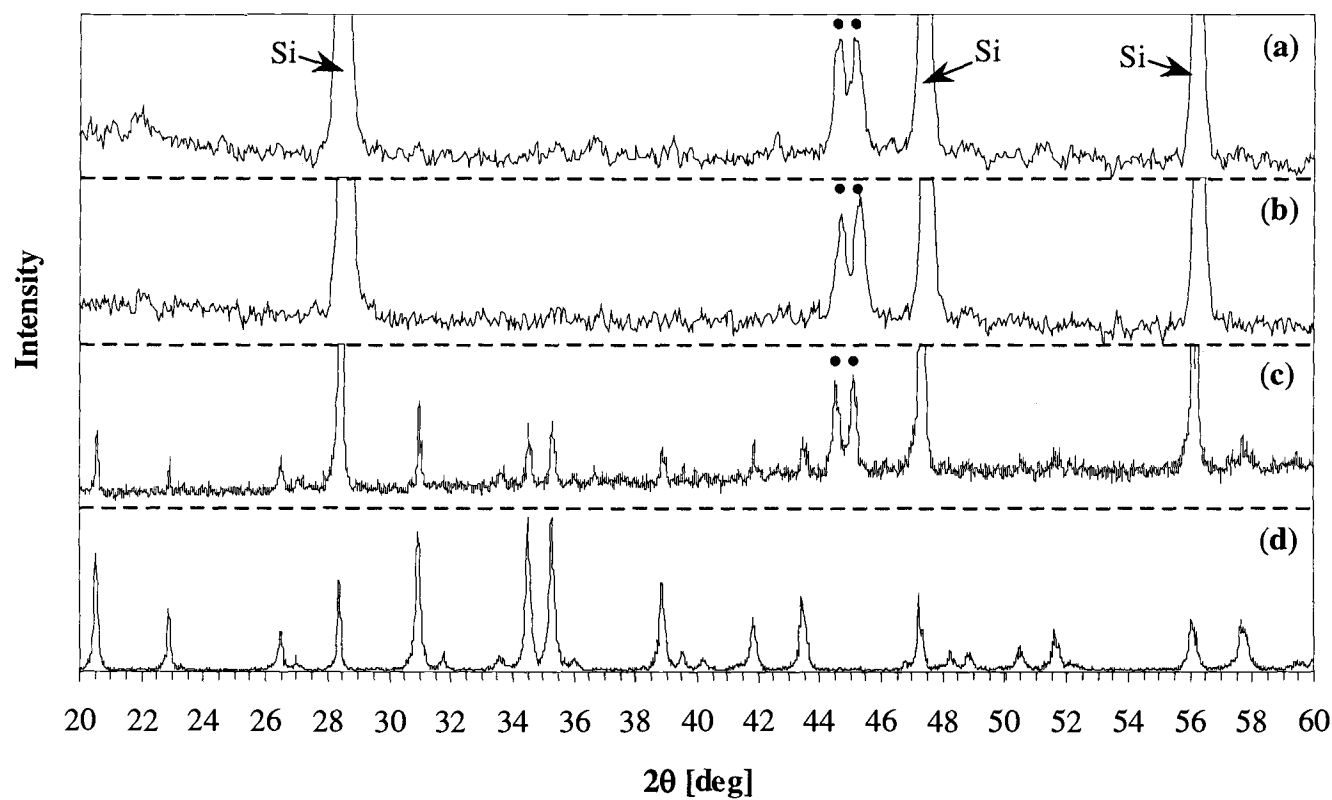


Figure B5 XRD patterns of the products from the nitridation of 20% copper-impregnated silicon: (a) after heating-up; (b) after 1-hour pretreatment; (c) after 3-hour nitridation; (d) product from the nitridation of bare silicon.

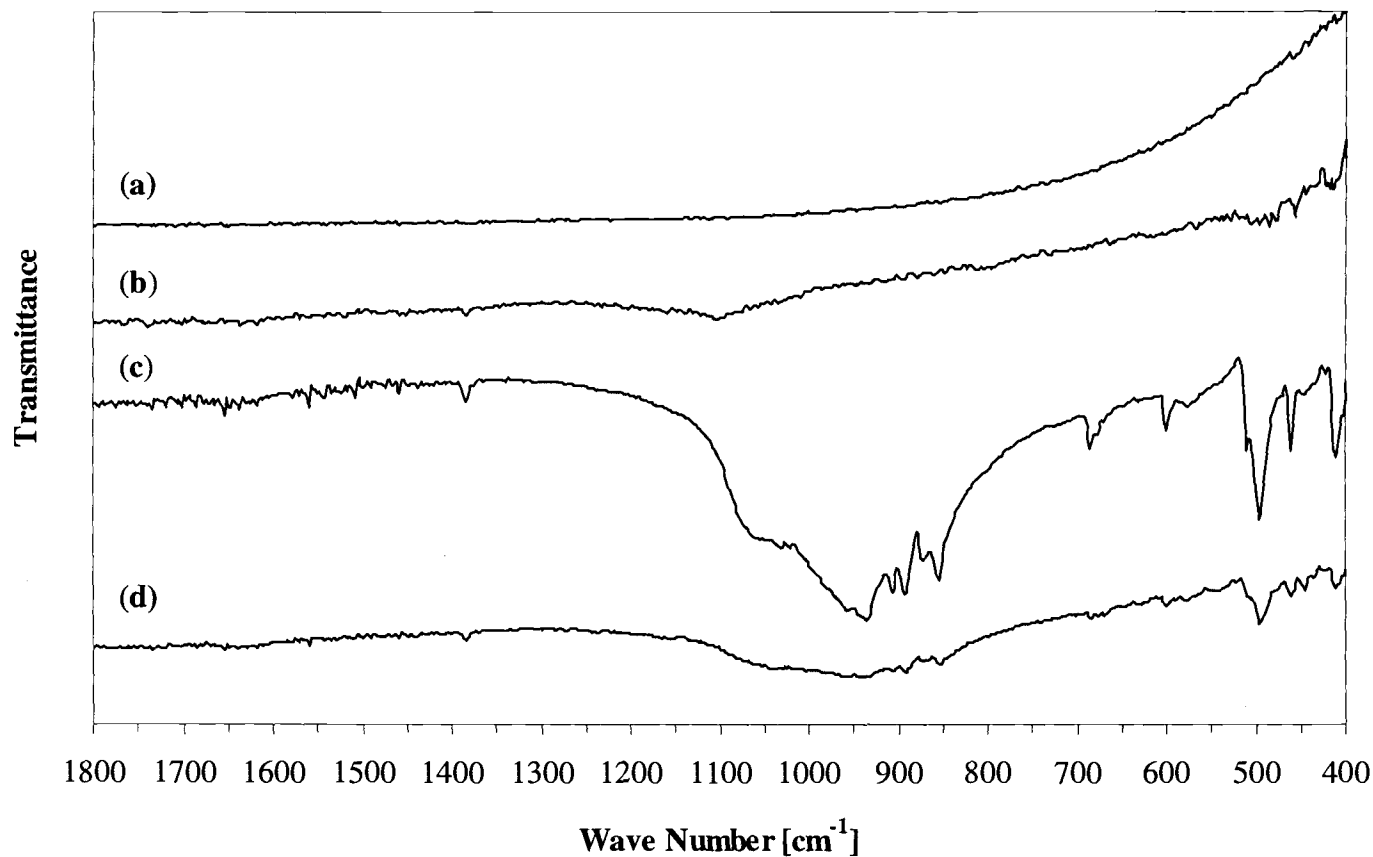


Figure B6 IR spectra of the products from the nitridation of 20% copper-impregnated silicon compared to that from bare silicon: (a) bare silicon, after 1-hour pretreatment; (b) 20% Cu impregnated silicon, after 1-hour pretreatment; (c) bare silicon, after 3-hour nitridation; (d) 20% Cu impregnated silicon, after 3-hour nitridation.